

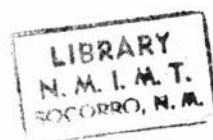
BULLETIN 80

Precambrian Geology of
La Madera Quadrangle,
Rio Arriba County,
New Mexico

by EDWARD C. BINGLER

1965

STATE BUREAU OF MINES AND MINERAL RESOURCES
NEW MEXICO INSTITUTE OF MINING & TECHNOLOGY
CAMPUS STATION SOCORRO, NEW MEXICO



NEW MEXICO INSTITUTE OF MINING & TECHNOLOGY Stirling
A. Colgate, *President*

STATE BUREAU OF MINES AND MINERAL RESOURCES Alvin J.
Thompson, *Director*

THE REGENTS

MEMBERS Ex OFFICIO

The Honorable Jack M. Campbell *Governor of New Mexico*
Leonard DeLayo *Superintendent of Public Instruction*

APPOINTED MEMBERS

William G. Abbott Hobbs
Eugene L. Coulson, M.D. Socorro
Thomas M. Cramer Carlsbad
Eva M. Larrazolo (Mrs. Paul F.) Albuquerque
Richard M. Zimmerly Socorro

For sale by the New Mexico Bureau of Mines and Mineral Resources
Campus Station, Socorro, N. Mex.—Price \$3.00

Contents

| | <i>Page</i> |
|--------------------------------|-------------|
| ABSTRACT | 1 |
| INTRODUCTION | 2 |
| Previous work | 2 |
| Location and access | 2 |
| Physical features | 4 |
| Methods of study | 5 |
| Acknowledgments | 6 |
| QUATERNARY GEOLOGY | 7 |
| Erosion surfaces | 7 |
| Recent deposits | 8 |
| TERTIARY GEOLOGY | 9 |
| Petrology | 9 |
| Sedimentary rocks | 9 |
| Conglomerate | 9 |
| Quartzite conglomerate | 11 |
| Volcanic conglomerate | 12 |
| Arkosic sandstone | 14 |
| Igneous rocks | 14 |
| Basalt | 14 |
| Pyroclastic unit | 15 |
| Faults | 16 |
| PRECAMBRIAN GEOLOGY | 17 |
| Petrology | 17 |
| Quartzite | 19 |
| Aluminous schist | 23 |
| Specularite schist | 24 |
| Kyanite-muscovite schist | 24 |
| Origin | 25 |
| Muscovitic quartzite | 25 |
| Origin | 27 |
| Tectonic breccia phase | 28 |
| Feldspathic schist | 29 |
| Origin | 34 |

| | <i>Page</i> |
|---|-------------|
| Quartz-albite-muscovite-biotite schist | 36 |
| Origin | 37 |
| Granitic gneiss | 37 |
| Origin | 39 |
| Hornblende-chlorite schist | 39 |
| Origin | 42 |
| Plagioclase-chlorite phyllite | 42 |
| Origin | 43 |
| Chlorite schist | 43 |
| Origin | 44 |
| Pegmatite and quartz dikes | 44 |
| Metamorphism | 44 |
| Facies of regional metamorphism | 45 |
| Later metamorphic effects | 47 |
| Pegmatitic metasomatism | 50 |
| Petaca aureole | 52 |
| Structural geology | 53 |
| Planar structures | 54 |
| Bedding | 54 |
| Flow cleavage | 59 |
| Fracture cleavage and slip cleavage | 59 |
| Joints | 63 |
| Relationship between rock cleavage and folds | 65 |
| Linear structures | 66 |
| Mineralogic lineation | 66 |
| Textural lineation | 68 |
| Intersecting planes | 71 |
| Boudins | 72 |
| Transposition of lineation | 73 |
| Relationship of lineation to megascopic folds | 75 |
| Orientation of lineation | 76 |
| Origin of lineation | 76 |
| Folds | 84 |
| Mesoscopic folds | 87 |
| Macroscopic folds | 90 |
| Relict structures | 91 |

| | <i>Page</i> |
|--|-------------|
| Structural history | 97 |
| First deformation structural features | 97 |
| Mesoscopic structures | 98 |
| Macroscopic structures | 101 |
| Summary of evidence | 102 |
| Effect upon original stratigraphic relations | 102 |
| Second deformation structural features | 103 |
| Mesoscopic structures | 103 |
| Macroscopic structures | 106 |
| Summary of evidence | 109 |
| Effect upon older structures | 109 |
| Third deformation structural features | 112 |
| Mesoscopic structures | 112 |
| Rotation of earlier structural elements | 114 |
| Macroscopic structures | 114 |
| Summary of evidence | 116 |
| Problem of the Petaca arc | 117 |
| Summary | 119 |
| Anomalous structure trends | 121 |
| Precambrian structural trends in New Mexico | 122 |
| Precambrian geologic history | 124 |
| REFERENCES | 127 |
| INDEX | 129 |

Illustrations

| | <i>Page</i> |
|--|-------------|
| TABLES | |
| 1. Facies of regional metamorphism | 46 |
| 2. Structural elements | 98 |
| FIGURES | |
| 1. Index map showing location of La Madera quadrangle . . | 3 |
| 2. Idealized representation of Tertiary stratigraphic relationships | 8 |
| 3. Modal composition of selected metamorphic rocks | 17 |
| 4a. Fracture cleavage in aluminous schist | 24 |
| 4b. Feldspathic schist | 31 |
| 4c. Preferred orientation of matrix muscovite in feldspathic schist | 32 |
| 4d. Micrographic intergrowth in gneissic phase of feldspathic schist | 35 |
| 5. Sketch of quartzite outcrop showing groups of arcuate layers | 56 |
| 6. Sketch of quartzite outcrop showing sigmoidal, recurved, and truncated hematite layers | 58 |
| 7. Slip cleavage transecting schistosity in feldspathic schist | 62 |
| 8. Alteration halo around joint in melanocratic phase of feldspathic schist | 64 |
| 9a. Crenulated schistosity in muscovitic quartzite | 69 |
| 9b. Wrinkled schistosity in muscovitic quartzite | 70 |
| 10. Second deformation fold in which L-lineation and first deformation axial-plane cleavage are folded | 81 |
| I 1a. Folded flow cleavage with incipient fracture cleavage developed parallel to the axial plane | 89 |
| 11b. Folded hematite layer in feldspathic schist | 89 |
| 12. Inferred continuity of amphibolite layer shown in perspective | 92 |

| | <i>Page</i> |
|--|-------------|
| 13. Pseudocross-bedding in sheared quartzite | 94 |
| 14. Sigmoidal segments of an older planar element truncated by fracture cleavage | 96 |
| 15. First deformation mesoscopic folds | 100 |
| 16. Second deformation mesoscopic folds | 105 |
| 17. Domains of second and third deformation folds | 107 |
| 18. Tectonic style of second deformation fold system | 108 |
| 19. Evolution of tectonic breccia | 111 |
| 20. Third deformation mesoscopic folds | 113 |
| 21. Schematic cross section of third deformation fold system | 115 |
| 22. Schematic diagram illustrating Precambrian geologic his- tory in La Madera quadrangle | 126 |

PLATES

| | |
|--|-----------|
| 1. Geologic map of La Madera quadrangle | In pocket |
| 2. Stereographic projection of structural data | In pocket |

Abstract

Precambrian rocks have been deformed by three episodes of regional dislocation. The earliest recognizable deformation was an integral part of the regional metamorphism. Pervasive shearing and flowage of material during the first deformation resulted in the formation of isoclinal shear folds with axial-plane flow and fracture cleavage that contains prominent textural and mineralogic lineations parallel to the fold axes. A second period of deformation, in which first deformation axial-plane cleavage is folded, produced nearly isoclinal similar folds overturned to the northeast with gently doubly plunging, northwest-trending axes. First deformation fold axes and b-lineation were transposed by the second period of folding and now trend south-southwest and plunge about 30 degrees. Second deformation axial-plane flow, fracture, and slip cleavage transect the first deformation axial-plane cleavage and form a prominent lineation parallel to second deformation fold axes. A third regional dislocation was primarily cataclastic and produced wide-spaced "step folds" with nearly vertical west-trending axial-plane cleavage. Small-scale third deformation folds trend west and plunge from 30 to 60 degrees. Fracture cleavage and slip cleavage are the usual types of axial-plane cleavage in these folds, but locally slip cleavage grades into axial-plane flow cleavage.

Quartzite, muscovitic quartzite, feldspathic schist, granitic gneiss, hornblende-chlorite schist, and phyllite are the major metamorphic rocks. Granitic pegmatite dikes and sills intrude the metamorphic complex. The first regional metamorphism resulted in the formation of quartzite, schist, and gneiss, from an original assemblage of quartz sandstone, shale, basic flow rock, granite or granitized rock, and silicic volcanic rock. First deformation equilibrium mineral assemblages are representative of the greenschist and almandine amphibolite facies of regional metamorphism. Thermal and/or hydrothermal metamorphism that followed the second period of regional folding induced regrowth of kyanite, hornblende, muscovite, and to a lesser degree feldspar in the form of porphyroblasts which include and cut across metamorphic textures formed during regional metamorphism. This stage of activity also locally converted kyanite to pyrophyllite and kaolinite plus muscovite to andalusite within the large quartzite masses. The circulation of hydrothermal fluid was controlled by pre-existing shear zones and rock cleavage. Cataclastic structures associated with regional dislocation cut across minerals formed during the thermal and/or hydrothermal metamorphism. Pegmatites are intrusive along the axial-plane cleavage of third deformation folds. Pegmatitic alkali metasomatism has converted some hornblende-chlorite schist to biotite schist and resulted in the growth of feldspar and muscovite in aureoles around some pegmatite bodies.

introduction

The Precambrian rocks of La Madera quadrangle have long been recognized as a structurally and petrologically complex sequence of quartzite, schist, and gneiss (Just, 1937; Jahns, 1946; Barker, 1958; Corey, 1960). Geologists interested primarily in the economic significance of pegmatites in the area have commented on the need for detailed structural analysis. Reconnaissance of the exposed Precambrian rocks substantiated structural complexity cited in other studies in the area; hence, detailed structural analysis became the principal motivating factor for this report. Information gathered in this study now bridges the mapped areas of Las Tablas quadrangle to the north and Ojo Caliente quadrangle to the south. The final link has been inserted in a chain of mapped areas extending from the Colorado—New Mexico line south to Ojo Caliente.

The purpose of this study has been to elucidate the sequence of tectonic and petrologic events that have so profoundly affected the Precambrian rocks of the area. The systematic collection of data on the attitude, style, and order of superposition of small-scale structural elements has been the principal means of deducing tectonic history. Thinsection data have provided the basis for most of the petrologic conclusions.

PREVIOUS WORK

A few scattered references to the Petaca area, mostly with regard to the pegmatites, appear in the literature prior to 1937 (Sterrett, 1913, 1923; Atwood and Mather, 1932). Just was the first geologist to present a geologic report of the area. His reconnaissance study of La Madera quadrangle as only a small part of a much more extensive area is remarkable in its excellent representation of rock distribution. He also recognized the structural complexity of the area, and several of the geologic names he applied to Precambrian rock units are still in use. Jahns studied the pegmatites in La Madera quadrangle as part of a more comprehensive study of pegmatites of the Petaca, Ojo Caliente, and Elk Mountain areas. Barker made a detailed study of the geology of Las Tablas quadrangle which adjoins La Madera quadrangle to the north. He subdivided the Ortega quartzite and Petaca schist of Just and named several new formations. The formal stratigraphic treatment given Precambrian rock units in Las Tablas quadrangle may have been premature in view of the structural complexity evident in the Precambrian of La Madera quadrangle. Corey reported on the occurrence and origin of kyanite deposits in La Madera and Las Tablas quadrangles.

LOCATION AND ACCESS

La Madera quadrangle, with an area of nearly sixty square miles, lies within the southeastern corner of Rio Arriba County in central northern New Mexico (fig. 1).

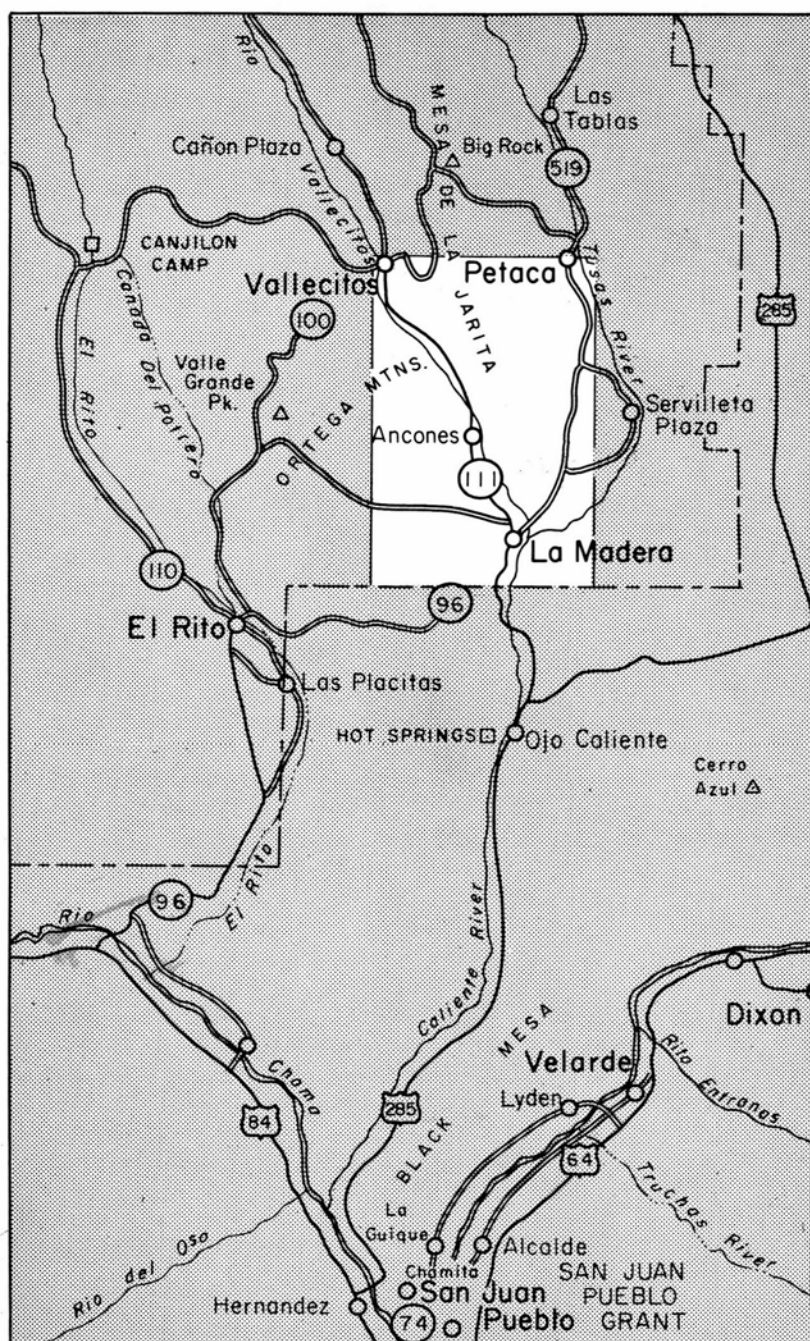


Figure 1

INDEX MAP SHOWING LOCATION OF LA MADERA QUADRANGLE

La Madera and Vallecitos are the principal villages and have a permanent population of several hundred inhabitants each. The villages of Ancones and South Petaca were occupied in 1963.

Good access within the quadrangle is provided by paved State Highway 111 which traverses the area from south of La Madera up the Vallecitos valley to Vallecitos. A graded gravel road along the eastern margin of the quadrangle joining South Petaca and La Madera connects graded roads which extend westward into the Cribbenville district southwest of South Petaca and the Globe district in the center of the quadrangle. Unimproved roads form a network of access roads throughout the pegmatite area east of Mesa de la Jarita. The Old Petaca road which climbs the dissected western flank of Mesa de la Jarita east of Vallecitos provides access for conventional automobiles to the summit of the northern part of the mesa. Unimproved dirt roads in Canon de la Madera, Canon del Agua, and near Rancho del Olguin provide the only access to the Ortega Mountains from State Highway 111. These mountains can be reached by automobile over an unimproved dirt road which connects with State Highway 100 joining El Rito and Vallecitos.

PHYSICAL FEATURES

La Madera quadrangle lies on the southeasternmost extension of the San Juan Mountains which separate the Rio Grande graben to the east from the eastern margin of the San Juan Basin to the west. The Precambrian core is flanked on all sides by Tertiary rocks.

The prominent topographic highs in La Madera quadrangle are the Ortega Mountains and Mesa de la Jarita. The Ortega Mountains are underlain by resistant quartzite and form an elongate range bounded on the east by the Rio Vallecitos. Mesa de la Jarita, an elongate ridge extending south-southeastward from the northern quadrangle boundary to about one mile north of La Madera, ranges in elevation from about 8460 feet near Vallecitos to about 7400 feet north of La Madera. The Ortega Mountains and Mesa de la Jarita are separated by the Rio Vallecitos.

The areas north and south of the Ortega Mountains are in sharp contrast. The area north of the mountains consists of steep-sided arroyos cut into surfaces developed on poorly consolidated Tertiary clastics. These surfaces dip gently toward the Rio Vallecitos and were apparently cut by streams graded to the Rio Vallecitos in the past when it flowed at a higher level. Isolated quartzite knobs stand above the broad, gently sloping surfaces and the one-half mile wide alluvial valley in which the Rio Vallecitos now flows. The area south of the Ortega Mountains is a broad surface sloping gently toward the Rio Vallecitos. This surface is deeply incised by ephemeral consequent and insequent streams graded to the main trunk stream. Two remnants of lower level stream terraces occur north and west of La Madera.

The area east of Mesa de la Jarita is a broad rolling upland incised by steep-sided arroyos cut by tributaries of the Rio Tusas. Patches of the high-level erosion surface north and west of La Madera are preserved on the east spur of La Madera Mountain, on the metamorphic complex in sec. 17, T. 25 N., R. 9 E., and along the southeastern margin of Mesa de la Jarita. There is a divide in secs. 19 and 20, T. 26 N., R. 9 E. which separates east-flowing streams to the north and south-flowing streams to the south. The upper part of Canon de los Alamos appears to have been cut by a subsequent stream controlled by the Precambrian—Tertiary contact.

The Rio Vallecitos and Rio Tusas are the only perennial streams in the area. The Rio Vallecitos enters the quadrangle about half a mile north of Vallecitos at an elevation of about 7400 feet, flows southeastward, and leaves the quadrangle one mile south of La Madera at an elevation of 6460 feet. A sharp change in gradient occurs two miles north-northwest of Ancones where the Rio Vallecitos flows through a 300-foot deep canyon cut in quartzite. The Rio Tusas enters the quadrangle north of South Petaca at an elevation of 7220 feet and flows southeast to a point about one and a half miles south of South Petaca where it leaves the quadrangle and flows into the Servilleta valley. It re-enters the quadrangle in sec. 17, T. 25 N., R. 9 E. and flows southwest to the Rio Vallecitos. The junction of these two streams east of La Madera is the beginning of the Rio Ojo Caliente. Drainage along the eastern margin of the quadrangle is through Canon de la Paloma and Canon de los Alamos, both of which join the Rio Tusas just north of La Madera Mountain. In many places along their meandering courses, the Rio Vallecitos, Rio Tusas, and their tributary intermittent streams have cut steep-sided canyons in metamorphic rock and soft Tertiary elastics in a random manner. This relation indicates that the principal drainage network has been superposed in this area.

The principal types of vegetation are trees and shrubs. Tree types are controlled largely by elevation. Ponderosa pine is generally restricted to areas above 7000 feet with pinon pine replacing it at lower elevations; juniper is present throughout the area. Sage is present in alluvial valleys at all elevations, but scrub oak is restricted to areas occupied by ponderosa pine.

METHODS OF STUDY

The Precambrian rocks of La Madera quadrangle were mapped at a scale of 1:24,000 using the United States Geological Survey 71/2 minute topographic map of La Madera quadrangle. Additional data were provided by aerial photographs supplied by the State Bureau of Mines and Mineral Resources, Socorro, New Mexico.

A total of six months was spent in the field during the summers of 1961, 1962, and 1963. The attitude and style of small-scale structural

features were recorded at more than 1000 outcrop stations. Two hundred and sixteen thinsections were studied. The identification of kaolinite, pyrophyllite, chloritoid, and numerous other mineral phases was verified by X-ray diffraction.

ACKNOWLEDGMENTS

The writer expresses his appreciation to Dr. W. R. Muehlberger for introducing him to the area, for the many profitable discussions regarding structural interpretations, and for invaluable aid in preparing the manuscript. Sincere appreciation goes to Drs. S. E. Clabaugh and E. F. McBride for critical suggestions and helpful comments during the preparation of the manuscript. Thanks are also due Mr. Max E. Willard of the State Bureau of Mines and Mineral Resources for many profitable discussions of the problems encountered in this study and for critical review of the manuscript. Other members of the Bureau staff gave freely of their time and made many helpful suggestions.

Special thanks go to Mr. A. J. Thompson, Director of the State Bureau of Mines and Mineral Resources, for providing encouragement and financial aid to defray the cost of field work and the preparation of thinsections. I also express my appreciation to the Department of Geology of The University of Texas for defraying much of the cost of thin-section preparation.

Quaternary Geology

Stream drainage that developed after the deposition of arkosic sandstone consists of the major through-flowing streams, the Rio Vallecitos and the Rio Tusas with their tributaries. The two major streams are superposed within the map area. The Rio Vallecitos, however, flows entirely within the Vallecitos fault zone, whereas the Rio Tusas crosses a northeast-trending zone of faults north of La Madera Mountain. The tributaries of the two major streams are consequent, having developed in response to local gradients established on gently sloping Tertiary sedimentary rocks.

EROSION SURFACES

Five erosion surfaces are recognized in La Madera quadrangle, based upon the criterion of elevation. Mesa de la Jarita is the highest and presumably the oldest erosion surface. Within the mapped area, it ranges in elevation from 8300 to 8400 feet. Gravel composed principally of Precambrian quartzite with only a small percentage of volcanic rock fragments caps the surface and in places has slumped down over the mesa edge to form a colluvial cover. This surface is cut entirely on Precambrian rocks.

A small remnant of an erosion surface graded to the Rio Vallecitos is exposed in secs. 16 and 21, T. 26 N., R. 8 E. This surface is covered with a thin mantle of gravel composed almost entirely of Precambrian rock types. No direct evidence exists to link this erosion surface with the widely developed 7000-foot surface along the southern part of the Rio Vallecitos, but the possibility that they developed at about the same time is very likely.

The best-developed and most widespread surface is located south of the Ortega Mountains and west of the Rio Vallecitos. It ranges in elevation from about 6900 to 7400 feet at the base of the Ortega Mountains. Gravel covers the entire surface west of the Rio Vallecitos. These deposits range in composition from primarily volcanic rock fragments near the main stream to entirely quartzite fragments at the base of the mountains. This surface is now deeply incised and dissected by branch streams of the Rio Vallecitos. Scattered remnants of this surface occur east of La Madera, but here the gravel cover is very thin.

Two low-level stream terraces cut on a variety of rock types are present at 6800 and 6600 feet north and west of La Madera. Gravel of mixed volcanic and metamorphic rock types covers these surfaces. Isolated remnants of these surfaces are also cut on Precambrian and Tertiary rocks along the Rio Tusas north of La Madera Mountain.

RECENT DEPOSITS

Recent stream alluvium consisting of gravel and silt occupies parts of all the major stream valleys. Isolated patches of alluvial silt occur at higher elevations in the north-central part of the quadrangle.

Colluvial deposits of talus and slope wash mantle much of the Ortega Mountains and the west face of Mesa de la Jarita.

A 20- to 30-foot thick deposit of calcareous tufa is exposed at Statue Spring. Similar material is being precipitated from the spring water at present.

Tertiary Geology

A thin sequence of sedimentary and igneous rocks of Tertiary age underlies about 50 to 60 per cent of La Madera quadrangle. Nearly one half of the Tertiary section is composed of volcanic conglomerate. Poorly consolidated conglomerate of Precambrian rock fragments of local derivation intertongues with part of the volcanic conglomerate and makes up about one third of the Tertiary rocks. Arkosic sandstone which intertongues with the upper part of the volcanic conglomerate comprises the remainder of the sedimentary sequence. Basalt, andesite to latite pyroclastic, and rhyolite porphyry are present but do not constitute a large part of the Tertiary sequence. The stratigraphic relationships of the Tertiary section are shown in Figure 2.

The average thickness of the Tertiary cover in the map area is about 300 feet. A composite section made up of segments from several different areas in the quadrangle suggests a maximum thickness of about 1000 feet. These thickness estimates of the entire Tertiary section may be considerably in error, however, because of unrecognized faults and the complex intertonguing of the major clastic units.

Ten lithologic units were utilized in mapping the Tertiary sequence. These are informal units that represent distinct lithologic types and were selected as a convenience in mapping rather than as an attempt to further subdivide the stratigraphic nomenclature used by others in this region (*see* Just; Butler, 1946; Barker; Smith, 1938). Some of the map units utilized in this quadrangle represent or are correlative to parts of or all the established formal stratigraphic units. Where this situation occurs, it is noted in the description of the rock unit.

PETROLOGY

SEDIMENTARY ROCKS

The sedimentary sequence is subdivided on a descriptive basis into four major units: conglomerate, quartzite conglomerate, volcanic conglomerate, and arkosic sandstone. This breakdown involves some genetic implications, for material size which separates conglomerate and sandstone and composition which separates various conglomerates are principally a function of distinctly different source areas contributing detritus to the map area during Tertiary time.

Conglomerate

Conglomerate composed entirely of metamorphic rock fragments in a matrix of quartz sand is exposed in SW1ANW1ANW1/4 sec. 17, T. 25 N., R. 9 E. and about three quarters of a mile west of South Petaca along the boundary between secs. 7 and 18, T. 26 N., R. 9 E. In the former locality, the conglomerate appears to be only 10 to 20 feet thick,

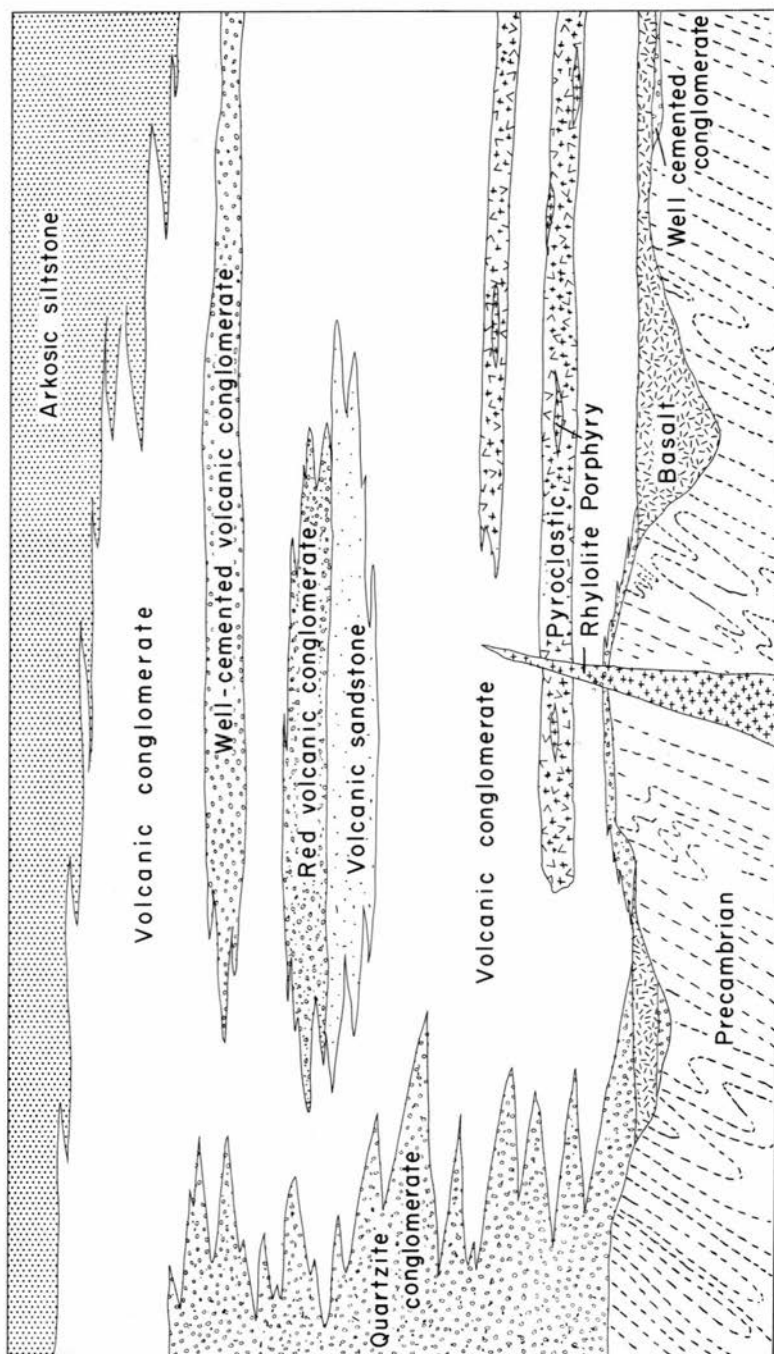


Figure 2

IDEALIZED REPRESENTATION OF TERTIARY STRATIGRAPHIC RELATIONSHIPS

to rest on the Precambrian, and to underlie basalt. These relationships are obscured in this area, however, by considerable slope wash derived from adjacent metamorphic rocks.

In Canada de los Tangues west of South Petaca, a maximum thickness of 175 feet of conglomerate is exposed in the arroyo floor. The unit ranges in color from red to yellowish brown and is well cemented. The clasts in the conglomerate consist of quartz muscovite schist, feldspathic schist, micaceous quartzite, and white quartz. They range in size from small pebbles up to boulders several feet in diameter. The matrix consists of quartz sand and sand-sized metamorphic rock fragments. Except for an ephemeral shingling of large, flaggy schist boulders, bedding is nonexistent. The conglomerate unconformably overlies metamorphic rocks and underlies amygdaloidal basalt.

The local origin of this unit is suggested by the composition of the clasts which is similar in all respects to surrounding metamorphic rocks. Butler (his geologic map) designated this conglomerate as part of the Biscara Member of the Los Pinos Formation; however, it lacks the volcanic rock clasts which presumably characterize this unit (Barker, p. 44). It is equally likely that this conglomerate may be equivalent in time to part of the El Rito Formation or may represent a more heterogeneous and locally well-cemented phase of the quartzite conglomerate.

Quartzite Conglomerate

Quartzite conglomerate refers to gray to brownish gray, loosely consolidated conglomerate of metamorphic quartzite fragments in a matrix of quartz sand. Clasts range in size from about one inch to one foot in diameter with the modal size in the four- to six-inch range. Individual fragments are angular to subangular. The monolithologic nature of the fragments and their angularity distinguish this unit from other Tertiary conglomerates in the area.

This sedimentary unit mantles the large quartzite masses which form the Ortega Mountains and La Madera Mountain. A minimum thickness of about 200 feet is present in the extensive exposures of conglomerate that form the northern fringe of the Ortega Mountains. Identical material at least 100 feet thick rims the northeastern margin of La Madera Mountain where it is prominently interbedded with volcanic conglomerate.

Elongate, irregular exposures of quartzite conglomerate occur along the southeastern margin of Mesa de la Jarita. At the southern margin of the mesa where quartzite is the bedrock, the conglomerate is identical to that described above. In the extreme southwest corner of sec. 31, T. 26 N., R. 9 E., the contact relations between underlying Precambrian and overlying volcanic conglomerate are excellently exposed. Here the cobbles in the quartzite conglomerate consist of muscovitic quartzite, feldspathic schist, amphibolite and quartzite in a zone 10 to 20 feet

thick at the base of the conglomerate unit. The composition of the clasts is the same as the bedrock lithology in this area. The heterogeneous basal zone is transitional vertically into typical quartzite conglomerate. The quartzite conglomerate is about 100 feet thick and intertongues at the top with volcanic conglomerate.

At the east-central part of sec. 18, loosely cemented conglomerate of angular metamorphic rock fragments in an argillaceous matrix was mapped as quartzite conglomerate. In this area, the conglomerate is brown to grayish brown, rests on basalt and muscovitic quartzite, and grades upward into the tuffaceous quartz sandstone of the lentil in the volcanic conglomerate.

The intertonguing of quartzite conglomerate and volcanic conglomerate demonstrates the partial time equivalence of these two units. The quartzite conglomerate is similar in appearance to conglomerate that Barker (p. 42) named Ritito Conglomerate. If the quartzite conglomerate of La Madera quadrangle and the Ritito Conglomerate of Las Tablas quadrangle are the same, Barker's statement that "It [Ritito Conglomerate] is older than the period of widespread volcanism" is not justified.

Volcanic Conglomerate

Volcanic conglomerate herein refers to the generally poorly consolidated conglomerate exposed over about 50 per cent of the map area east of the Rio Vallecitos and consists of gray, green, pink, and purple andesite porphyry, minor latite porphyry, and gray aphanitic rhyolite in a sandy tuffaceous matrix. It includes a well-cemented horizon about 20 feet thick in the eastern and southeastern part of the quadrangle, a well-cemented cobble to boulder conglomerate in the northeastern part of the quadrangle, and a small lentil consisting of two distinct lithologic types exposed principally in sec. 8, T. 25 N., R. 9 E. Within the map area, volcanic conglomerate rests on Precambrian rocks and basalt and is intertongued at the base with quartzite conglomerate. This unit grades upward into arkosic sandstone, and the intertonguing is best shown in secs. 7 and 18, T. 26 N., R. 9 E. Pyroclastic and rhyolite porphyry occur at the base and within the volcanic conglomerate.

The great bulk of volcanic conglomerate consists of subrounded to rounded fragments of volcanic and metamorphic rock types that range from sand to boulder size. Bedding is prominent and marked by alternating layers of coarse sandstone and cobble to boulder conglomerate. There is a gradual change in the unit from north to south in the map area marked by a general decrease in the thickness and number of boulder beds. This transition is most noticeable from the general area of the township line in the east-central part of the map area south to La Madera Mountain. The color of the conglomerate is primarily gray, but locally, where the percentage of tuff in the matrix is high, it is more

nearly grayish white. Metamorphic rock fragments generally make up from 5 to 30 per cent of the conglomerate, with the highest percentages being in areas where the volcanic conglomerate rests upon Precambrian rocks. Similarly, basalt cobbles constitute from 10 to 20 per cent of the fragments where the conglomerate rests upon basalt.

A lentil of conglomerate and quartz sandstone, 250 to 300 feet thick, occurs at the base of the volcanic conglomerate and has an outcrop area of about a quarter of a square mile along Canon de la Paloma in the E1/2 sec. 8, T. 25 N., R. 9 E. The lentil consists of an upper volcanic conglomerate unit that is distinguished from the usual type of volcanic conglomerate by its red color and the presence of from about 10 to 30 per cent red andesite to latite porphyry clasts. The conglomerate unit is about 150 feet thick and contains a basal zone of coarse volcanic sandstone 10 to 20 feet thick which grades upward into cobble conglomerate. The lower unit in the lentil is a tuffaceous quartz sandstone that is gradational upward into the distinctive red conglomerate and coarse sandstone mentioned above, gradational downward into quartzite conglomerate, and gradational laterally into typical gray volcanic conglomerate. This basal unit is characterized by its variegated gray and pink color, the presence of numerous quartz bipyramids, and numerous local erosion surfaces marked by color change, thin conglomeratic layers, and truncated layers.

A well-cemented horizon in the gray volcanic conglomerate with a maximum thickness of about 100 feet is a prominent cliff-forming horizon in the southeastern part of the quadrangle. This layer is similar in all respects to the more widespread, loosely cemented volcanic conglomerate, except for the presence of secondary silica that forms the cementing agent.

A well-cemented, cross-bedded basal conglomerate is exposed locally around South Petaca. This conglomerate is about 20 feet thick and composed of well-rounded cobbles of volcanic and metamorphic rock types. It is well exposed in cliffs around the abandoned mica mill about one mile south of South Petaca. Exposures of this local conglomerate are restricted to secs. 17 and 20, T. 26 N., R. 9 E.

Rock mapped as volcanic conglomerate in La Madera quadrangle was designated the Cordito Member of the Los Pinos Formation by Butler. Similar conglomerate was mapped as Abiquiu tuff by Jahns, Muehlberger, and Smith (unpublished map) in the Ojo Caliente quadrangle. Volcanic conglomerate mapped in La Madera quadrangle differs from the Cordito Member of the Los Pinos Formation in secs. 11 and 14, T. 26 N., R. 8 E., where conglomerate that underlies basalt was mapped as volcanic conglomerate. Using the redefined Los Pinos Formation in Butler's system of nomenclature, the conglomerate overlain by basalt would be grouped into either the Biscara or Esquibel members.

Arkosic Sandstone

Uniformly fine-grained, pinkish brown to yellowish brown arkosic sandstone underlies about one fourth of La Madera quadrangle. The bulk of this unit is exposed in the triangular area bounded on the east by the Rio Vallecitos, on the north by the Ortega Mountains, and on the south by the quadrangle boundary. An elongate exposure of arkosic sandstone occupies the valley of the Rio Vallecitos in the central part of the quadrangle and is the bedrock in the eastern part of the valley east and southeast of Vallecitos. Small exposures are scattered along the eastern boundary of the quadrangle east of South Petaca, along the Old Petaca road, and north of La Madera Mountain along the lower reaches of the Rio Tusas.

The map unit consists of an upper and a lower part. The lower part is composed of generally well-cemented brown to yellowish brown arkosic sandstone beds interlayered with distinctive purplish gray to gray beds of volcanic conglomerate. This section of the arkosic sandstone is best exposed around La Madera Mountain and in the two exposures along the Old Petaca road. The upper part of the arkosic sandstone is poorly consolidated, contains prominent festoon cross-beds and rare grayish white tuff beds, and is the most commonly exposed variant of this unit. The thin strip of arkosic sandstone that occupies the Rio Vallecitos valley in the central part of the quadrangle contains numerous yellowish to greenish zones of claystone and clayey siltstone that appear to be within and near the base of the upper unit.

The arkosic sandstone in La Madera quadrangle is part of the widespread Santa Fe Formation. This formation ranges in age from Miocene to Pliocene and is the youngest Tertiary unit exposed in the mapped area. The intertonguing of arkosic sandstone (Santa Fe Formation) and volcanic conglomerate (Cordito Member of Los Pinos Formation) demonstrates the partial time equivalence of these two units.

IGNEOUS ROCKS

Volcanic rocks constitute only a small part of the Tertiary section exposed in La Madera quadrangle. They range in composition from basalt to rhyolite, are complexly intertongued with volcanic sediments, and locally exhibit a wide range in color, composition, degree of alteration, and mode of occurrence.

Basalt

Basalt crops out in small isolated areas along the eastern and northern margins of the quadrangle. The largest areas are at the confluence of Canon de los Alamos and the Rio Tusas and in a narrow, north-trending strip about half a mile west of South Petaca.

The map unit is readily divisible into two parts: a lower sequence

of three flow units of amygdaloidal, highly altered, red to purplish green basalt and an uppermost flow unit of unaltered, brown, vesicular basalt with locally prominent flow folding. The lower sequence of three units is exposed only in the two larger areas just mentioned, but the uppermost vesicular basalt is exposed in all areas where basalt is indicated on the geologic map.

Basalt rests upon Precambrian rocks and conglomerate and is overlain by volcanic conglomerate except in secs. 11 and 14, T. 26 N., R. 8 E., where the vesicular basalt unit is intertongued with volcanic conglomerate. The maximum exposed thickness of basalt is 160 feet; the average thickness of the vesicular basalt exposed in the north-central part of the quadrangle is about 30 feet.

Butler (p. 65) gave the name *Jarita Basalt* to the vesicular basalt unit exposed along the northwest flank of Mesa de la Jarita east of Vallecitos. He designated it a member of the Los Pinos Formation.

Pyroclastic Unit

Reddish purple pyroclastic rock, primarily of andesitic composition but ranging from andesite through latite to rhyolite, occurs at the base and within the volcanic conglomerate. It is exposed as isolated masses along the northeastern quadrangle boundary. Numerous lenses and dikes of gray to white rhyolite porphyry are characteristically associated with the pyroclastic unit. The intercalation of pyroclastic rock with volcanic conglomerate is best illustrated south of South Petaca, west of the Rio Tusas, and along the Old Petaca road.

In most exposures, the pyroclastic unit is composed of angular fragments of red to purplish pink andesite porphyry set in a matrix of similar composition. The distinctive brecciated texture of the unit is emphasized by surface weathering. The size of the fragments ranges from about six inches to less than one inch, with an average diameter of one to two inches. In a few exposures, the color of the unit ranges from grayish brown to brown, and the rock is nearly devoid of phenocrysts. Thinsections of this unit reveal a wide range in the quartz content and plagioclase/potassium feldspar ratio of the phenocrysts, suggesting a variation of the composition of the rock unit as a whole within the map area.

Lenses of sanidine-bearing, white to grayish white rhyolite porphyry are present in all the masses of the pyroclastic unit. These lenses are generally 5 to 10 feet thick, with an average length of about 30 feet. Along the northern boundary of sec. 20, T. 26 N., R. 9 E., a small dike and a pluglike mass intrude the pyroclastic unit. Xenoliths of reddish purple pyroclastic rock occur within the rhyolite porphyry intrusive bodies. In this same area, a small amount of perlitic vitrophyre agglomerate is exposed at the base. It consists of grayish black clasts of perlitic vitrophyre two to three inches in diameter enclosed in a tuff matrix.

Barker (p. 49) noted the presence of rhyolite flow rock and tuff within the Cordito Member of the Los Pinos Formation. This reference apparently includes the pyroclastic unit mapped in La Madera quadrangle. The relations shown in the northeastern part of La Madera quadrangle and the apparent range in composition suggest a more complex history for this unit than has generally been appreciated.

FAULTS

The bedrock of La Madera quadrangle is cut by many high-angle faults with normal separation. All faults in the area truncate arkosic sandstone (Miocene—Pliocene) or older rock units. No unequivocal faults of pre-Tertiary age were observed.

With orientation serving as the basis for classification, faults can be separated into three groups: a northeast-trending set, a northwest-trending set, and an east-trending set. Most of the northeast-trending set are exposed in the southeast corner of the quadrangle and there form a zone of faults that have isolated the mass of Precambrian quartzite in La Madera Mountain and have produced a structural depression along the southern part of Canon de los Alamos. The northwest-trending set is represented principally by faults along the Vallecitos valley which have a down-to-the-west separation. This major zone of faults is designated the *Vallecitos fault zone*. A few northwest-trending faults are inferred along the eastern quadrangle boundary and in the Ortega Mountains. East-trending faults are common in nearly all parts of the quadrangle. Within the Vallecitos fault zone, they appear to link the major set of northwest-trending faults. The absence of major offsets of northwest- and northeast-trending faults suggest that all three sets formed at about the same time rather than during separate periods of dislocation.

Where the faults of the Vallecitos fault zone are exposed, the country rock on both sides of the fault is characteristically brecciated and crushed. At the fault contact between arkosic sandstone and quartzite in sec. 11, T. 25 N., R. 8 E., the quartzite has been reduced to a mylonite by intense crushing associated with movement along the fault. The crushing that distinguishes the faults of the Vallecitos fault zone may indicate a long history of movement and is the only evidence for pre-Tertiary faulting in the area.

Precambrian Geology

PETROLOGY

Rocks of Precambrian age in La Madera quadrangle occupy slightly less than one half of the map area. The largest continuous exposure is in the Ortega Mountains. Other exposures occur in a two-mile-wide belt underlying Mesa de la Jarita extending from Vallecitos to within one and a half miles of La Madera, in and around La Madera Mountain, and in a roughly circular area one mile west of South Petaca (pl. 1). Principal rock types are quartzite, muscovitic quartzite, feldspathic schist, granitic gneiss, and hornblende-chlorite schist. The modal composition of selected samples from these units is given in Figure 3.

Figure 3. MODAL COMPOSITION (IN PER CENT) OF METAMORPHIC ROCK UNITS

| Mineral | Unit numbers* | | | | | | | | | | | | | | |
|--------------|---------------|----|----|----|----|----|----|----|----|----|----|----|----|----|----|
| | 1 | 2 | 3 | 4 | 5 | 6 | 7 | 8 | 9 | 10 | 11 | 12 | 13 | 14 | 15 |
| quartz | 94 | 59 | 83 | 21 | 81 | 76 | 74 | 58 | 43 | 52 | 80 | 61 | 24 | 8 | 28 |
| microcline | | | | | | | | | 25 | 7 | | | | | |
| plagioclase | | | | | | | Tr | | 23 | 22 | 16 | 24 | 16 | 28 | |
| muscovite | Tr | 4 | 2 | 2 | 18 | 23 | 26 | 42 | 1 | 19 | Tr | 9 | Tr | | |
| biotite | | | | | | | | | 8 | | 3 | 4 | | 29 | |
| chlorite | | | | | Tr | | | | | | Tr | Tr | 24 | | |
| epidote | | Tr | | | Tr | 1 | Tr | | | | 2 | Tr | 4 | | |
| specularite | 1 | 10 | 4 | 35 | Tr | 1 | Tr | Tr | Tr | Tr | Tr | 2 | 2 | Tr | Tr |
| rutile | Tr | Tr | Tr | 5 | | | | | | | | | | | |
| sphene | | | | | | Tr | | | | | | | | 2 | Tr |
| pyrophyllite | | | | | | | | | | | | | | 29 | |
| garnet | | Tr | | | Tr | | Tr | Tr | Tr | | | | | | |
| apatite | | | | | | | | | | | | | Tr | Tr | |
| zircon | Tr | Tr | Tr | | | | | Tr | | | | | | | |
| kyanite | 4 | 27 | Tr | 36 | | | | | | | | | | | 43 |
| sillimanite | | | 12 | 1 | | | | | | | | | | | |
| hornblende | | | | | | | | | | | 31 | 46 | | | |
| kaolinite | | | Tr | | | | | | | | | | | | |

- *1. kyanite quartzite, SE $\frac{1}{4}$ SW $\frac{1}{4}$ SE $\frac{1}{4}$ sec. 2, T. 25 N., R. 8 E.
 2. kyanite quartzite, SE $\frac{1}{4}$ SW $\frac{1}{4}$ NE $\frac{1}{4}$ sec. 21, T. 26 N., R. 8 E.
 3. sillimanite quartzite, S $\frac{1}{2}$ NE $\frac{1}{4}$ SW $\frac{1}{4}$ sec. 20, T. 25 N., R. 9 E.
 4. kyanite-specularite-quartzite, center SW $\frac{1}{4}$ SW $\frac{1}{4}$ sec. 19, T. 25 N., R. 9 E.
 5. muscovitic quartzite, SE $\frac{1}{4}$ NE $\frac{1}{4}$ NW $\frac{1}{4}$ sec. 35, T. 25 N., R. 9 E.
 6. muscovitic quartzite, NW $\frac{1}{4}$ SE $\frac{1}{4}$ SE $\frac{1}{4}$ sec. 2, T. 25 N., R. 8 E.
 7. muscovitic quartzite, NE $\frac{1}{4}$ SW $\frac{1}{4}$ NE $\frac{1}{4}$ sec. 30, T. 26 N., R. 9 E.
 8. muscovitic quartzite, SE $\frac{1}{4}$ SE $\frac{1}{4}$ NE $\frac{1}{4}$ sec. 26, T. 26 N., R. 8 E.
 9. granitic gneiss, SE $\frac{1}{4}$ NE $\frac{1}{4}$ NW $\frac{1}{4}$ sec. 19, T. 26 N., R. 9 E.
 10. granitic gneiss, SW $\frac{1}{4}$ NE $\frac{1}{4}$ SE $\frac{1}{4}$ sec. 12, T. 26 N., R. 8 E.
 11. quartz-albite-muscovite-biotite schist, SW $\frac{1}{4}$ SW $\frac{1}{4}$ SW $\frac{1}{4}$ sec. 24, T. 26 N., R. 8 E.
 12. quartz-albite-muscovite-biotite schist, center NE $\frac{1}{4}$ sec. 24, T. 26 N., R. 8 E.
 13. hornblende-chlorite-schist, NE $\frac{1}{4}$ SW $\frac{1}{4}$ NE $\frac{1}{4}$ sec. 23, T. 26 N., R. 8 E.
 14. biotite amphibolite, NE $\frac{1}{4}$ NE $\frac{1}{4}$ SW $\frac{1}{4}$ sec. 32, T. 26 N., R. 9 E.
 15. quartz-kyanite-pyrophyllite hornfels, SE $\frac{1}{4}$ SW $\frac{1}{4}$ SW $\frac{1}{4}$ sec. 25, T. 26 N., R. 8 E.

The most conspicuous general features of the Precambrian rocks are (1) the high silica content indicated by the great bulk of quartzite and muscovitic quartzite and the presence of quartz in all rocks examined and (2) the absence of unfoliated granites. Granitic pegmatites are the only unmetamorphosed rocks of Precambrian age.

The separation of metamorphic rock units is based on differences in their composition and texture. This is a purely descriptive approach; hence, the Precambrian map units, for the most part, reflect metamorphic petrogenesis and do not necessarily reflect original composition.

Montgomery (1953, p. 8), in the Picuris Range, and Barker (p. 10), in Las Tablas quadrangle, have interpreted composition and textural layering to be largely coincident with a premetamorphism stratification. They have erected an order of superposition and created a stratigraphic nomenclature based upon the position of presumed meta-sedimentary units in a single system of folds.

In La Madera quadrangle, however, Precambrian rocks have been deformed three times by periods of regional folding. This history of dislocation has resulted in systems of folds which trend south-southwest, northwest, and west (oldest to youngest). Prominent axial-plane cleavage and lineation parallel to fold axes are associated with the first deformation fold system. Fracture cleavage and slip cleavage are common structural parameters of the second and third deformation folds. This structural rearrangement has complicated, if not completely obscured, original stratigraphic relationships and led the writer to interpret much of the compositional layering as tectonic intercalation rather than simple stratigraphic succession. The descriptive approach utilized in mapping the Precambrian, however, is intended to be free of inferences derived from any structural interpretation.

The metamorphic petrology discussed below is separated into two sections. The first section is intended to be purely descriptive and consists of a detailed description of each map unit. The units are discussed in the order of their abundance; that is, quartzite, the most extensively exposed metamorphic rock type is discussed first, and chlorite schist, which constitutes less than one per cent of the exposed Precambrian, is discussed last. Some map units such as quartzite and feldspathic schist include several rock types which are mappable on the scale of 1:24,000, but which are closely allied compositionally or texturally. The second section includes the interpretative and speculative facets of the petrology in which problems of metamorphic process relevant to observed features are reviewed. The application or, more accurately, the inability to rigorously apply the regional facies concept to some of the metamorphic assemblages found in the map area is considered in an attempt to unravel the history of these rocks.

QUARTZITE

Remarkably pure quartzite comprises about one third of the exposed Precambrian in La Madera quadrangle. In general, it is a compact, hard, coarse-grained, gray, vitreous quartzite composed of more than 95 per cent quartz. In nearly all outcrops it contains prominent grayish black to blue-black layers composed principally of specular hematite. These layers are commonly arcuate and believed by some to represent relict cross-bedding. Just (p. 11) named this unit the *Ortega quartzite* and designated the Ortega Mountains as the type area. The name has been applied to quartzite of similar appearance north and west of the Ortega Mountains by Barker and by Muehlberger (1960a, p. 45) and in the Picuris Range by Montgomery. Continuous exposures do not link the extreme limits of quartzite exposure in central northern New Mexico; hence, correlation rests solely upon lithologic similarity. In La Madera quadrangle the quartzite contains various amounts of kyanite, sillimanite, rutile, and sphene, in addition to the specular hematite already mentioned. Discontinuous schistose layers, containing an unusually high proportion of alumino-silicate minerals, and three isolated masses of quartz-kyanite schist occur within the otherwise monotonously uniform quartzite masses.

The areal distribution of quartzite is shown in detail on Plate 1. The largest single mass forms the Ortega Mountains west of the Rio Vallecitos. Another great bulk of quartzite underlies La Madera Mountain, of which only the northern end is within the map area. Large areas of quartzite also occur at the south end of Mesa de la Jarita just south of Ancones and in a string of isolated knobs in the northern part of the Vallecitos valley extending from Rancho del Olguin northward to west of Vallecitos. An outlier of quartzite is exposed in sec. 29, T. 26 N., R. 8 E., where erosion has stripped off some of the Tertiary conglomerate that elsewhere mantles most of the quartzite masses. A small, elongate exposure of quartzite occurs in sec. 17, T. 26 N., R. 8 E., where Tertiary faulting and subsequent erosion have brought it to the surface. Two small exposures of gray quartzite without hematite layering and associated with granitic gneiss are exposed in sec. 32, T. 26 N., R. 9 E. and in sec. 19, T. 26 N., R. 9 E. Augen of hematite-layered quartzite ranging in average diameter from one to three feet are intercalated with mica schist in the south-central part of sec. 30, T. 26 N., R. 9 E.

The quartzite has an exposed width of about four and one-half miles in the Ortega Mountains measured along a northeast line perpendicular to the generally northwest trend of the foliation and hematite layering. If the foliation, which has an average dip of 30° SW, is assumed to represent bedding, the quartzite could be construed to represent about 12,000 feet of original quartz sandstone. That this estimate of original thickness has little value is indicated by the facts that the foliation is an axial-plane cleavage and not bedding foliation and that

repetition of layers by folding and very probably by faulting have increased the apparent thickness in the Ortega Mountains. Also the style of folding exhibited by the quartzite in outcrop indicates considerable translation along axial-plane shear surfaces and substantial flowage of material. These factors invalidate estimates of original thickness based on simple trigonometric calculations utilizing strike and dip of foliation and outcrop width. In view of the complex folding which these rocks have undergone, the great mass of quartzite now exposed could conceivably have been derived from an original sandstone layer or layers only a few hundred feet thick.

In most quartzite outcrops the rock is grayish white to blue-gray, is vitreous, and contains many thin black layers composed principally of specular hematite. It is compact, tough, and brittle, with a conchoidal to hackly fracture. A foliation that ranges considerably in prominence as a function of kyanite content is present in nearly all quartzite exposures. Where the foliation is least conspicuous, it is still visible under a hand lens as hairlike subparallel lines on joint and rock cleavage surfaces. Most often the foliation is marked by a tendency for the rock to part parallel to it. Where the quartzite contains from 5 to 10 per cent kyanite laths, the rock is subschistose. Massive, sugary-textured, greenish gray quartzite devoid of hematite layers crops out in thin (5 to 20 feet) bands near the north-facing summit of La Madera Mountain and on the southeast flank of the Ortega Mountains in sec. 9, T. 25 N., R. 8 E. This phase of the quartzite is gradational into the more typical gray, hematite-layered variety.

Layers ranging in thickness from about one inch to about one foot and composed of white quartz aggregates in the form of triaxial ellipsoids are common in the quartzite and are parallel to foliation and hematite layering. They are more numerous and closer-spaced in zones which crop out in the isolated quartzite knob in NE1/4 sec. 9, T. 25 N., R. 9 E., in the gorge of the Rio Vallecitos in NEN sec. 11, T. 25 N., R. 8 E., and in the quartzite exposure west of Vallecitos in the extreme northwestern corner of the quadrangle. Both the individual layers and the zones are discontinuous along their strike with rapid changes in the number of quartz aggregates. Geologists who have observed similar layers in the Ortega quartzite elsewhere in central northern New Mexico have interpreted them as relict pebble beds. This writer could find no conclusive evidence to support or refute this interpretation.

Where the Vallecitos fault zone is exposed in quartzite in sec. 11, T. 25 N., R. 8 E., the rock has been crushed to an aggregate of breccia and mylonite. This crushed rock is well cemented, white, and seamed with red hematite.

The quartzite associated with granitic gneiss noted above is a massive, even-grained, noticeably granular, gray rock devoid of hematite laminae. The foliation in both exposures is very faint, but recognizable. At the exposure in sec. 19, T. 26 N., R. 9 E., the foliation in the quartz-

ite is parallel to the quartzite-granitic gneiss contact and to the barely discernible schistosity in the granitic gneiss.

Quartzite is in contact with other metamorphic rock types on the southern margin of Mesa de la Jarita east of Ancones, at the southern tip of the wedge-shaped outcrop of Precambrian which separates the Rio Tusas and Canon de los Alamos, and in the small quartzite exposure described in the paragraph above. Near Ancones the contact is between quartzite and muscovitic quartzite; here it is largely concealed by slope wash and talus. The contact along the Rio Tusas is well exposed and illustrates the transitional nature of the boundary between quartzite and muscovitic quartzite. The boundary between these two units consists of a zone about 15 to 20 feet wide. Homogeneous quartzite grades into alternating layers of quartz and muscovite-rich layers, through a medial zone of alternating layers about three to six inches thick of quartzite and muscovitic quartzite, and then into muscovitic quartzite. The contact between quartzite and granitic gneiss south-southwest of South Petaca is sharp, although the quartz content of the granitic gneiss in this area is higher than the average for that rock type.

In thinsection, the typical hematite-layered quartzite consists of a mosaic of equant xenomorphic quartz grains which range in size from about 2 mm to less than 0.1 mm, with an average diameter of about 1 mm. Intergranular fringes and patches of very fine-grained quartz in many samples and pronounced undulatory extinction and Böhm lamellae in nearly all sections studied indicate mild cataclasis after the crystalloblastic quartz fabric had formed. Foliation is marked by the arrangement of parallel trains of stubby kyanite prisms with an average diameter of 0.2 mm. The foliation is parallel to hematite layering which consists of aggregated subhedral grains of specular hematite. Individual hematite grains range in size from 0.2 mm to dustlike flakes less than 0.01 mm in diameter. Xenomorphic red rutile and sphene are invariably associated with the hematite concentrations and commonly occur as patchy aggregates and rare individual grains scattered throughout the opaque layers. In many sections, sphene partly rims hematite grains. Many, but not all, of the hematite concentrations contain or are closely associated with zircon, which always occurs as single grains. Most of the zircon grains are highly rounded, but in some sections euhedral prisms and rounded grains occur together. Fracture cleavage marked by parallel fractures, which cut across the xenomorphic quartz fabric, is a common structural feature. These planes are generally wide-spaced (5 to 10 mm), but individual quartz grains between the cleavage planes contain numerous microfractures parallel to the dominant fracture cleavage planes. In some sections the fracture cleavage plane contains kyanite. The average quartz content is about 95 per cent. Kyanite and hematite make up the bulk of the accessory minerals with trace amounts of rutile, sphene, and zircon.

There is considerable range in the kyanite content of quartzite

which forms the isolated knobs in the upper Vallecitos valley and in the quartzite of La Madera Mountain. One sample from the upper Vallecitos valley contains 27 per cent modal kyanite along with 4 per cent muscovite. Kyanite occurs in this sample as nearly equigranular, subhedral, tabular aggregates, which are parallel to the preferred orientation of interstitial muscovite flakes. Specularite forms plates, with an average length of 0.4 mm, whose long dimension is also parallel to the kyanite-muscovite layering. Unlike the typical quartzite, this sample contains disseminated epidote idiomorphs and two porphyroblasts of pink garnet. A sample of sillimanite-bearing quartzite from La Madera Mountain contains a trace amount of kyanite intergrown with a small amount of muscovite. Both kyanite and muscovite exhibit a high degree of preferred orientation, whereas sillimanite occurs as scattered tufts of acicular needles with a random orientation. The tufts of sillimanite and prisms of kyanite occur side by side in the quartz matrix, but there is no evidence that sillimanite has nucleated on either muscovite or kyanite.

A sample of one of the layers of elongate quartz aggregates (pebble bed?) has a granoblastic-hiatal fabric. Hematite-rutile-zircon concentrations rim domains of xenomorphic quartz with prominent undulatory extinction. The quartz aggregates are elliptical to slightly flattened with the long dimension of the aggregates parallel to a crude layering in the interaggregate segregations that is defined by trace amounts of kyanite and kaolinite with a preferred orientation. Individual quartz grains in the aggregates average 1 to 2 mm in diameter, whereas xenomorphic quartz between the aggregates has an average diameter of less than 0.3 mm.

Quartzite in the large augen or boudins intercalated with mica schist has a xenomorphic-seriate quartz fabric containing very thin, short, muscovite flakes with an average length of 0.1 mm dispersed throughout the section. Grains of specularite are also dispersed except for a planar zone near the margin of the section where they form a typically clotted segregation marking a hematite laminae. Muscovite flakes within the specularite segregation are about twice as large as matrix muscovite. All muscovite in the rock, however, exhibits a high degree of preferred orientation with the flakes nearly parallel to the hematite layers.

In summary, the bulk of the quartzite in the map area is uniform in composition and texture. It has been completely recrystallized to form a xenomorphic aggregate of quartz which in many samples shows indications of later mild cataclasis. The average combined kyanite and specularite content is about 5 per cent with trace amounts of rutile, sphene, and zircon. Subhedral to anhedral kyanite exhibits a high degree of preferred orientation within foliation planes. Major textural and compositional variation is present in the quartzite within the Vallecitos valley fault zone and in La Madera Mountain. Accessory mus-

covite is usually present in rocks from these areas, and invariably exhibits a preferred orientation with (001) nearly parallel to foliation and specularite laminae.

Aluminous Schist

Thin, discontinuous, red-brown schistose layers are enclosed in hematitic quartzite in La Madera Mountain, in the quartzite spur west of Vallecitos in the northwest corner of the quadrangle, and in the quartzite knob in sec. 21, T. 26 N., R. 8 E. These layers range in thickness from approximately six inches to three feet and on La Madera Mountain can be traced several hundred feet along the strike. The contacts between schist and quartzite are sharp and parallel to hematite layering and foliation in the enclosing quartzite. In hand specimen, the schist is prominently layered with folia of medium-grained quartz separated by red-brown seams which range in thickness from 2 to 3 mm. Fine-grained white mica in the red-brown seams imparts a phyllitic appearance to the layers. In a section cut normal to a faint lineation in the red-brown interquartz seams, the quartz layers have the form of flattened ellipsoids; hence, the texture most resembles a pencil gneiss in which quartz aggregates form the pencils.

The texture and mineralogy of this unit are both variable. A sample from the upper Vallecitos valley contains 45 per cent kyanite, all of which is concentrated in seams ranging in thickness from 0.1 to 0.6 mm. Kyanite occurs as nearly equigranular subhedra with a trace of specularite and 5 to 10 per cent muscovite interstitial to the kyanite grains. A sample from the eastern prong of La Madera Mountain in the SW1/4 sec. 20, T. 25 N., R. 9 E. consists of a granoblastic matrix of quartz containing thin layers composed of kyanite and muscovite with a little kaolinite intergrown with the muscovite. The kyanite layering is parallel to the preferred orientation of micas within the layers and to hematite layering marked by subhedral grains. The mineralogic layering is crosscut by fracture cleavage which also transects numerous sillimanite tufts scattered throughout the section. The fracture cleavage bifurcates in places around islands of microbreccia.

A sample from the western spur of La Madera Mountain also consists of islands of xenomorphic quartz rimmed by concentrations of other minerals. Most of the seams are filled with anhedral andalusite which poikiloblastically includes equant kyanite grains, quartz, specularite, and minor muscovite. However, in one part of the sample, the seams consist of mutually intergrown kaolinite and muscovite surrounding kyanite grains (fig. 4a). In another sample from this same locality, the rock consists of xenomorphic quartz containing complexly swirled specularite trails throughout the quartz matrix. Large kyanite idiomorphs in random orientation poikiloblastically include the folded hematite layers.

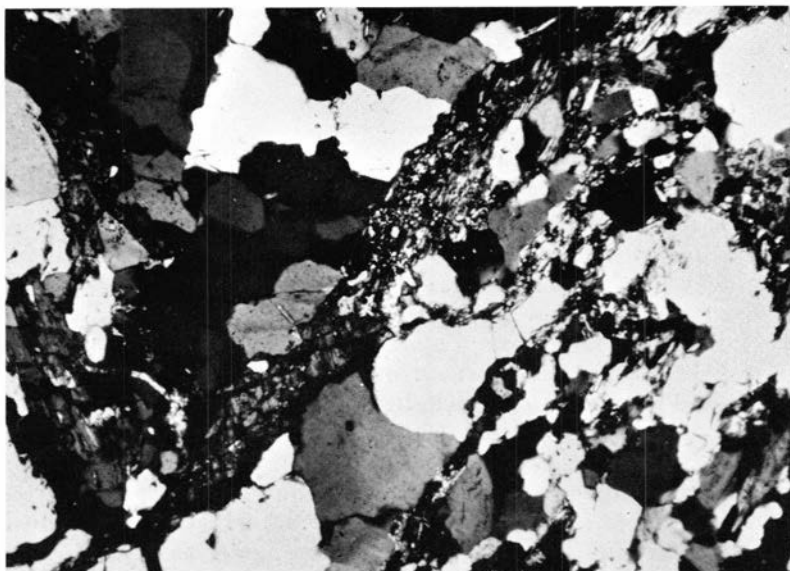


Figure 4a
FRACTURE CLEAVAGE IN ALUMINOUS SCHIST

Specularite Schist

A lens of specularite-kyanite-quartz schist with an exposed thickness of from three to four feet and a length of about forty feet crops out on the northwest flank of the western spur of La Madera Mountain. The outcrop trace of the lens strikes nearly west, parallel to the trend of the foliation in enclosing quartzite. In outcrop, it is grayish green to black, compact, and coarsely crystalline. The essential constituents are kyanite, 36 per cent; specularite, 35 per cent; and quartz, 21 per cent. It contains accessory amounts of rutile, muscovite, and sillimanite. In thinsection, xenomorphic quartz with sharp extinction includes porphyroblastic kyanite idiomorphs and faint planar segregations of hematite. Most hematite occurs as large irregular patches of subhedral to anhedral grains. Numerous small orange anhedral rutile grains are associated with the larger masses of hematite. Individual hematite grains range in size from submicroscopic to 0.7 mm, kyanite has an average prism cross-section diameter of 0.8 mm, and matrix quartz averages 0.35 mm in diameter.

Kyanite—Muscovite Schist

Three tabular bodies of kyanite-muscovite schist were mapped in quartzite in the Ortega Mountains (pl. 1). In outcrop, the rock is

bluish black and distinctly schistose due to a high mica content. Kyanite blades ranging in length from one to two centimeters lie with their long axes in the plane of schistosity, but have no marked preferred orientation within that plane. The unit is characterized by the presence of numerous rods and flattened lenticles of white quartz which lie within the plane of schistosity. The contacts of the schist with enclosing quartzite are sharp and parallel to the foliation in quartzite. The average thickness is about thirty-five feet. The schist is uniform in composition and texture with about 10 per cent idiomorphic kyanite set in a lepidoblastic fabric of fine-grained xenomorphic quartz and from 40 to 50 per cent muscovite which defines the schistosity.

Origin

The great mass of quartzite exposed in the map area represents the metamorphic equivalent of quartz sandstone. Relic bedding is indicated by the presence of gray to black laminae which consist of the suite specularite-kyanite-sphene-rutile-zircon. The isolated grains of rounded zircon constitute the only feature that distinguishes these laminae from megascopically similar laminae that in places represent second-deformation fracture cleavage. The kyanite, which has a high degree of preferred orientation, occurs both in specularite layers and in foliation that transects the specularite layers.

MUSCOVITIC QUARTZITE

Muscovitic quartzite is the second largest metamorphic rock unit in La Madera quadrangle, occupying about 20 per cent of the exposed Precambrian. It is a distinctive lithologic type consisting of alternating thin laminae of quartz and muscovite. The muscovite content ranges from about 10 per cent to more than 60 per cent, with an average of 30 per cent. Hence, it grades from quartzite to quartz-mica schist, but the end members are rare and the unit generally has a uniform composition and texture. The contacts between muscovitic quartzite and other rock units are usually sharp and well marked except where the muscovitic quartzite grades into granitic gneiss about 1.3 miles southwest of South Petaca. Just (p. 43) gave the name *Petaca schist* to this unit from exposures he observed along the southwestern margin of Mesa de la Jarita. He considered it a variety of the Ortega quartzite.

The fact that the schist is restricted to the pegmatite area near the Tusas granite and the abrupt transition along the strike of a considerable thickness into typical Ortega quartzite suggest that the entire schistose phase owes its development to the granite intrusion, the granite having provided the materials and possibly the physical conditions that permitted the formation of a schist.

Muscovitic quartzite crops out in a one- to two-mile wide north-trending belt under the southern margin of Mesa de la Jarita. A thin-

section of this belt extends along the eastern flank of the mesa to within a few hundred feet of the northern boundary of the quadrangle one and a half miles east of Vallecitos. It is also well exposed in the Cribbenville district southwest of South Petaca where it is complexly interlayered with feldspathic schist. Small isolated segments crop out along Canon de la Paloma in the east-central part of the quadrangle. Small remnants of muscovitic quartzite intercalated with feldspathic schist are preserved in some of the faceted spurs along the northern part of the west flank of Mesa de la Jarita. The isolated mass of Precambrian rocks bounded on three sides by normal faults in the southeastern corner of the map area is shown on the map as muscovitic quartzite. Locally, many sections of this mass have lithologic features similar to quartzite, feldspathic schist, and granitic gneiss, but the boundaries of these local varieties are vague and the lithologic character of the mass as a whole is more nearly that of muscovitic quartzite with an unusually small muscovite content.

Most of the muscovitic quartzite mapped appears in outcrop and hand specimen as a grayish white to greenish white prominently layered rock. Laminae, with an average thickness of 0.5 mm, composed of muscovite flakes nearly parallel to the lamination exhibit a greenish silky sheen. The layers which regularly alternate with the micaceous folia are composed principally of quartz with only a few scattered flakes of mica. The quartz in these layers is generally equant and medium-grained, but in a few exposures near the northern end of Mesa de la Jarita, superindividuals of quartz 1 to 3 mm in diameter are common. A prominent textural lineation in the plane of schistosity is present in most exposures of the rock. The unit has a slightly different texture in the area along the southwestern flank and extending across the southern tip of Mesa de la Jarita. There the rock is uniformly finer-grained and the otherwise prominent lamination is vague to absent. The composition and relative proportion of muscovite and quartz are unchanged, but the rock in this area is more nearly a fine-grained aggregate of evenly distributed quartz and muscovite. The degree of preferred orientation of muscovite flakes defining the schistosity is no less than in the bulk of the unit. A very faint hematite layering is also present in this area, whereas the bulk of the muscovitic quartzite contains no compositional layering other than the quartz-muscovite layers already described. A fine-grained, muscovite-rich variety surrounds the elongate body of feldspathic gneiss exposed in secs. 10 and 15, T. 26 N., R. 8 E. In this corona, the muscovite content is in excess of 60 per cent and the rock is better termed a muscovite schist. A conspicuous feature of this unit is the large number of quartz rods and lenticles around which the schistosity pinches and swells. The intermediate axis of these small bodies of quartz ranges in diameter from one to six inches. They are so numerous that the bulk composition of the corona is probably not very different from that typical of muscovitic quartzite.

The microscopic fabric of typical muscovitic quartzite is granoblastic to lepidoblastic with equant xenomorphic quartz grains averaging about 0.3 mm in diameter. Muscovite plates from 0.1 to 0.4 mm in length have a nearly parallel orientation and occur, in part, concentrated into layers, in addition to being distributed throughout the quartz matrix. In several samples, large quartz superindividuals and aggregates of equant grains 2 to 3 mm in diameter form rounded to ellipsoidal masses. Here the schistosity defined by muscovite pinches and swells around the quartz concentrations. Nearly all specimens contain trace amounts of specularite and epidote; two samples contain poikiloblastic, colorless to pale pink garnet, and one section contains a patch of optically continuous pale green chlorite. Most samples exhibit minor cataclastic effects indicated by incipient mortar texture, undulatory extinction, and Boehm lamellae in quartz. In one sample, the plane formed by the preferred orientation of muscovite plates is also marked by fracturing in quartz, although the micas in the fracture plane are not flexed or fractured. Many samples contain a later planar element which ranges from a slip cleavage to a flow cleavage that transects the older schistosity. A sample of the mica schist from the northern end of Mesa de la Jarita is composed of a fine-grained (0.3 mm) aggregate of xenomorphic quartz and idiomorphic muscovite with a high degree of preferred orientation. Mica flakes are very close-spaced and have been folded and torn to form a later slip cleavage. A sample of muscovitic quartzite from the northern part of the west-facing scarp of Mesa de la Jarita exhibits a well-marked schistosity which flows around quartz superindividuals and aggregates. The network of mica-rich layers that surround the quartz aggregates is enclosed by amoeboid poikiloblastic plagioclase porphyroblasts. These grains are untwinned but have an index of refraction slightly less than balsam; hence, they are probably calcium-albite. Two other samples from this same area contain trace amounts of biotite and chloritoid. One sample contains biotite flakes identical in size and orientation with the muscovite that delineates the schistosity. The other sample contains flakes of chloritoid 2 to 3 mm long which are transverse to the schistosity.

Origin

The ideas set forth for the presence of large amounts of muscovite in quartzite by other writers have already been mentioned. Two alternatives seem equally likely: (1) The muscovite is a reconstituted form of potassium aluminosilicate already present in quartzose sediment, possibly as illite, potassium feldspar, or both; or (2) potassium was introduced during a regional metasomatic event prior to the first deformation. The gradational nature of the boundary between granitic gneiss and muscovitic quartzite already discussed suggests that emanations from the granite could have affected quartzite intercalated with

feldspathic schist. However, in some areas the granitic gneiss is in sharp contact with quartzite free of muscovite and feldspar, a relationship not particularly in harmony with widespread metasomatism. Also, hornblende-chlorite schist enclosed within muscovitic quartzite contains no potassium-bearing phase, and it would seem unlikely that potassium could be freely introduced into quartzite, yet not into the parent of the hornblende-chlorite schist. These drawbacks to the thesis of regional introduction of potassium prompt this writer to favor a sedimentary source for the muscovite in the muscovitic quartzite.

TECTONIC BRECCIA PHASE

A lithologic unit compositionally transitional between hematitic quartzite and muscovitic quartzite, which owes its present appearance to tectonic processes, is distinguished as a separate map unit on Plate 1. It is here designated the tectonic breccia phase of muscovitic quartzite, and its tectonic origin is discussed in the section on Precambrian structural geology.

The tectonic breccia crops out along the eastern summit of Mesa de la Jarita in a narrow northwest-trending belt with an outcrop width of about one tenth of a mile. Along this belt it lies between muscovitic quartzite and feldspathic schist and pinches out abruptly at both ends. Midway along the outcrop trend, this unit includes a thin wedge of feldspathic schist. A thin layer of tectonic breccia, too small to appear on the map, occurs within muscovitic quartzite near the Pineapple Group mine in sec. 30, T. 26 N., R. 9 E.

The tectonic breccia is similar in appearance to stretched pebble conglomerate. The weathered surface is studded with numerous flattened dish- to rod-shaped fragments of very fine-grained, gray hematitic quartzite and spherical to ellipsoidal fragments of white quartz. The ratio of quartzite fragments to white quartz aggregates ranges from about 1:1 to 2:1, but together these fragments seldom exceed about 10 per cent of the entire rock. The fragments of hematitic quartzite are aligned with their short and intermediate axes in the plane of schistosity of the enclosing muscovite quartzite; their long axes form a lineation which bears and plunges south-southwest. The intermediate axis of these fragments ranges in size from about one inch to eight inches. The associated quartz fragments range from about one-fourth inch to two inches in diameter. A conspicuous feature of this unit is the dissemination of the two types of fragments throughout the matrix of muscovitic quartzite. In none of the outcrops examined are the fragments closely packed. With decreasing content of the "clasts," the spacing between them increases proportionally.

Near the boundary between tectonic breccia and melanocratic feldspathic schist in NW1A sec. 15, T. 26 N., R. 8 E., the breccia consists of numerous angular fragments of white quartz from 1 to 2 mm in diame-

ter with rare fragments of hematite quartzite. Here the rock contains about 10 per cent white to pink idiomorphs of feldspar in addition to the usual components described above.

The contacts between the tectonic breccia and other metamorphic units are sharp. In the northern part of sec. 15, T. 26 N., R. 8 E., the contact between tectonic breccia and muscovitic quartzite is drag-folded, as shown on Plate 1.

FELDSPATHIC SCHIST

Feldspathic schist is the name given here to a sequence of metamorphic rocks characterized by a very fine-grained matrix of quartz, potassium feldspar, and mica that surrounds beadlike quartz individuals and aggregates, and feldspar ten to thirty times as large as the matrix grain size. The feldspathic schist unit includes three mapped phases: (1) feldspathic schist composed of quartz, feldspar, and muscovite which constitutes the great bulk of the unit, (2) a melanocratic phase in which biotite is the principal mica with trace amounts of muscovite, and (3) a gneissic phase which has a very low muscovite content.

Just (p. 44) gave the name *Vallecitos rhyolites* to this unit on the basis of six criteria:

The following features support the classification of the Vallecitos rhyolites as extrusive rocks: a) Flow banded structure is well developed; b) the aphanitic groundmasses are too fine for intrusive bodies of such size; c) the long axes of the outcrops and the flow banding strike consistently parallel to the sediments; d) in the NE 1/4 sec. 15, T. 26 N., R. 8 E. the flows are interbedded with conglomeratic quartzite; e) the masses are elongate and lenticular; f) the phenocrysts of quartz and orthoclase indicate an order of crystallization common in acidic extrusive rocks but rare in intrusive rocks of similar composition, such as granites.

Barker (p. 55) renamed similar rock in Las Tablas quadrangle the *Burned Mountain Metarhyolite* and accepted the volcanic origin advocated by Just. Montgomery (p. 25) named similar-appearing rock felsite in the Picuris Range and stated that "Much of the rock is meta-rhyolite, and some of it represents metavolcanic types of quartz latite or dacite affinities."

This writer prefers to use the descriptive name of *feldspathic schist* for this rock type to avoid the genetic implications of the rock name *metarhyolite*. Of Just's six criteria, only the aphanitic groundmass and presumed relict phenocrysts are relevant to the origin of this mass. The intercalation and form of feldspathic schist, as will be shown, are of tectonic rather than primary origin. Also, inasmuch as the aphanitic groundmass and relict phenocryst interpretations are open to question and alternative explanation, the application of a genetic name is believed to be more misleading than useful.

In the field, feldspathic schist was identified by the presence of large, rounded quartz grains and euhedral to subhedral feldspars set in a very fine-grained, and in many places, flinty matrix. Only rock with these three features occurring together was identified as feldspathic schist, for some parts of the muscovitic quartzite and hematitic quartzite, as already noted, contain quartz superindividuals and small sections of quartzite contain isolated euhedral feldspar crystals. The only unique feature of the feldspathic schist is the very fine-grained, quartz-feldspar matrix.

The leucocratic or typical feldspathic schist comprises about 20 per cent of the metamorphic rocks in the map area. It underlies the bulk of Mesa de la Jarita and is exposed along the western flank from a point two miles north of Ancones to SW1/4 sec. 15, T. 26 N., R. 8 E. In Canon de los Alamos, it forms two large lenticles; a tapered, lens-shaped isolated western mass and a pronged eastern mass. The southern end of the major body of schist splits into several wedges which terminate in muscovitic quartzite half a mile east of Ancones. Numerous thin sheets occur in muscovitic quartzite where the Tertiary conglomerates lap onto the Precambrian along the southeastern margin of Mesa de la Jarita and along the Petaca road near the eastern margin of the map area. The western half of the exposed Precambrian southwest of South Petaca is composed of complexly interlayered feldspathic schist and muscovitic quartzite.

The melanocratic or biotite-bearing variety of feldspathic schist is exposed in a thin belt along the northern part of the west flank of Mesa de la Jarita and as an elongate lens across the summit of Mesa de la Jarita in sec. 26, T. 26 N., R. 8 E. This part of the melanocratic variety is marked by a phyllitic schistosity as opposed to the small arcuate mass exposed in secs. 10 and 15, T. 26 N., R. 8 E., which is gneissic. One thin layer enclosed by leucocratic feldspathic schist crops out for several hundred feet one mile west of South Petaca.

The gneissic phase forms three small elongate bodies in secs. 10, 15, and 16, T. 26 N., R. 8 E. The two western lenses are surrounded by the mica schist part of the muscovitic quartzite mentioned earlier. The longer eastern mass abuts quartz-albite-biotite-muscovite schist and muscovitic quartzite.

The color and texture of leucocratic feldspathic schist range considerably in different parts of the map area. In the large canyon cut into the western flank of Mesa de la Jarita one and a half miles east-southeast of Vallecitos, the rock is red to pinkish red, compact and flinty with prominent black hematite layers spaced from less than an inch up to six inches apart. This part of the feldspathic schist is similar in appearance to *Hartschiefer*. It contains a marked fissility along which the rock tends to split, and these surfaces have a lustrous sheen due to segregations of very fine-grained muscovite. A well-developed textural and mineralogical lineation is present on the parting surfaces. Small

patches of this compact, hematite-layered phase are present along the west flank of Mesa de la Jarita and several layers of this type were traced across the summit of the mesa in sec. 26, T. 26 N., R. 8 E. This phase of the feldspathic schist grades into the more representative schistose variety. The transition is marked by increase in the content and grain size of muscovite and disappearance of the hematite layering. Typical feldspathic schist is markedly foliated and pinkish white. The thin laminae consist of alternating muscovite-rich and quartz-feldspar-rich layers with an average thickness of less than one millimeter. Along the west flank of Mesa de la Jarita in secs. 22 and 27, T. 26 N., R. 8 E. and in the central northern part of sec. 15, T. 26 N., R. 8 E., the feldspathic schist is white to greenish white and contains streaks and small drusy cavities lined with manganese oxide. In the latter locality, these cavities make up about 30 to 40 per cent of the rock. This white, manganese-bearing phase also contains trace amounts of piemontite visible in hand specimen. All of the feldspathic schist exposed in the Cribbenville district and in the isolated exposures along the eastern margin of the quadrangle is the pink, markedly schistose variety. A small exposure north of the Petaca road in sec. 5, T. 25 N., R. 9 E. is exceptional in that it contains very little mica and is sugary and crumbles under the hammer.

Under the microscope, most of the leucocratic feldspathic schist (fig. 4b) consists of a very fine-grained matrix made up of equant xenomor-

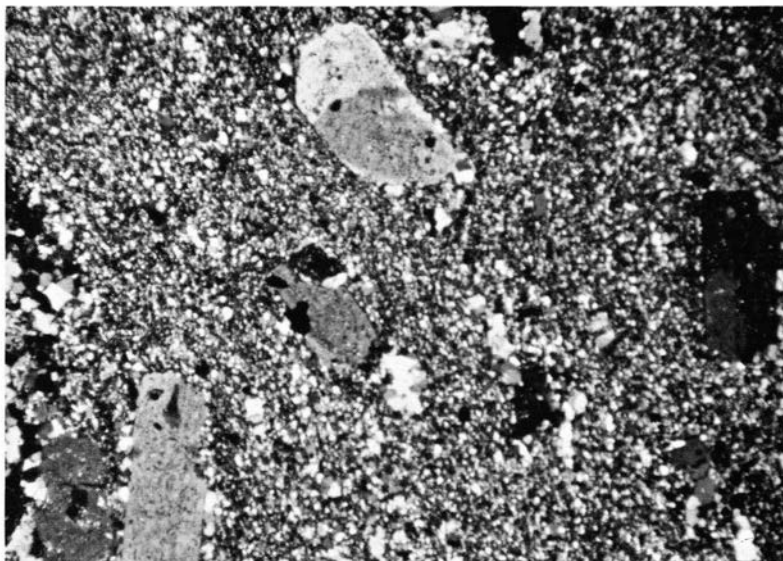


Figure 4b
FELDSPATHIC SCHIST

phic quartz and untwinned potassium feldspar. Small interstitial muscovite flakes that are very nearly parallel throughout the matrix define the schistosity (fig. 4c). The matrix grains range in size from about 0.05 mm to submicroscopic. Nearly circular quartz superindividuals and xenomorphic aggregates with an average diameter of 1 mm are set in the matrix which wraps around these larger grains. Almost all quartz superindividuals contain arcuate planes of mica inclusions. A few elliptical aggregates of xenomorphic quartz are present with the long axes of the aggregates parallel to the schistosity. Large euhedral to subhedral feldspar crystals also occur scattered throughout the matrix with no apparent preferred orientation. In most samples, large grains of microcline patch perthite and sodium-oligoclase are present. In a few samples, patch perthite composed of an untwinned feldspar (biaxial (—); 2V approximately 60°) includes perthitic patches of plagioclase with albite twinning. Large plagioclase crystals twinned according to the Albite law, combined Albite-Carlsbad laws, or combined Albite-Acline laws are common. Aggregates of large subhedral to euhedral twinned plagioclase crystals are present in some samples. Most of the plagioclase exhibits simple albite twins. The plagioclase-potassium feldspar ratio for the large crystals of perthite and plagioclase is variable. In some samples, all the coarse-grained feldspar is **plagioclase and in others it is**

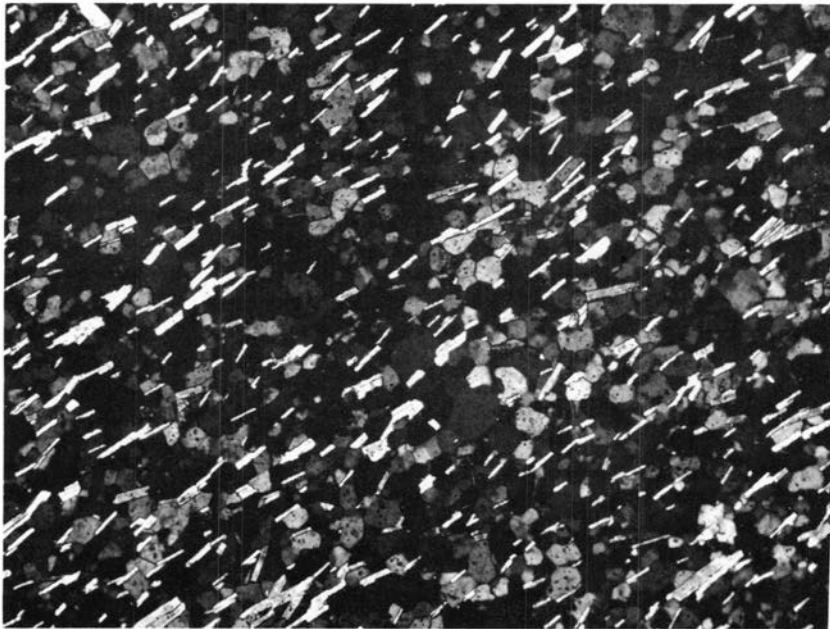


Figure 4c

PREFERRED ORIENTATION OF MATRIX MUSCOVITE IN FELDSPATHIC SCHIST

all perthite. Nearly all samples contain a mixture of these two types of feldspar, but in no section observed does feldspar in the form of large grains exceed 10 per cent. The ratio of plagioclase to potassium feldspar is also variable. The whole spectrum from microcline perthite through microcline antiperthite is present in the feldspathic schist. All samples contain accessory subhedral to anhedral epidote and specularite.

Several thinsections contain features found both in leucocratic feldspathic schist and muscovitic quartzite and are considered transitional. In several samples, muscovite occurs as individual flakes scattered throughout the matrix and in sheaves which form a braided network in the slide. Very fine-grained aggregates occur as irregular patches and networks around ellipsoidal concentrations of coarser xenomorphic quartz. Microcline patch perthite and highly altered plagioclase subhedra are present in small amounts. Another sample similar to that just described contains irregular patches of untwinned xenomorphic plagioclase which poikiloblastically includes muscovite and specularite. In some of the transitional varieties, plagioclase with albite twinning and fresh microcline occur as equant porphyroblasts with an average diameter three to four times the diameter of matrix feldspar. Several specimens have the characteristic texture of mylonite; irregular sinuous veinlets of finely comminuted material bound rounded augen of coarse-grained xenomorphic quartz. The fine-grained aggregate is quartz and potassium feldspar, not a single crushed mineral.

The melanocratic variety of feldspathic schist differs from the leucocratic variety in color, mica content, and to a small degree in texture. In outcrop, it is generally gray-brown to brownish black with prominent pink feldspar euhedra and rounded quartz blebs. The darker color is due to very fine-grained biotite in the matrix. It is compact with a pronounced, though wide-spaced, foliation along which the rock tends to part. In good exposures on the south canyon wall in sec. 15, T. 26 N., R. 8 E., numerous flattened feldspars occur on the parting surfaces. The arcuate mass exposed in secs. 10 and 15, T. 26 N., R. 8 E. differs from the melanocratic phase mapped elsewhere in being coarser-grained, markedly schistose, and containing 20 to 30 per cent more feldspar euhedra. The schistosity pinches and swells around the large feldspars which have a random orientation.

In thinsection, the melanocratic phase consists of a very fine-grained matrix (0.02 to 0.03 mm average grain size) of equant xenomorphic quartz, untwinned feldspar, biotite flakes in parallel orientation, and a trace of calcite. Large crystals in this matrix are subhedral to euhedral albite-twinned sodium-oligoclase and microcline perthite which occur as laths and stubby equant grains. Accessory specularite occurs as very small subhedra in the matrix. One sample contains a trace of poikiloblastic pink garnet, and several samples contain skeletal books of mus-

covite averaging 0.4 mm across, which are randomly distributed and randomly oriented in the rock.

The gneissic variety of feldspathic schist occupies the smallest outcrop area of the three varieties. It is compact, pinkish white to grayish white, crudely foliated, and glassy. It contains numerous large pink feldspar euhedra in addition to the omnipresent quartz superindividuals. Under the microscope, a sample from the ridge that rises above the surface of Mesa de la Jarita in secs. 10 and 15, T. 26 N., R. 8 E. has the texture of the leucocratic feldspathic schist and large skeletal books of muscovite, but no matrix mica. Layering in the rock is defined by trains of disseminated specularite both as large subhedral grains (0.3 mm) and as numerous equant xenomorphic grains less than 0.1 mm in diameter. The matrix consists of a granoblastic aggregate of quartz, untwinned feldspar, and rare microcline and albite. Large grains set in this matrix, in addition to the skeletal muscovite already mentioned, are (1) microcline perthite, (2) untwinned potassium feldspar (orthoclase?) perthite, and (3) antiperthite with patches of untwinned potassium feldspar. A dusty alteration product which is transparent under high magnification and convergent light (epidote?) is restricted to the untwinned potassium feldspar. Three grains composed of a micrographic intergrowth of quartz and untwinned feldspar form a clot several millimeters in diameter (fig. 4d). Many of the patch perthites in which the dominant phase is untwinned potassium feldspar show marginal rims of polysynthetic microcline-type twinning. The twinned areas are free of the dusty inclusions noted above.

Feldspathic schist is structurally intercalated and in sharp contact with other metamorphic rocks except where it grades into granitic gneiss in the Cribbenville district. The only gradational contact between varieties of feldspathic schist observed by the writer is exposed along the Old Petaca road on the north canyon wall in sec. 15, T. 26 N., R. 8 E. Here the hematite-layered leucocratic feldspathic variety passes into the melanocratic variety with only an increase in biotite and decrease in hematite marking the transition. The boundary zone between the two distinct rock types is about 20 feet wide.

Origin

All previous workers have regarded the feldspathic schist as metamorphosed rhyolite porphyry. Their conclusion is based upon the very fine-grained quartz-feldspar groundmass, large subhedral to euhedral crystals of microcline perthite and plagioclase, quartz superindividuals, which in some samples appear to have the bipyramidal form of high quartz, and chemical composition similar to average rhyolite. The presence of perthite crystals in the unit within La Madera quadrangle in which an untwinned potassium feldspar host is transitional into microcline also supports this opinion. Clusters of coarse-grained, complexly twinned plagioclase and micrographic intergrowths of quartz

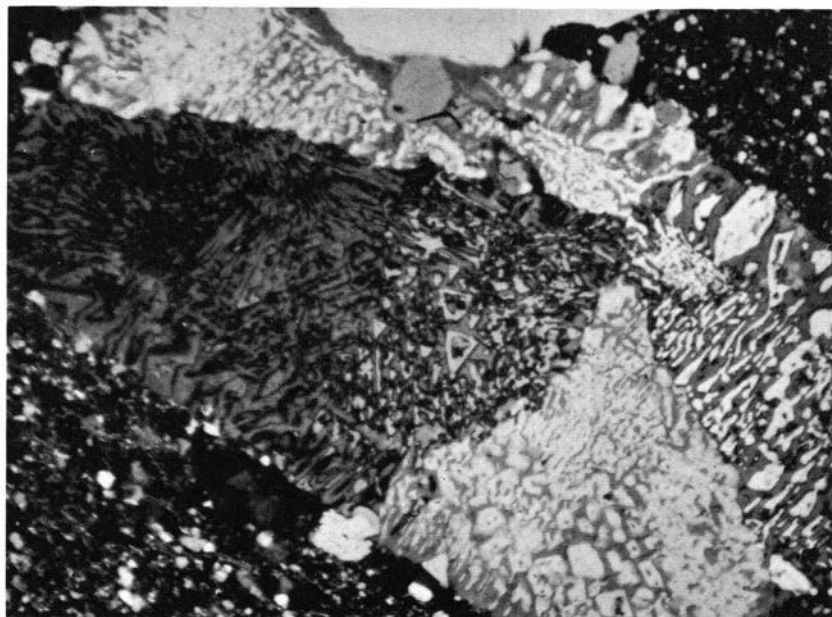


Figure 4d

MICROGRAPHIC INTERGROWTH IN GNEISSIC PHASE OF FELDSPATHIC SCHIST

and feldspar as large grains are common in volcanic textures. Although all these features suggest that the feldspathic schist was at one time a rhyolite porphyry, no single feature is unequivocal proof.

The gneissic phase surrounded by an aureole of quartz-muscovite schist which is gradational into muscovitic quartzite may be construed as representing an original hypabyssal intrusive mass. The sheath of muscovite-rich schist which envelops this rock is an expectable result of alteration of original wall rock during intrusion. In this small unit there is a scarcity of the textures of volcanic character noted above, and the composition appears to be constant throughout.

Alternatively, it is possible that the fine-grained matrix containing the rounded quartz aggregates and superindividuals is the result of cataclasis of an arkosic sandstone and that the plagioclase and perthite were introduced after the pronounced dislocation had ceased. The fact that no perthite or large plagioclase crystals were found in any of the enclosing muscovitic quartzite or quartz-albite-muscovite-biotite schist samples, however, does not favor a regional alkali metasomatism. Late feldspar in these rock types is xenomorphic and poikiloblastic micro-dine and untwinned albite.

However, the advocates of metarhyolite must account for the preservation of delicate patch and string perthites and their lack of pre-

ferred orientation in a matrix containing a penetrative and pervasive flow cleavage. They must also account for a wide range in the content of large feldspar species from about equal proportions of perthite and plagioclase to sections of the schist in which all the large crystals are either plagioclase or perthite. Another factor which must be explained is the presence of numerous textural relicts within one map unit, whereas the fabric of all other map units in the area is entirely crystalloblastic.

QUARTZ-ALBITE-MUSCOVITE-BIOTITE SCHIST

A fine-grained, equigranular, quartz-rich schist composed of quartz, untwinned plagioclase, muscovite, and biotite as essential minerals constitutes about 15 per cent of the exposed metamorphic rocks. It crops out in a one-half- to three-quarter-mile wide northwest-trending belt along the eastern base of Mesa de la Jarita, in a small wedge-shaped mass in the Vallecitos valley two miles north of Ancones, in a very small isolated area in the lower part of Canon de los Alamos, and in a thin layer in sec. 30, T. 26 N., R. 9 E. This unit is uniform in composition and texture in all samples examined. The largest area of exposure, in the upper part of Canon de los Alamos, is bounded by muscovitic quartzite on the west and covered by Tertiary rocks in the east. The southern part of the outcrop area bifurcates into an eastern prong bounded by muscovitic quartzite and feldspathic schist and partly covered by Tertiary rocks and into a thin western wedge which pinches out abruptly in muscovitic quartzite. The northern part of this mass includes the largest body of gneissic leucocratic schist. The contacts between quartz-albite-muscovite-biotite schist and other metamorphic rock units are sharp.

This unit is uniformly soft, fine- to medium-grained, gray to yellowish gray, and speckled with small flakes of biotite. The schistosity is well developed, and elongate plates of biotite in the plane of schistosity form a pronounced lineation. Poorly defined, widely spaced hematite laminae commonly occur parallel to the schistosity. The thin layer in sec. 30, T. 26 N., R. 9 E. contains large boudins of hematite-layered quartzite similar in appearance to the quartzite in the Ortega Mountains. In this area also, the schistosity and hematite layering are folded and cut by west-trending axial-plane cleavage.

In thinsection, this rock has a lepidoblastic-seriate fabric and contains, in order of decreasing amount, quartz, albite, muscovite, and biotite with accessory amounts of epidote, specularite, and rare retrograde chlorite. Equant xenomorphic quartz (1 mm or less in diameter) is intergrown with mostly untwinned plagioclase (0.5 to less than 0.1 mm in diameter). Plagioclase with faint albite twinning is rare, and many of the plagioclase xenomorphs exhibit a broad concentric zoning. Interleaved biotite and muscovite flakes averaging 0.3 mm in length

are uniformly dispersed throughout the quartz-plagioclase matrix and the preferred orientation of these plates defines the schistosity. Many of the biotite flakes exhibit incipient alteration along the cleavage traces, and a few grains have been completely altered to pale green pleochroic chlorite. In a sample of this schist from the axial-plane region of one northwest-trending fold, the fabric includes a fracture cleavage which grades into thin rift zones containing islands of crushed quartz and plagioclase. Muscovite flakes define a schistosity, but slightly larger biotite flakes have no preferred orientation and are transverse to the schistosity. Many of the biotite flakes have been partly altered to chlorite. In the first sample described, biotite is pleochroic from yellowish brown to brownish black (opaque), but in the latter sample it is pleochroic from colorless to greenish brown.

Origin

The average composition of this unit falls within the pelitic field of an ACF diagram (Fyfe, Turner, and Verhoogen, 1958, p. 200) which suggests derivation from aluminous material. It differs mineralogically from enclosing muscovitic quartzite in the presence of biotite, epidote, and albite. The presence of these minerals indicates that the original material contained substantial amounts of calcium, sodium, and magnesium. The equilibrium assemblage in this unit could equally well have been derived from a dolomitic quartz sandstone or a tuffaceous sandstone. The high quartz content argues against an original graywacke. The relatively high albite content could be due to an unusually high sodium content in a siliceous tuff.

GRANITIC GNEISS

Fine-grained, schistose, locally biotite-bearing, granitic gneiss crops out in the eastern and northeastern parts of La Madera quadrangle. It is even-grained, yellowish brown, and relatively homogeneous except where it is gradational into muscovitic quartzite and feldspathic schist in the Cribbenville district. The rock has a mineralogic composition similar to granite but does not have characteristic igneous textures either in outcrop or under the microscope. The schistosity and lineation in the map unit are similar in style and orientation to structural features of the same generation present in the other metamorphic rock units of the area. Granitic gneiss mapped in La Madera quadrangle is lithologically similar to the Tres Piedras granite (Barker, p. 59) which crops out in Las Tablas quadrangle. In La Madera quadrangle, granitic gneiss constitutes about 5 to 10 per cent of the exposed Precambrian rocks.

The granitic gneiss is a fine- to medium-grained, slightly schistose rock composed of quartz, microcline and microcline microperthite, untwinned plagioclase, and small amounts of biotite and muscovite in

widely ranging proportions. In outcrop, the schistosity ranges from moderately well developed to nearly absent. This structural parameter is directly related to the total mica content of the rock which varies from place to place. Most exposures contain 10 to 20 per cent mica; low mica phases are rare. In the Cribbenville district, granitic gneiss grades into interlayered muscovitic quartzite and feldspathic schist through a broad transitional zone; hence, no contact is indicated on the geologic map in these areas. In a few places, layers of muscovitic quartzite can be traced into granitic gneiss along the strike for several hundred feet beyond the area where feldspathic schist has graded into granitic gneiss (pl. 1). Thin layers of highly altered garnitiferous-muscovite schist and large areas of rock texturally and compositionally transitional between feldspathic schist and granitic gneiss occur within the southern part of the large mass of granitic gneiss along the central eastern boundary of the quadrangle. Most of the transitional rocks contain scattered superindividuals of quartz and large feldspars. They are set in a coarse-grained lepidoblastic matrix which imparts a texture and color in hand specimen more akin to granitic gneiss than feldspathic schist. A small lens of very fine-grained, biotite-rich granitic gneiss occurs within feldspathic schist enclosed by muscovitic quartzite that forms the elongate mass of Precambrian rock in sec. 32, T. 26 N., R. 9 E. Small masses of granitic gneiss occur in Canon de la Paloma where it forms a deep gorge in the Precambrian rocks in sec. 17, T. 25 N., R. 9 E.

The microscopic fabric and quartz-feldspar composition of the granitic gneiss exhibits little variation in the samples studied. The rock consists of a crystalloblastic aggregate of quartz rarely having undulatory extinction and ranging in size from 1.0 to less than 0.1 mm, fresh xenomorphic microcline and microcline perthite with an average grain diameter of 0.7 mm, and uniformly sericitized, rarely twinned plagioclase. Total mica content ranges from about 10 to 20 per cent, but the ratio of muscovite to biotite ranges widely. In most samples, there is slightly more muscovite than biotite, but some specimens contain only muscovite and others only biotite. No recognizable trend of the muscovite-biotite ratio was found within the map unit. The ratio of microcline to microcline microperthite is also variable, but in most samples it is about 2:1. The microperthite is composed of from about 1 to 5 per cent untwinned plagioclase in the form of parallel thin films or layers within the microcline host. In one microperthite grain several of the lamellae are composed of a material with high birefringence, probably muscovite. Several samples from the Cribbenville area contain large poikiloblastic porphyroblasts of microcline patch perthite to antiperthite in which the plagioclase is fresh to mildly altered and untwinned. Large quartz individuals and xenomorphic aggregates are also present in these samples. Muscovite and biotite plates are uniformly distributed throughout the matrix and range in length from 0.8 to less than 0.1 mm. In most samples, the plagioclase forms amoeboid patches and small

xenomorphic grains interstitial to quartz and microcline. In only a few samples is any of the plagioclase twinned, but many grains show a broad concentric zoning. Common accessories are epidote disseminated in small equant subhedra, small xenomorphic grains of specularite, a trace of poikiloblastic pink garnet, and rare myrmekite composed of quartz and untwinned albite. Xenomorphic quartz, slightly elongate in the plane of the schistosity, is commonly found in mica-rich granitic gneiss.

Origin

As the name implies, the modal composition of this metamorphic rock approaches that of granite. Barker (p. 60) considers the Tres Piedras granite to be of magmatic origin. No positive statement regarding the premetamorphic form of the granitic gneiss (lithologically indistinct from the Tres Piedras granite) is warranted for La Madera quadrangle. The gradational nature of the boundary relations between granitic gneiss and other metamorphic units has already been discussed; however, in several localities the gneissic granite is in sharp contact with quartzite and muscovitic quartzite. The microscopic texture of the gneiss is entirely crystalloblastic and no unequivocal relict textures were found. Perhaps the most significant relationship bearing on the origin of this unit is the presence of discontinuous lenses of highly altered garnetiferous quartz-muscovite-feldspar schist within the otherwise homogeneous unit. These layers could represent sediment which escaped the metasomatic influence of granite magma not identified in the area. They could also represent septa in a granite subsequently converted to granitic gneiss, or they could be remnants of original quartzose sediment, incompletely granitized.

HORNBLende-CHLORITE SCHIST

Bluish green to greenish black schists and gneisses composed of various amounts of hornblende, chlorite, plagioclase, and quartz are included in this map unit. Biotite-rich phases, within and marginal to some schist layers and too small to appear as a separate map unit, are included with hornblende-chlorite schist. This unit consists of relatively thin layers averaging thirty to thirty-five feet thick whose contacts with enclosing rocks are nearly always parallel to schistosity within the unit. A notable exception to the parallelism of contacts and schistosity is illustrated by the two west-southwest-trending lenses of schist in NE1/4 sec. 23, T. 26 N., R. 8 E. The largest exposure of schist in which a single layer, well defined within muscovitic quartzite, can be traced for thousands of feet lies along the southeast flank of Mesa de la Jarita. In this area, the outcrop thickness is variable because of the relationship between the uniformly dipping schist and irregular topography. Isolated lenses of schist crop out in the upper part of Canon de los Alamos.

A single layer of schist is enclosed within muscovitic quartzite in sec. 32, T. 26 N., R. 9 E. and in secs. 17 and 18, T. 25 N., R. 9 E. Muscovitic quartzite and quartz-albite-biotite-muscovite schist are the only metamorphic rock units which enclose hornblende-chlorite schist layers.

Just (p. 44) considered the hornblende-chlorite schist in the La Madera area to be equivalent to similar rocks from the Picuris area to which he gave the name *Picuris basalts*. Barker (p. 25) designated similar rocks the amphibolite member of the Kiawa Mountain Formation.

The degree of compactness, composition, and development of schistosity varies considerably within some, and among most, of the hornblende-chlorite schist bodies. Most of the unit which crops out east of Ancones consists of hard, compact, greenish black, homogeneous schist. It is composed of about 40 per cent blue-green hornblende, 25 per cent sodic andesine, 20 per cent quartz, and 10 per cent chlorite, with accessory amounts of epidote, specularite, and apatite. The average grain size is from 0.2 to 0.3 mm. The schistosity is defined by small parallel flakes of chlorite and prisms of hornblende, most of whose c-axes lie in the foliation plane. Idiomorphic hornblende tends to be segregated in layers set in a granoblastic quartz-plagioclase matrix. Usually a few hornblende grains lie transverse to the schistosity. Specularite forms small tablets which parallel the schistosity. The preferred orientation is displayed in outcrop by a pronounced lineation in the plane of schistosity. In several exposures, white to greenish white blebs composed of partly sericitized plagioclase, subhedral to anhedral epidote, and minor quartz are disseminated throughout a zone one to three feet thick along one margin of the schist layer. Usually these blebs are elongate in the plane of the schistosity and form a prominent lineation parallel to the hornblende lineation. In a few exposures, the schist exhibits a pronounced color banding composed of alternating grayish white and greenish black layers which are isoclinally drag-folded and parallel to the schistosity except where it passes through the hinges of the folds.

Near the base of the scarp in the southern part of sec. 35, T. 26 N., R. 8 E. and in the drag-folded margins of the amphibolite layer a quarter mile due east of Ancones, the schist boundary consists of alternating layers of muscovitic quartzite and a gneissic phase of the hornblende-chlorite schist. The gneissic variety consists of layers of xenomorphic quartz and untwinned andesine (0.2 to 0.3 mm in diameter) alternating with layers of chlorite and hornblende. In some parts of this variety, biotite occurs in the chlorite-hornblende layers as books about one millimeter long oriented normal to the gneissic layering. Most blue-green hornblende has a preferred orientation in the plane of schistosity and defines a lineation, but in some samples individual idiomorphs 2 to 3 cm long cut across the layering and have a random orientation in the rock. Hornblende has also grown in the form of radiating aggregates of

slender prisms whose c-axes lie in the schistosity defined by the chlorite-rich layers. Biotite and some of the hornblende have been partly replaced by chlorite. In sec. 35, T. 26 N., R. 8 E., a granitic pegmatite has intruded hornblende-chlorite schist and converted all the hornblende and chlorite to biotite.

The isolated layers of hornblende-chlorite schist exposed in the upper part of Canon de los Alamos differ from the units described above in that the rock is generally light green to greenish gray, markedly schistose, and tends to crumble under the hammer. The schist exposed in the west-central part of sec. 24, T. 26 N., R. 8 E. is more nearly like the hornblende-chlorite schist east of Ancones than any of the other isolated exposures in this belt. It contains about 24 per cent quartz, 46 per cent plagioclase uniformly altered to sericite (paragonite?), and 24 per cent chlorite. Quartz and altered feldspar form equant xenomorphic grains averaging 0.2 mm in diameter, and ranging in size from 0.3 to less than 0.1 mm. Chlorite flakes 0.2 mm long outline the quartz and plagioclase and define the schistosity, together with parallel plates of specularite. Idiomorphic hornblende prisms, 0.7 to 5.0 mm long, pleochroic from yellowish brown to olive-green to blue-green are randomly oriented in the quartz-plagioclase-chlorite matrix. Accessory apatite, epidote, and rutile are present as xenomorphic grains disseminated throughout the rock. The southernmost mass of schist exposed in sec. 25, T. 26 N., R. 8 E. is markedly porphyroblastic in hand specimen and consists of 25 per cent quartz, 30 per cent chlorite, 30 per cent andesine, and 10 per cent specularite. The preferred orientation of chlorite flakes defines the very marked schistosity. Large poikiloblastic hornblende prisms occur randomly oriented in the quartz-andesine-chlorite matrix. Most of the porphyroblasts are surrounded by a thin halo markedly deficient in chlorite, but several hornblende crystals include chlorite flakes. The hornblende-chlorite schist exposed at the base of the eastern flank of Mesa de la Jarita is composed of 50 per cent blue-green hornblende set in a granoblastic matrix of quartz and untwinned oligoclase. A weak schistosity is defined by the preferred orientation of hornblende and tabular plates of specularite. Many hornblende idiomorphs lie transverse to the schistosity. This section of the rock contains no chlorite, but two small books of corroded biotite are present in the matrix.

Hornblende-biotite schist and biotite schist comprise a thin layer two of three feet wide enclosed by feldspathic schist in sec. 32, T. 26 N., R. 9 E. The schist ranges in color from greenish black to black and is very soft and crumbly. It consists of 30 to 50 per cent biotite with an average grain size of 0.5 mm, 5 to 45 per cent blue-green hornblende, 10 to 30 per cent untwinned albite, and 10 to 20 per cent quartz. The high degree of preferred orientation of hornblende and biotite define the schistosity in most of the layer, but in one sample where biotite has partly replaced hornblende, the biotite books have a random orientation in the quartz-plagioclase matrix. The plagioclase is mildly seri-

citized and exhibits a broad concentric zoning. In sections where hornblende is partly replaced by biotite, the former is pleochroic from greenish brown to grass green to bluish green.

Origin

The assemblage chlorite-andesine (sodic oligoclase) which characterizes this map unit is not an expectable equilibrium assemblage in a conventional facies classification. Field relations and bulk composition suggest that this unit has been derived from an original basalt. The continuity of a single thin layer such as that exposed east of Ancones, the plagioclase-epidote-quartz blebs restricted to one margin of the layer which could represent reconstituted amygdules, and the extremely low potassium content inferred from the near absence of biotite suggest derivation from basic rock. The alternative explanation that these schists have been derived from a calcareous pelite is seriously weakened by the absence of a widespread potassium-bearing phase.

PLAGIOCLASE-CHLORITE PHYLLITE

Plagioclase-chlorite phyllite is restricted to the central part of the west scarp of Mesa de la Jarita and the Vallecitos valley. On the flank of the mesa it appears on the map as an arcuate layer which thins to the south where it passes under Tertiary conglomerates. It is exposed in a road cut near Rancho del Olguin within a fault block and is in fault contact with feldspathic schist and muscovitic quartzite at the base of the scarp in sec. 22, T. 26 N., R. 8 E.

The unit ranges in color from grayish white to grayish green. It is highly variable in texture, being a phyllite near Rancho del Olguin and changing from a gray flinty hornfels with elongate flattened blebs at the base of the fault scarp to a grayish green chlorite phyllite along the arcuate trace of this unit where it curves east and south up the face of the scarp. Just north of the fault which intersects the phyllite in sec. 35, T. 26 N., R. 8 E., it contains abundant black tourmaline prisms up to two inches in length and arranged in sheaves and bundles parallel to the layering.

This rock unit is composed principally of plagioclase, chlorite, muscovite, and quartz with accessory amounts of epidote, hematite, and tourmaline.

Under the microscope, the typical fabric is lepidoblastic with various amounts of minute chlorite and muscovite flakes defining the phyllitic layering. The micas are arranged in very thin layers separated by layers of xenomorphic quartz and untwinned plagioclase. Hematite forms small plates whose long axes are parallel to the mica flakes and also rare equant porphyroblasts. Some samples contain flattened augen of xenomorphic quartz. In one section, the phyllitic layering is defined by minute parallel chlorite flakes interstitial to plagioclase and quartz

in islands separated by a braided network of matted fine-grained muscovite. Dichroic tourmaline (pink to bluish gray) occurs as idiomorphic prisms in all samples examined. A sample from the crest of Mesa de la Jarita consists of quartz, plagioclase, and muscovite in a fine-grained matrix. It also contains muscovite books (0.3 to 2.0 mm) as idiomorphic porphyroblasts transverse to the phyllite layering. Most of the rock, however, consists of large (about 2 mm diameter) irregular grains of al-bite which poikiloblastically include swirled phyllitic layering marked by the preferred orientation of specularite plates. Most of the albite is untwinned and fresh and exhibits a broad concentric zoning. A few grains exhibit albite twinning.

Origin

The small areal distribution and unusual mineralogy of this phyllite distinguish it from the other map units in the Precambrian. The low quartz content in the equilibrium assemblage albite-chlorite-muscovite indicates an original bulk composition intermediate between pelitic and ferromagnesian. Graywacke, sodic tuff, or perhaps bentonite could conceivably be converted to the existing assemblage, but these choices are purely speculative. The possibility of a premetamorphic event such as local hydrothermal activity or metasomatic alteration of pre-existing rock should be considered. At best, the origin of this metamorphic unit is uncertain.

CHLORITE SCHIST

Chlorite schist is areally the smallest of the map units, yet it exhibits some of the most unusual mineralogic features found in the map area. It forms a small tongue in chlorite-plagioclase phyllite where that unit is exposed on the west side of the northwest-trending fault in sec. 22, T. 26 N., R. 8 E. A single layer with a maximum thickness of about twenty feet crops out in SW1/4 sec. 25, T. 26 N., R. 8 E. It is a compact, strongly foliated, green to greenish black schist composed of individual chlorite flakes with an average diameter of 3 mm. Schistosity surfaces have a speckled appearance due to the presence of poikiloblastic xenomorphic clinozoisite. At the northern end of the layer west of Sunnyside mine, the margins of the schist are prominently layered. The layering consists of planar segregations of red euhedral garnet ranging in size from 1 mm to 3 cm, pseudomorphs of red hematite after idiomorphic pyrite which attain a diameter of several centimeters, and typical chlorite schist. The schist layer is enclosed by muscovitic quartzite and the schistosity in chlorite schist and muscovitic quartzite is parallel to the litho-logic contacts.

The chlorite schist consists of 50 to 60 per cent chlorite arranged in nearly parallel plates. Muscovite flakes about 2 mm long occur intergrown with chlorite in the form of planar segregations parallel to the

schistosity defined by chlorite and as broad irregular patches of parallel-oriented muscovite. A subfabric is marked by optically continuous skeletal remnants of chlorite nearly perpendicular to the prominent schistosity. These remnants of chlorite exhibit various degrees of replacement by biotite which surrounds and extends along the cleavage traces of the chlorite patches. Quartz forms xenomorphic equant grains in the chlorite-muscovite framework. Leucoxene occurs as small plates whose long axes are parallel to the schistosity. Clinozoisite forms large poikiloblastic porphyroblasts (1 to 3 cm) composed of small individual grains in various optic orientations. Many of these grains exhibit an anomalous Berlin blue interference color. Poikiloblastic garnet and minute subhedra of epidote are scattered throughout the matrix in trace amounts. A thin layer of kyanite quartzite associated with chlorite schist consists of randomly oriented kyanite prisms in a granoblastic quartz matrix. The kyanite is largely replaced by very fine-grained felty pyrophyllite.

Origin

The quartz-muscovite-chlorite assemblage, like the albite-muscovite-chlorite assemblage, is intermediate between the typical pelite and magnesian compositional groups. The unit is so small, however, that it could easily represent a metamorphic segregation formed during regional metamorphism. As a sedimentary unit, it could have been a dolomitic arkose or some form of basic pyroclastic accumulation.

PEGMATITE AND QUARTZ DIKES

Numerous dikes and lenses of granitic pegmatite and tabular bodies of quartz intrude the Precambrian metamorphic rocks. Most of these dikes have a west trend and dip steeply south or north. The petrology of the pegmatites has been treated in detail by Jahns. The structural significance of these rock bodies lies in the fact that most of the dikes were intruded parallel to the axial-plane cleavage of third deformation folds, placing them late in the sequence of Precambrian structural and petrologic events that have affected the Precambrian rocks in La Madera quadrangle.

METAMORPHISM

Precambrian rocks in La Madera quadrangle are polymetamorphic. Regional metamorphism resulted in the formation of equilibrium mineral assemblages characteristic of the greenschist and almandine amphibolite facies. Later folding, metamorphism, and localized pegmatitic metasomatism have modified the fabric and mineral composition established during regional metamorphism. The principal effects

of later thermochemical processes are the replacement of pre-existing mineral phases and the growth of new minerals lacking a preferred orientation.

Facies of Regional Metamorphism

Facies of regional metamorphism set forth by Turner and Verhoogen (1960, p. 531-560) are used to classify the metamorphic rocks in La Madera quadrangle. During regional metamorphism in the area, recrystallization accompanied by penetrative shear and componental movement resulted in the formation of schists and schistose rocks which contain a pervasive axial-plane flow cleavage with a prominent b-lineation. Hence, rocks with a homogeneous fabric in which the component minerals have a high degree of preferred orientation represent the product of regional metamorphism. Minerals formed by neocrystallization and/or replacement which postdate the regional metamorphism have a random orientation and are not considered in designating the position of rock units in the facies classification.

With the exception of hornblende-chlorite schist, the mineral components of the first deformation fabric represent equilibrium assemblages and consequently are amenable to treatment as metamorphic facies. The structural criterion of equilibrium is the mutual inter-growth of minerals with a high degree of preferred orientation in a single movement picture. Goldschmidt's mineralogic phase rule (number of phases is equal to number of components) is the chemical criterion of equilibrium. All the major map units exhibit a first deformation fabric; thus, they satisfy the structural criterion. The hornblende-chlorite schist, however, contains one more phase than the number of components and consequently represents a disequilibrium assemblage.

The equilibrium assemblages of regional metamorphism which occur in the map area are given in Table 1. With the exception of the hornblende-chlorite schist, all the assemblages could be placed in either the greenschist facies or in both the greenschist and amphibolite facies because of the presence of characteristic minerals of each facies and the absence of critical minerals of either the greenschist or almandine amphibolite facies.

Chlorite schist, chlorite phyllite, granitic gneiss, and quartz-albite-biotite-muscovite schist are placed in the greenschist facies by virtue of the plagioclase composition and the characteristic micas, chlorite, and biotite. Chlorite schist and chlorite phyllite are grouped in the chlorite subfacies and granitic gneiss and quartz-albite-muscovite-biotite schist are placed in the biotite subfacies based on the transition of chlorite to biotite in the presence of muscovite. The two smallest map units areally, chlorite schist and plagioclase-chlorite phyllite, represent the lowest grade of regional metamorphism in the area. The absence of biotite in these schists can not be attributed to lack of available K_2O , for mus-

covite is a member of the equilibrium assemblage in both units. Granitic gneiss and quartz-albite-biotite-muscovite schist represent the intermediate grade of the greenschist facies.

Quartzite, muscovitic quartzite, and feldspathic schist do not contain plagioclase as a member of the equilibrium assemblage, and the minerals present fit equally well into the greenschist or almandine amphibolite facies.

Attempting to place the hornblende-chlorite schists in the facies classification presents a problem. They all contain sodic oligoclase to andesine, which warrants placing them in the almandine amphibolite facies. However, the presence of ubiquitous chlorite, which defines the foliation, intimately intergrown with hornblende is more characteristic of greenschist than of almandine amphibolite facies. Abnormally high

TABLE 1. ASSIGNMENT OF METAMORPHIC MAP UNITS TO FACIES OF REGIONAL METAMORPHISM
(Critical minerals in *italics*)

| ROCK UNIT | EQUILIBRIUM ASSEMBLAGE (+ QUARTZ) | FACIES |
|---|--|--------------------------------------|
| Quartzite | kyanite | Greenschist or almandine amphibolite |
| Muscovitic quartzite | muscovite | Greenschist or almandine amphibolite |
| Quartz-albite-muscovite-biotite schist | <i>muscovite-albite-biotite-epidote</i> | Greenschist; biotite subfacies |
| Granitic gneiss | <i>microcline-albite-biotite-muscovite</i> | Greenschist; biotite subfacies |
| Feldspathic schist (leucocratic variant) | K-feldspar-muscovite | Greenschist or almandine amphibolite |
| Feldspathic schist (melanocratic variant) | K-feldspar-biotite | Greenschist or almandine amphibolite |
| Plagioclase-chlorite phyllite | <i>albite-chlorite-muscovite</i> | Greenschist; chlorite subfacies |
| Chlorite schist | chlorite-muscovite | Greenschist; chlorite subfacies |
| Hornblende-chlorite schist | <i>hornblende-chlorite-andesine</i> (Na-oligoclase) | No assignment |

partial pressure of water would tend to extend the stability field of chlorite to the higher temperatures commensurate with the assumed P-T realm of the almandine amphibolite facies (Nelson and Roy, 1958), but it would also facilitate the breakdown of andesine to albite plus epidote. The real problem lies in a lack of knowledge regarding the stability relations of chlorite under different partial pressures of water and FeO/MgO ratio. An alternative possibility is that biotite originally formed the matrix mica and that subsequent removal of K₂O has converted biotite to chlorite. However, there is no evidence to indicate that this has occurred; hence, it should be considered purely speculative.

Later Metamorphic Effects

Later metamorphic effects include the enlargement of pre-existing mineral phases, growth of new minerals, and retrograde hydration of anhydrous aluminosilicates. Such mineralogic changes can be grouped into two categories based upon textural criteria: those in which the new mineral phase owes its orientation or position in the rock mass to pre-existing textural anisotropy and those in which the new mineral phase has a random orientation and whose distribution is not directly related to older structural elements. Examples of the first group are the growth of kyanite in fracture cleavage, the formation of andalusite at the expense of kaolinite and kyanite in shear zones, and the conversion of kyanite to pyrophyllite. Relatively local effects of this type are the partial chloritization of hornblende and biotite, the migration of iron oxide into fracture cleavage, and alteration along joints in hornblende-chlorite schist.

In the description of kyanite quartzite, it was noted that in many outcrops kyanite has grown in cleavage planes with some prisms, generally 10 to 20 per cent, having a random orientation within the cleavage plane. In the foliation plane of quartzite (first deformation fracture cleavage), most of the kyanite blades have a high degree of preferred orientation and mark the first deformation b-lineation. In second deformation axial-plane cleavage, kyanite forms a less well-developed lineation which is the result of transposition of the first deformation lineation. Radial aggregates and randomly disposed kyanite blades occur in both planar structures, but they tend to be more prominent in second deformation axial-plane cleavage.

Kaolinite-muscovite-kyanite-andalusite forms one of the most complex assemblages in the map area. It is restricted to the schistose mylonitic quartzite layers which crop out in La Madera Mountain. Similar layers in the Vallecitos fault zone and in the quartzite spur west of Vallecitos consist of kyanite-muscovite-kaolinite filling a network of finely granulated quartz seams. In all parts of the mylonite where the assemblage kyanite-kaolinite-muscovite exists, the minerals have a high degree of preferred orientation defining a schistosity and lineation

whose attitude is congruent with first deformation structural features. Where andalusite forms a fourth mineral phase, it occurs as optically continuous layers filling the seams in the mylonite and poikiloblastically including kyanite, quartz, and corroded flakes of muscovite. Several alternative explanations may be set forth for the origin of the kaolinite interleaved with muscovite. First, the original sandstone may have contained mixed-layer kaolinite-illite which was converted to kaolinite-muscovite during regional metamorphism. Second, the assemblage kyanite-muscovite, stable in the absence of potassium feldspar, may have formed during regional metamorphism and muscovite may have been partly replaced by kaolinite during subsequent hydrothermal metamorphism. Third, the assemblage quartz-kyanite may have formed during regional metamorphism while concomitant fluids containing some K_2O circulated through shear zones and converted some kyanite to muscovite. Hydrothermal alteration then effected the partial replacement of muscovite by kaolinite as an intermediate step in the conversion of the kyanite-muscovite assemblage to andalusite.

Some K_2O must necessarily have been added and removed by processes operating at different times. This thesis is strengthened by the presence of small flakes of muscovite interstitial to the xenomorphic quartz arranged parallel to the crude layering in the mylonite. Muscovite is absent in all other parts of the quartzite, with the exception of the quartz-kyanite schist in the Ortega Mountains.

Slightly different aspects of the hydrothermally metamorphosed rocks occur locally throughout the quadrangle. Several samples of kyanite quartzite from La Madera Mountain and a thin layer of similar rock associated with the chlorite schist exhibit patchy coronas of very fine-grained pyrophyllite replacing kyanite. In many outcrops of quartzite, second deformation fracture cleavage is filled with specularite. These layers are bounded by zones, ranging in thickness from about 0.5 to 1.0 cm, of white quartzite enclosed in gray quartzite. Iron may have migrated into the fracture cleavage under the influence of a concentration gradient aided by freely circulating hydrothermal solutions. The lens of quartz-hematite-kyanite-rutile schist which crops out in the west spur of La Madera Mountain may be the result of hydrothermal deposition from solutions carrying silicon, aluminum, iron, and titanium derived from the great mass of quartzite. An alternative explanation is that it represents a metamorphic segregation of the component minerals whose constituents were mobilized during regional metamorphism. It does not seem likely that it represents a primary sedimentary accumulation of iron and alumina-rich material because of the lack of preferred orientation of its components relative to the well-developed structural features in the enclosing quartzite.

Manganese-lined solution cavities are present in bleached feldspathic schist in NW1A sec. 15, T. 26 N., R. 8 E. The presence of accessory piemontite in the same unit indicates that manganese was locally

available. These vugs are cogent evidence that metamorphic processes were active after the tight folding of the second deformation, for it is doubtful that large amounts of pore space could be preserved during an episode of deformation that involved large-scale flowage of the metamorphic rocks.

Chloritization of hornblende is a minor feature of the hornblende-chlorite schists and is believed to represent reconstitution of a high temperature mineral to a lower temperature ferromagnesian phase.

Altered joints in amphibolite are rare but deserve mention, for they represent removal of iron, magnesium, and aluminum along an obvious structure.

The most striking example of the growth of randomly oriented minerals is the presence of euhedral hornblende prisms in the marginal zones of the hornblende-chlorite schist exposed on the southwest flank of Mesa de la Jarita. In the small mass of hornblende-chlorite schist exposed north of the Sunnyside mine, euhedral hornblende porphyroblasts are set in a fine-grained schistose matrix of quartz, plagioclase, and chlorite. In this rock, hornblende appears to have grown at the expense of chlorite as evidenced by chlorite-deficient rims around hornblende porphyroblasts. Kyanite in quartzite and garnet and clinozoisite in associated chlorite schist form large porphyroblasts, some of which are optically continuous grains five to ten times as large as the matrix grain size. In some parts of the muscovitic quartzite and feldspathic schist, muscovite occurs as flakes several times larger than the average for the unit and with a very weak preferred orientation. The amoeboid patches of untwinned plagioclase in these units probably represent enlargement of matrix plagioclase, for the large xenomorphic and poikiloblastic grains include smaller parallel-oriented grains, indicating post-tectonic growth. The sillimanite tufts which occur in the quartzite underlying La Madera Mountain are believed to be the most reliable indicator of a later metamorphic event. These aggregates of acicular prisms are randomly distributed in the quartz mosaic and the tufts form three-dimensional patches throughout the rock. One of the most puzzling features of the sillimanite occurrence is the absence of any spatial relationship of sillimanite to either kyanite or andalusite in the same rock. The sillimanite porphyroblasts exhibit no tendency to nucleate on the kyanite prisms or andalusite veinlets, which are clearly older. In the writer's opinion, this is not expectable regardless of whether the sillimanite formed by diffusion in a dry environment or through growth induced by hydrothermal solutions.

Several lines of evidence suggest that the features described above and the metamorphic event they indicate occurred after the second stage of deformation and prior to the third deformation. First, enlarged crystals would not be expected to preserve a random orientation through a period of regional folding accompanied by considerable flowage of material. Although second-deformation structural features are

not so uniformly developed regionally as first deformation structures, large porphyroblasts of mica, hornblende, kyanite, and sillimanite are present in many places. Also, some of the most striking specimens of transverse mica and hornblende occur in the tightly folded belt along the east flank of Mesa de la Jarita. The only direct evidence which establishes the metamorphic event in time prior to the third cataclastic deformation is found in the sillimanite-bearing quartzite of La Madera Mountain and the chlorite schist north of the Sunnyside mine. In the former, sillimanite bursts and individual prisms are cut by third deformation fracture cleavage as are the andalusite veinlets. Parts of the sillimanite needles have been removed by solution where the fracture cleavage intersects them. In the latter, the chlorite schist is cut by third deformation fracture cleavage which passes through idiomorphic hematite pseudomorphs after pyrite and individual garnet idiomorphs. Thus, there is strong evidence for placing the thermal event between the second and third regional dislocations. However, there are no data available that justify an estimate of the duration of time during which the metamorphic processes were active or the amount of time between the two periods of deformation.

The presence of specularite in all rock types indicates that the partial pressure of oxygen was high at one time during the evolution of the metamorphic rocks. Quartzite and muscovitic quartzite best exhibit the textural evidence for this phenomenon. Nearly all the hematite laminae consist of xenomorphic specularite either rimmed or intimately intergrown with sphene or rutile. The distribution and the lack of preferred orientation of these mineral aggregates suggest that an original iron-titanium mineral dissociated and recrystallized in the form of separate titanium and iron phases in an isotropic stress environment. In several thinsections of quartzite, this same association occurs in second deformation axial-plane cleavage, indicating that the reconstitution in an oxidizing environment took place after the second deformation. It appears that this reconstitution is genetically associated with the thermal event already discussed, although no direct evidence was found which would establish the time of change in oxidizing conditions prior to the third deformation.

Pegmatitic Metasomatism

A phase of pegmatitic metasomatism of local significance can be identified in La Madera quadrangle. It has resulted in the conversion of chlorite and hornblende to biotite, minor feldspathization and muscovitization, and the introduction of tourmaline. The products of introduced potassium and sodium, although restricted to small areas, occur in several localities in the Petaca district. The occurrence of tourmaline in pegmatites closely associated with tourmaline-bearing plagioclase-chlorite phyllite is restricted to the central part of the western scarp of Mesa de la Jarita.

Biotite-bearing varieties of hornblende-chlorite schist have already been described in detail. They appear in sec. 32, T. 26 N., R. 9 E. and in secs. 17 and 18, T. 25 N., R. 9 E. near the confluence of Canon de los Alamos and Canon de la Paloma. A layer, two to three feet thick, of biotite schist completely enclosed by muscovitic quartzite crops out in a roadcut in SW1ASW1A sec. 8, T. 25 N., R. 9 E., but is too small to appear on the map. All the biotite-rich phases are closely associated with exposed pegmatites and are enclosed by muscovitic quartzite and feldspathic schist containing an abnormally high muscovite content. Many books of biotite and muscovite cut across the schistosity. These textural relations suggests that the regrowth of muscovite and formation of biotite after chlorite and hornblende occurred in an isotropic stress environment with the pre-existing schistosity acting as a structural control for the migration of the potassium-bearing pegmatitic solutions.

The pegmatite which crops out near Salt Lick Spring in sec. 8, T. 25 N., R. 9 E. is surrounded by an aureole containing porphyroblastic muscovite and garnet. The biotite schist mentioned above, which is not shown on Plate 1, lies within this metasomatic aureole and demonstrates the genetic relationship between pegmatitic emanations and introduction of potassium into hornblende-chlorite schist. The garnetiferous aureole surrounding this pegmatite has a thickness of about 150 feet and constitutes the largest observed zone of alteration associated with a pegmatite.

Thin sheaths of feldspathized and muscovitized wall rock surround many of the pegmatite bodies in the map area. The distribution of introduced feldspar and muscovite has been described in detail by Jahns (p. 53), who recognized a wide range in the degree of alteration surrounding the emplaced pegmatites.

Some of the pegmatite bodies were confined between the walls of the fractures into which they were injected and the adjacent country rock has been little affected by them. Others broke through the fracture walls to send out many small branches or apophyses, and still others literally soaked through the walls both before and during their consolidation.

The pegmatite with its wide zone of alteration exposed near Salt Lick Spring is an example of the latter type. Pegmatite dikes with an alteration zone only a few inches thick crop out in the fresh roadcuts within NW1/4 sec. 17, T. 25 N., R. 9 E.

Metasomatic tourmaline spatially related to tourmaline-bearing pegmatites is illustrated in secs. 26 and 35, T. 26 N., R. 8 E. Plagioclase-chlorite phyllite near the west-trending fault and north along the strike of the unit contains from 14 to 60 per cent schlorite. In this same area, west-trending, quartz-rich, tourmaline-bearing pegmatites three to four feet thick with an exposed strike length of from five to twenty feet are

enclosed in muscovitic quartzite. The tourmaline content varies from place to place within a single pegmatite. Some concentrations exceed 80 per cent of the rock.

No tourmaline-bearing pegmatites were observed in any other part of the quadrangle. The close spatial relationship of the tourmaline-bearing pegmatites and the tourmaline-bearing schists suggests a genetic relationship. However, no tourmaline-bearing pegmatites were observed to intrude the tourmaline-bearing schists and no tourmaline was observed in the muscovitic quartzite which encloses the pegmatites.

Petaca Aureole

Just (p. 43) considered the muscovite in muscovitic quartzite to have been metasomatically introduced into typical quartzite by emanations from the Tusas granite. Barker (p. 87), in a discussion of pegmatitic-hydrothermal metamorphism in Las Tablas quadrangle, notes that "... two general rock types have been affected by an aureole of metamorphism that surrounds the area of pegmatites on Mesa de la Jarita." He asserts, "The direct association of the altered quartz-feldspar rocks and amphibolite with the La Jarita pegmatites implies that fluids emanating from the pegmatites were the cause of the alteration." The southern extension of the pegmatite area referred to by Barker as the La Jarita pegmatites includes the Precambrian rocks exposed in the Cribbenville district and the schists and muscovitic quartzite which underlie and flank Mesa de la Jarita. On the basis of structural data, the thesis of Just is possible, but Barker's contention that the muscovite-rich rocks in the Petaca area are the result of pegmatitic metasomatism is untenable, as shown below.

Small-scale structural features associated with the first deformation are constant in style and orientation in the granitic gneiss (Tusas granite of Just which was subdivided into the Tusas and Tres Piedras granite by Barker) and in all other metamorphic map units within the area. That is, they are uniformly developed throughout the Precambrian rocks, excluding the pegmatites. The presence of first deformation structures in the granitic gneiss and the gradational nature of the boundary between this unit and the muscovitic quartzite-feldspathic schist complex in the Cribbenville district indicate that the granite (or granitized sediment) existed prior to the regional metamorphism which affected this area. Hence, the hypothesis that granitic intrusion accompanied by metasomatism that affected a wide area around the granite before the first deformation is acceptable in view of the available structural evidence.

The thesis that the muscovite content of the feldspathic schist and muscovitic quartzite is directly related to pegmatites which intrude the Precambrian is untenable for two reasons. First, the muscovitic layers in

feldspathic schist and muscovitic quartzite define the first deformation axial-plane cleavage and b-lineation. The preferred orientation of muscovite demonstrates internal rotation and penetrative componental movement. The monoclinic fabric indicates the presence of the deformation plane normal to first deformation fold axes. There is no evidence to support the contention that muscovite has formed as a growth fabric controlled by bedding planes. Second, pegmatite dikes have been intruded along third deformation axial-plane cleavage which truncates older structures. The occurrence of the pegmatites has been preceded in time by three periods of deformation and an episode of granite intrusion or granitization. There is ample evidence of pegmatitic metasomatism in aureoles surrounding the emplaced bodies, but this process should not be regarded as an explanation of the muscovite content of feldspathic schist and muscovitic quartzite.

STRUCTURAL GEOLOGY

Detailed investigation of Precambrian rocks which underlie nearly one half of La Madera quadrangle reveals the presence of three spatially and temporally distinct systems of folds. This interpretation is based upon the collection of data regarding the style, orientation, and superposition of small-scale planar and linear structural elements. The over-all structural interpretation which constitutes the Precambrian structural history hinges upon a few fundamental assumptions and the valid ordering of detailed structural data into a geologically rational scheme.

Structural study of the Precambrian rocks has produced the following results. First, the form and style of three distinct fold systems have been established. The areal distribution, attitude, and trend of individual folds have been determined for the second and third fold systems. Second, the geometry and interference effects, resulting from the superposition of successive stages of pervasive regional deformation, have been to a large extent determined. Third, the temporal relations of the superposed fold systems have been established. This is not meant to imply that each folding event has been assigned an absolute age or that the amounts of intradeformational time have been determined, but only that the relative order of superposition of spatially distinct fold systems has been resolved. Structural data are shown in map form (pl. 1) and as stereographic projections (pl. 2).

It is conceivable that the results of this local detailed structural study may contribute to a better understanding of regional Precambrian structural trends in New Mexico. If the conclusions presented herein stimulate a more detailed approach to the examination of Precambrian exposures within the state of New Mexico and vicinity, it will have served a useful purpose.

PLANAR STRUCTURES

Planar structures are well developed in all exposures of metamorphic rocks examined. With the exception of bedding, all planar structures identified and mapped in the field are of tectonic origin. No evidence of a primary magmatic foliation exists in the granitic gneiss which crops out in the eastern and northeastern parts of the quadrangle.

Bedding

The identification of bedding in metamorphic rocks is of major importance. Once a planar element is designated bedding in a metamorphic sequence, it becomes the fundamental building block in reconstructing structural and stratigraphic history. Conversely, if bedding can not be recognized, there is no firm starting point. Reconstruction of structural history must start with the earliest recognizable structural elements and important questions of original sedimentologic and stratigraphic conditions may be indeterminate. Although the latter alternative may leave the geologist uneasy, it is preferable to a completely erroneous reconstruction based on an uncritical acceptance of any compositional layering as *prima facie* evidence for bedding. For these reasons, several mechanisms are discussed which may result in planar features easily mistaken for bedding.

Compositional layering is the planar feature most commonly designated as bedding in metamorphic rocks. Observation of sedimentary rocks substantiates the fact that alternating laminae of contrasting composition represent bedding planes or sedimentation units, and it is known that such primary compositional intercalations may be preserved as thinly laminated metamorphic rocks.

Similar-appearing sequences of interlaminated metamorphic rocks may also be produced by metamorphic differentiation and/or metasomatic activity along pre-existing planes of structural weakness. Turner (1948, p. 137), with respect to the former, states that ". . . metamorphic differentiation has now assumed an established status among the recognized processes of rock metamorphism. . . ." Perhaps the best example of the regional development of contrasting mineralogic lamination related to a structural planar element as opposed to bedding is afforded by the Otago schists in New Zealand (Turner, p. 144); isochemical metamorphism of graywackes has resulted in a sequence of laminae alternately rich in quartz-albite and chlorite-albite-epidote.

Evidence for metasomatic activity resulting in compositional layering is present in La Madera quadrangle. Along the margin of the amphibolite exposed east of Ancones, biotite has grown at the expense of chlorite in axial-plane cleavage. The product of this process is a prominently layered rock composed of biotite-rich layers interspersed with chlorite-hornblende-epidote-plagioclase matrix.

Compositional layering unrelated to original bedding may also arise through intense regional shearing. *Hartschiefer*, the recrystallized mylonite commonly found in Europe and Scandinavia, is characterized by a striking alternation of layers produced by the natural milling of rock under high pressure followed by bulk recrystallization.

Schistosity is sometimes considered a reflection of bedding in terranes containing moderate- to high-grade metamorphic rocks. The simplifying assumptions generally are made that the growth of a micaceous phase is controlled by static load, the classical "load metamorphism"; is facilitated by interbed shear during folding; or mimetic crystallization emphasizes pre-existing bedding planes. Detailed and critical investigation has generally revealed little direct evidence that such processes are significant in the development of schistosity. Gilluly (1934, p. 182-201), for example, investigated the schists of the Shuswap Series, presumably a classic example of "load metamorphism," and found fabric evidence to support the contention that schistosity formed by componental movements. Interbed shearing movements could conceivably contribute to the formation of schistosity parallel to bedding, but such a mechanism is by definition restricted to the genesis of concentric folds which are relatively uncommon in metamorphic rocks.

In areas where folding is completely isoclinal, original bedding is parallel to the axial plane of individual folds, except in fold hinges. The statement of many writers that "schistosity is parallel to bedding except in the noses of folds" attests to the frequency of this process. The statement that "schistosity is parallel to bedding" is not sufficiently explicit, for this condition may obtain because of isoclinal folding or through a process of static mimetic recrystallization. The question of whether schistosity represents bedding in a given area can only be answered convincingly by a detailed and critical study of all aspects of the metamorphic terrane.

To summarize, the recognition of bedding in a given area of metamorphic rocks should be given critical consideration for two reasons. First, the recognition of bedding in an area constitutes a fundamental conclusion upon which structural history is built. Second, there is a variety of processes whose end result is the formation of compositional layering. Before any planar element may be justifiably designated bedding, it must be subjected to a thorough and critical analysis.

In Precambrian rocks which underlie La Madera quadrangle, some arcuate layers composed principally of specular hematite and zircon are believed to be relic bedding. Groups of arcuate layers are commonly arranged within tabular domains, here termed *sets* and outlined in Figure 5. Where the hematite layering is best developed, parallel sets of arcuate layers are continuous throughout individual outcrops. The average set thickness is about six inches. The quartzite layers within a set range in thickness from vanishingly small up to about one foot. Their average thickness is about four inches. The average length

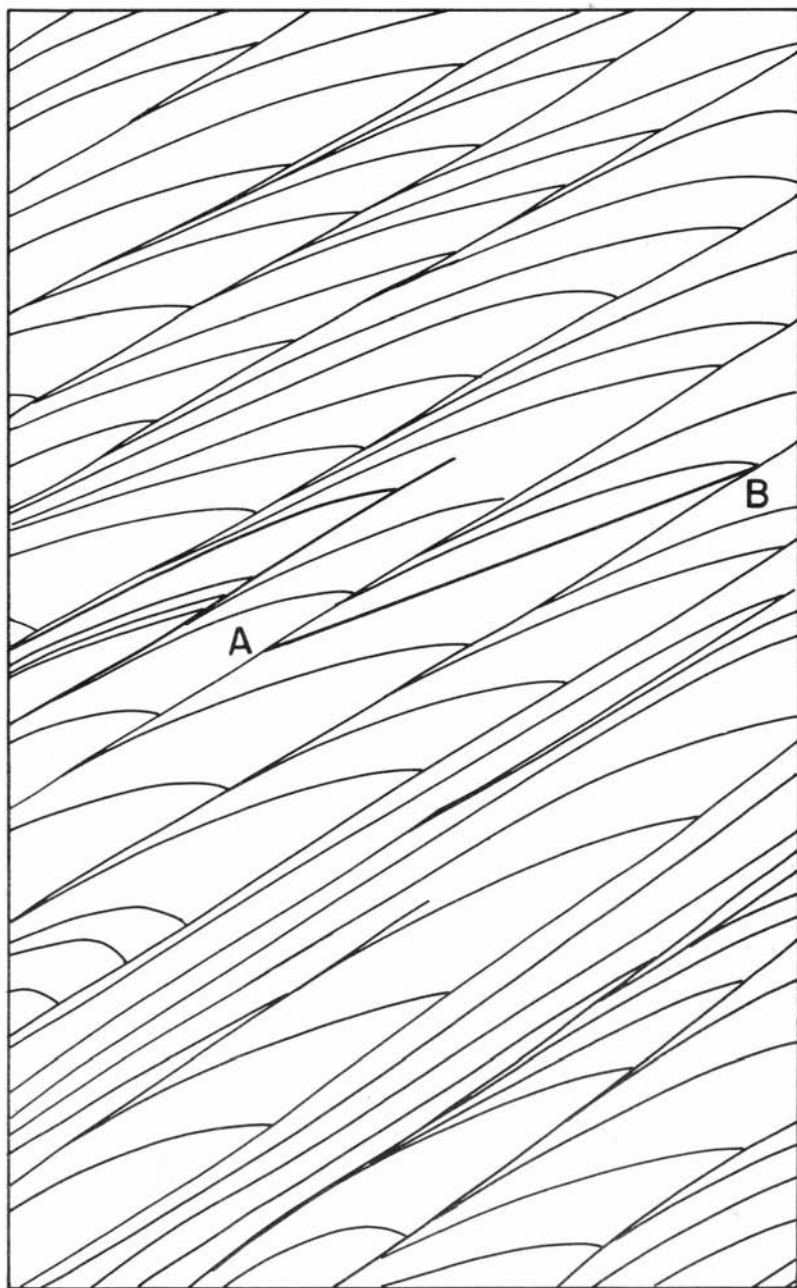


Figure 5

SKETCH OF QUARTZITE OUTCROP SHOWING GROUPS OF ARCUATE LAYERS

of the arcuate layers, as shown by the line A-B in Figure 5, is about two feet. There is considerable variation in the length of layers, however, which ranges from less than six inches to about five to six feet. The association of zircon in the gray-black laminae was described earlier in the discussion of the kyanite quartzite, and it was there concluded that the zircon-opaque concentrations were most readily explained by assuming concomitant deposition in a sedimentary environment; that is, that they represent bedding.

The radius of curvature of the arcuate layers is variable. Within a single quartzite exposure, the arcuate hematite laminae range from nearly flat to sharply curved with a radius of curvature on the order of several inches. This variation exists in sets measured normal as well as parallel to the greatest planar dimension. In a few quartzite outcrops, individual laminae contain an inflection point and in rare instances are recurved as illustrated in Figure 6. The laminae in these exposures range from the simple arcuate form, tangential to the set boundary at one termination and sharply truncated by the set boundary at the other end, through hook-shaped to an asymmetric S-shaped form with both terminations tangential to the set boundaries. These forms are best illustrated in exposures at an elevation of 7400 feet on the nose of the quartzite ridge, SW1/4 sec. 2, T. 25 N., R. 8 E. At this exposure, the axial lines of the S-shaped and hook-shaped laminae are coincident with the line of intersection produced by the intersection of the intra-set arcuate layers with the set boundaries. This linear element has a bearing of S. 20° W. and a plunge of 40° W.

Sets of arcuate layers exposed in the quartzite of the Ortega Mountains have an average strike and dip of N. 30° W., 35° W. By inspection, only 1 to 2 per cent of the intraset layers are concave upward; the remainder are concave downward.

As noted earlier, the amphibolite exposed on the west-facing scarp of Mesa de la Jarita east of Ancones contains irregular, crudely planar zones of small quartz-feldspar blebs which are parallel to the amphibolite schist contact. If the blebs are relict amygdules, these zones could represent a marginal surface parallel to the upper boundary of a flow, and, as such, might well be parallel to original bedding in overlying sediments.

Planar zones of quartz augen in a matrix of fine-grained xenomorphic hematite and quartz are common in quartzite exposures and are fully described in the section *Metamorphic Petrology*. If these layers are interpreted as relict pebble beds, as implied by Barker (p. 10), the zone margins represent bedding planes. These zones are typically discontinuous along their strike and are concordant with sets of arcuate laminae. Because of the possible tectonic origin of these "pebbly" zones, as discussed under *Relict Structures* and *Structural History*, they are not accepted as strong evidence of original bedding.

The amphibolite-muscovitic quartzite contacts exposed east of



Figure 6

SKETCH OF QUARTZITE OUTCROP SHOWING SIGMOIDAL, RECURVED, AND
TRUNCATED HEMATITE LAYERS

Ancones probably represent bedding because the fold form resulting from the first deformation is recognizable. Where recognizable fold forms are absent, this reasoning can not be extended to other lithologic boundaries that are concordant with first deformation axial-plane cleavage. Because of pronounced tectonic transport and attenuation which accompanied the formation of the first deformation fold system, it is possible that many of the contacts between Precambrian map units are structural and not depositional.

Flow Cleavage

Flow cleavage as defined by Leith (1905, p. 23) and used in this report is "the cleavage dependent on the parallel arrangement of the mineral constituents of the rock." In La Madera quadrangle it is best developed in rocks containing more than 30 per cent mica, but it is readily recognizable in amphibolite which contains an abundance of prismatic hornblende. In the former, flow cleavage is synonymous with schistosity.

Flow cleavage is present in all metamorphic rocks of the area. In quartzite, it is marked by layers rich in kyanite and sillimanite whose long and intermediate axes lie within the plane of flow cleavage. With a decrease in the kyanite and sillimanite content, flow cleavage in quartzite grades into foliation. Flow cleavage in muscovitic quartzite consists of alternating quartz and muscovite laminae. Within the muscovite layers, large (0.5 to 2.0 mm) individual flakes are subparallel and commonly have a preferred orientation in two sets with a dihedral angle of 5 to 10 degrees. In feldspathic schist, flow cleavage consists of minute sericite flakes (<0.1 mm) arranged in subparallel trains throughout the matrix of the rock. Some specimens of feldspathic schist exhibit a pronounced lamination due to alternating sericite and quartz-feldspathic layers. Typically, however, the sericite flakes are uniformly distributed throughout the fine-grained matrix. In nearly all samples of feldspathic schist, the flow cleavage marked by minute mica flakes is deflected around quartz blebs and feldspar idiomorphs. Uniformly distributed subparallel plates of biotite and/or muscovite define flow cleavage in granitic gneiss. In this rock, however, the micas are similar in size to the muscovite in muscovitic quartzite, rather than being minute flakes as in feldspathic schist. Flow cleavage in the amphibolites is the result of a high degree of preferred orientation of hornblende prisms and chlorite flakes. In quartz-albite-muscovite-biotite schist, flow cleavage is equivalent to schistosity as delineated by the subparallel arrangement of ubiquitous muscovite and biotite.

Fracture Cleavage and Slip Cleavage

Leith (p. 139) defined fracture cleavage as "a capacity to part along parallel planes, usually in intersecting sets, along which there has been

either incipient fracturing or actual fracturing followed by cementation or welding." He broadened the definition by stating that fracture cleavage is a structure which develops in shearing planes. Thus he added a genetic facet to an otherwise descriptive formulation. Slip cleavage was considered by Leith to be a variety of fracture cleavage best developed in micaceous rocks. Fracture cleavage, *sensu stricto*, is marked by minute close-spaced fractures which pass through component crystals of the fabric, whereas slip cleavage involves the dislocation and rotation of an earlier planar element in such a way as to produce sets of micro drag folds, waves, and wrinkles. Hence, slip cleavage is always associated with direct evidence of shear and rotational effects and is not included with fracture cleavage in this report.

The terms *fracture* and *slip cleavage*, though primarily descriptive, indicate a later deformational event when found to be superimposed on an earlier metamorphic structure. When found in schists whose schistosity is an axial-plane cleavage, fracture and slip cleavage are *prima facie* evidence of superposed deformation. This generalization is based upon the observations of many geologists in which these types of rock cleavage parallel axial planes of superposed folds.

The genetic connotations of fracture and slip cleavage admittedly weaken their usefulness, and in using these terms, a purely descriptive approach to the mapping of such structures is virtually impossible. Yet, in the opinion of this writer, the alternative of designating various planar elements as S-planes is less desirable. The introduction of the expression *S-plane* by Sander (1930) for a set of parallel planes of mechanical inhomogeneity permits a purely descriptive approach, in general. However, most studies incorporate specific usage of S-planes; for example, **S₁**—bedding, **S₂**—schistosity, **S₃**—younger schistosity based on local evidence of superposition. These terms used specifically have greater genetic association than Leith's terms discussed above, for their designation is based upon a recognition of all the criteria requisite for the identification of fracture and slip cleavage, and they conclude an identity or grouping based upon an interpretation of relative age.

For these reasons, Leith's terms *fracture* and *slip cleavage* were used in mapping the small-scale structural features in the metamorphic complex. However, another problem is encountered in applying these terms to planar structures in La Madera quadrangle. It is that Leith's terminology applies to end member phenomena which are a response to the independent variables of rock composition, chemical environment, and pressure-temperature realm. Fracture cleavage represents dislocation by brittle failure, yet its development in rock may be enhanced by the recombination of various mineral components in such a way that new minerals may grow in the fracture cleavage plane. Such a process may occur during a single deformational phase or, more commonly, it may be the result of superimposed tectonic, chemical, and thermal events. A bedded sequence of sandstone and shale, metamor-

phosed once, may be expected to exhibit many examples of planar structures which are distinctly fracture cleavage or slip cleavage. But if the same sequence of rock is subjected to several successive metamorphic events, the earliest structural features become blurred by growth of new minerals and further dislocation. What formerly were distinct examples of end member categories of structural features now exhibit features of both end members and fall in a broad medial zone not amenable to a "pigeonhole" approach to classification.

A wide range of style is exhibited by the planar structures in the Precambrian of La Madera quadrangle. Fracture cleavage as defined by Leith is common in nearly monomineralic quartzite. It generally consists of close-spaced (0.5 to 2.0 mm) fractures visible as hairlike lines on joints and other planar structures. Likewise, well-developed slip cleavage is present in many outcrops of quartz-albite-muscovite-biotite schist. The majority of measurements, however, is from exposures of feldspathic schist and muscovitic quartzite and it is in these rocks that the broad area of overlap exists. Figure 7 illustrates the character of a superposed planar structure on an earlier flow cleavage. The specimen consists of tablets or plates bounded by subparallel shear fractures. Within the plates, the older flow cleavage has been contorted into sinusoidal and attenuated S-shaped crenulations. In this sample, the younger shear planes best fit the criteria for slip cleavage; yet, in the same outcrop, only six inches from where this sample was taken, the shear planes transect the flow cleavage with no visible rotation or deflection of the older planar element. The recognition of such circumstances has led to considerable latitude in the application of the terms *fracture cleavage* and *slip cleavage* in exposures of muscovitic quartzite and feldspathic schist. The significant point is the recognition of superposition of structural elements, and little significance should be attached to the categorical identification of fracture cleavage or slip cleavage in these two rock types.

In this report, crudely parallel fracture planes within quartzite which do not cut across individual quartz grains are termed *relict fracture cleavage*. This structure is transitional into flow cleavage in samples which contain more than 5 per cent kyanite or sillimanite on the cleavage planes. The cleavage planes are parallel or nearly parallel to hematite layering in quartzite, except in the cusplike terminations of arcuate hematite layers where they transect compositional layering at high angles. Where observed, relict fracture cleavage planes are invariably close-spaced, ranging from less than a millimeter up to one centimeter. In hand specimen, they are similar in appearance to fracture cleavage and parallel to the axial planes of isoclinal folds. In thin-section, however, planes mapped as relict fracture cleavage were never observed to transect individual quartz grains in the fabric of the rock.

Two styles of shear planes were mapped as slip cleavage. Planes of dislocation and translation parallel to the axial planes of microcrenu-

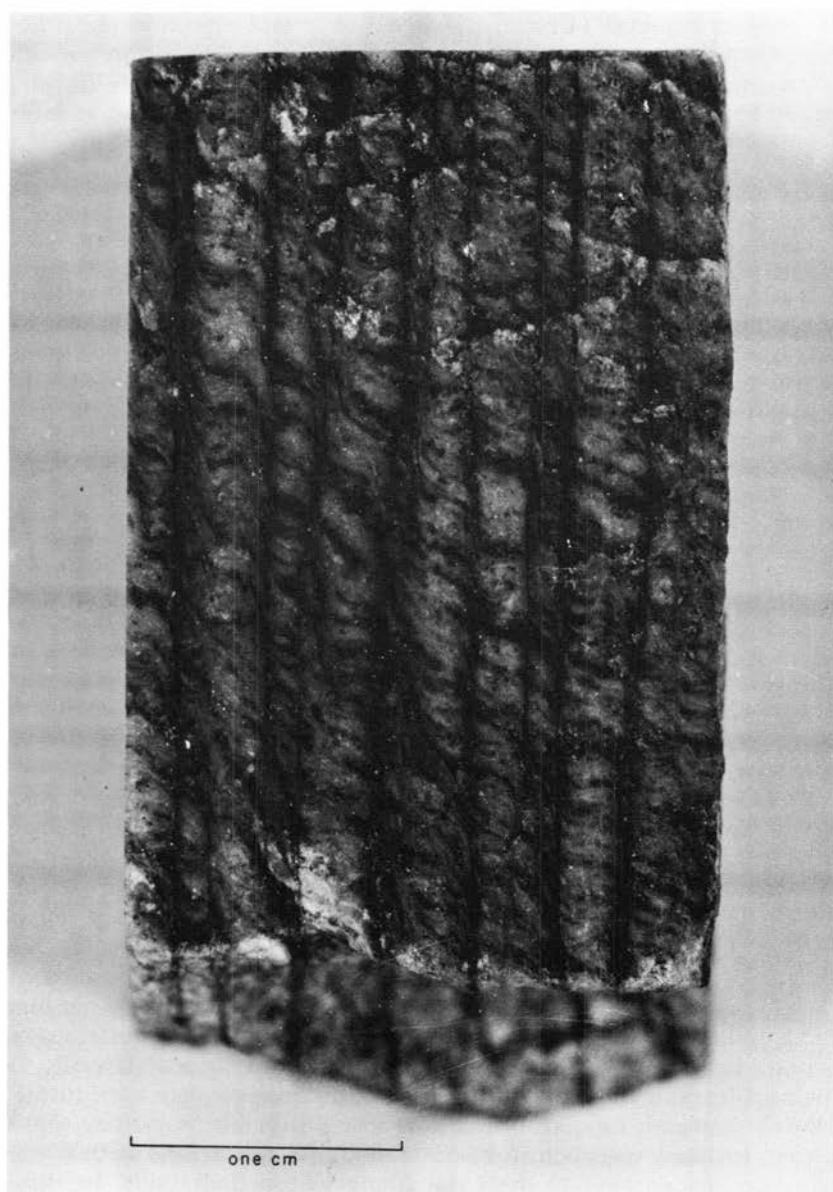


Figure 7

SLIP CLEAVAGE TRANSECTING SCHISTOSITY IN FELDSPATHIC SCHIST

lations and corrugations constitute the most common type of slip cleavage. Most shear planes of this type are close-spaced (less than 1 cm apart) and developed extensively in individual outcrops. That this type of slip cleavage grades into schistosity can be demonstrated in an isolated outcrop of quartz-feldspar-muscovite-biotite schist in the NE $1/4$ sec. 7, T. 25 N., R. 9 E. The schistosity of this rock consists of very close-spaced slip cleavage planes (<1 mm). An older schistosity marked by finely comminuted mica flakes now forms very tightly compressed microcorrugations whose limbs are nearly parallel to the slip cleavage planes. This sample of schist demonstrates that at least some schistosity in La Madera quadrangle is formed through rotational componental movements, suggesting the mechanical equivalency of slip cleavage and schistosity. This postulate is in accord with the similar findings of White (1949, p. 587) in east-central Vermont. The less common style of slip cleavage consists of wide-spaced shear planes. Interslip-plane distance ranges from about 1 inch to greater than 50 feet. The average spacing is about 1 foot. No systematic variation was observed in the interslip-plane distance. In hand specimen, the individual slip-planes are similar in appearance to the more common style of slip cleavage. In highly schistose rocks, the slip cleavage is the result of bending of older micaceous layers into the shear plane. In prominently laminated feldspathic schist, the shear plane is marked by a zone in which the micaceous laminae are bent and the quartzo-feldspathic laminae are splintered.

The origin of the rare, widely spaced slip cleavage planes is largely unknown. The fact that they are a shear phenomenon is attested to by the physical nature of the planar dislocation and slip movement. It is not known, however, whether they were formed during the terminal phase of a regional deformation, or whether they are in some way associated with the regional fault pattern as antithetic shear fractures.

Joints

Joints in La Madera quadrangle may be classified in one of three categories: (1) extension joints, (2) mineralized joints, and (3) other joints. The third group includes nearly all joints in the area. The first category includes joints exhibiting plumose surfaces, the so-called "feather fractures." The second group consists of isolated fractures that exhibit evidence of introduction or loss of material along the joint surface. An example of introduction along joint surfaces is exposed on the Old Petaca road 1.4 miles east of Vallecitos. One joint of a set cutting feldspathic schist exhibits a zonal arrangement of limonite, quartz, K-feldspar, and muscovite, as shown in Figure 8. Altered joints occur in amphibolite east of Ancones. The joint surfaces are bounded by a 1- to 2-inch-thick zone in which hornblende is absent.

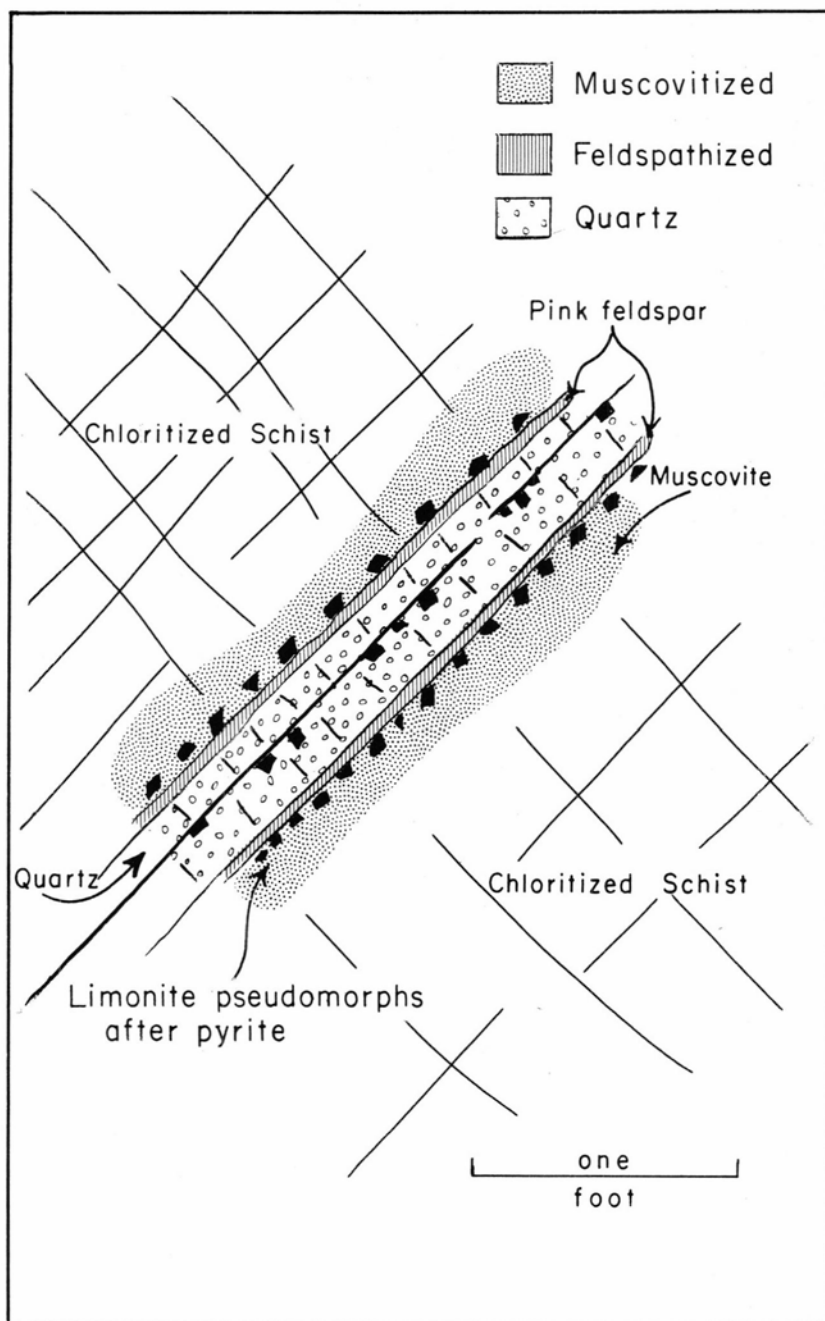


Figure 8
ALTERATION HALO AROUND JOINT IN MELANOCRATIC PHASE OF
FELDSPATHIC SCHIST

The hornblende-free zone is marginal to a quarter-inch fringe rich in limonite that grades into normal amphibolite. Altered points are uncommon and probably represent joints of group one or three along which chemical interchange has taken place. The circulation of pegmatitic, hydrothermal, or meteoric fluids could account for the observed alteration.

It is difficult to classify parallel fractures as fracture cleavage or joints when the spacing between planes is on the order of several inches. Most fracture cleavage planes are close-spaced, less than 1 inch, but the spacing can range as high as 30 to 50 feet. Most joints have an interplanar spacing of from 2 to 5 feet but can range down to a fraction of an inch. Because of this overlap in interplanar distance, some joint sets have probably been included as fracture cleavage and vice versa in mapping the Precambrian. This error due to overlap is reduced somewhat by two factors. First, close-spaced extension fractures were mapped as joints because they are not shear phenomena, hence, are not fracture cleavage by definition. Second, wide-spread fracture cleavage planes are in some instances associated with drag folds as axial-plane cleavage, thus ruling out the possibility of including them in the category of joints. For these reasons, an error due to overlap exists but is not considered significant in the structural analysis of this area.

Relationship Between Rock Cleavage and Folds

In all instances where flow cleavage, fracture cleavage, and slip cleavage are found associated with drag folds in individual outcrops, these planar structures are subparallel to parallel to the axial planes of small-scale folds. In relatively open folds, incipient or well-formed cleavage is parallel to fold axial planes within the error of field measurement. In appressed folds in which there is evidence for flowage of material, flow cleavage and slip cleavage planes are subparallel to the axial planes and commonly are arranged in a fan shape. In appressed and attenuated isoclinal drag folds, flow cleavage is parallel to the axial planes. The disposition of rock cleavage as parallel versus subparallel to the fold axial plane is believed to be a function of the influence of "flattening" movements during deformation and of the temporal relationship between cleavage and fold form. The latter thesis is considered at greater length in the discussion of folds.

Direct observation has demonstrated that in La Madera quadrangle planes of rock cleavage do not deviate more than 10 degrees from parallelism with the axial planes of associated drag folds. On the basis of this evidence, it is assumed that rock cleavage measured in outcrops devoid of drag folds may be used to define the attitude of fold axial planes at that locality. Stated another way, the generalization that rock cleavage is essentially axial-plane cleavage is accepted. In the

absence of such a premise, the reconstruction of the form and extent of major fold systems would be impossible.

LINEAR STRUCTURES

Linear structural elements, exclusive of fold axes, are omnipresent and well developed in the Precambrian rocks of La Madera quadrangle. Mineralogic lineation, resulting from the preferred orientation of prismatic and platy minerals, is present in nearly all outcrops of metamorphic rocks. Textural lineation within rock cleavage is best developed in quartzite and common in feldspathic schist with relatively low mica content. Lineation produced by the intersection of two planar structures is less common but is evenly distributed areally.

Lineation of all types is genetically related to fold structures. Each generation of folds has associated with it all the above types, but in most places mineralogic and textural lineations are the product of the first deformation.

Evidence for the transposition of early linear structures by later deformation has been found. In the writer's opinion, this process contributes significantly to the difficulty involved in deducing the Precambrian structural history.

Mineralogic Lineation

Lineation resulting from the preferred orientation of prismatic and platy minerals is termed *mineralogic lineation*. This type of lineation is common in all metamorphic rocks of the area but is best developed in amphibolite, quartzite, and quartz-albite-muscovite-biotite schist.

The preferred orientation of hornblende and, to a lesser degree, epidote constitutes a prominent lineation in amphibolite. As noted earlier, the composition and texture are variable among different bodies of amphibolite and within the amphibolite exposed east of Ancones. This compositional and textural variation is directly related to the prominence of mineralogic lineation. The preferred orientation of hornblende, and therefore the prominence of the lineation in outcrop, is best developed in the fine-grained, dense phases of amphibolite. Individual hornblende prisms, averaging 2 mm in length, are set in a quartz-feldspar matrix with their c-axes nearly parallel. The preferred orientation of (110) in hornblende (pl. 3j) results in a slabby parting in the rock. In the heterogeneous marginal phase of the amphibolite east of Ancones, about 80 per cent of the hornblende in one sample exhibits a high degree of preferred orientation of the c-axes (pl. 3m). The remainder of the grains have a nearly random orientation in part modified by growth in a pre-existing planar structure. Hornblende crystals having an apparent random orientation commonly occur as porphyroblasts in a matrix of plagioclase, epidote, and chlorite. In a single hand specimen of the marginal amphibolite phase, individual

hornblende crystals up to 3 cm long cut across the layering of the rock and have no preferred orientation with respect to the lineation defined by most of the small matrix hornblende crystals in the dark-colored bands. The lineation resulting from the preferred orientation of epidote is not evident in hand specimen or outcrop. Evidence for the preferred orientation of this mineral is furnished by measuring the orientation of b-axes in thinsection. Plate 31 demonstrates that epidote possesses a higher degree of preferred dimensional orientation than does hornblende in the same sample.

A prominent lineation defined by the nearly parallel alignment of prismatic kyanite is widely distributed in quartzite. The size of individual crystals composing the lineation has considerable range. The length of kyanite blades ranges from several millimeters up to 3 to 4 cm with an average length of between 1 and 2 cm. There is, however, generally little size variation within individual outcrops. Kyanite lineation is commonly developed on the foliation plane—less frequently on fracture cleavage planes which cut the foliation.

The preferred orientation of kyanite is megascopically similar to the orientation of hornblende in amphibolite. In all outcrops where kyanite was observed, most of the prisms exhibit a parallel alignment. There are always some crystals, however, which have a variety of orientations within the foliation plane. It is also not unusual to find well-developed "sunbursts" of kyanite in the foliation plane. Irregular pods of kyanite containing individual blades up to two inches long were noted in two outcrops of quartzite. The pods have no preferred orientation with respect to foliation in the rock, but blades of kyanite are arranged with their long axis normal to the walls of the pods.

Mineralogic lineation resulting from the preferred orientation of platy or tabular minerals such as feldspar, mica, and specularite is common in quartzite, feldspathic schist, and quartz-albite-muscovite-biotite schist.

Of all the mineralogic lineations encountered in this study, the most vague is that formed by the preferred orientation of tabular euhedra of microcline perthite. This lineation is largely restricted to the small mass of biotite-bearing feldspathic schist which crops out along the east side of the Old Petaca road in the northwestern corner of sec. 15, T. 26 N., R. 8 E. Even though the rock contains a high percentage of feldspar euhedra, the lineation is so ill-defined that its orientation is difficult to determine. The megascopic fabric of this rock differs in two respects from structural features shared by all other metamorphic rocks of the area. First, flow cleavage defined by nearly parallel flakes of biotite is not well developed and, second, where flow cleavage is recognizable, the components of the matrix are not arranged in such a way as to produce a visible textural lineation. It is not known whether the large number of feldspar crystals have contributed to an interfering effect by inducing waves and humps in the flow cleavage, or

whether the irregularity and tenuous nature of the planar structure is the result of processes which are manifested differently in bordering rocks. However, planar and linear structures, prominently developed in neighboring rock bodies, are indistinct in the biotite-bearing feldspathic schist.

Elongate plates of specular hematite arranged in subparallel trains form a lineation in quartzite which becomes visible under magnification. The plates have an approximate length-width ratio of 2:1 to 3:1, are generally less than 1 mm long, and commonly occur in elongate clusters which form a megascopic lineation in the foliation plane.

Muscovite and biotite that comprise flow cleavage commonly form a linear element in the flow cleavage. This is because the axial-plane flow cleavage does not consist of a single plane, but rather a family of nearly parallel planes (usually two or three) which intersect in a group of parallel lines. These planes have a very small dihedral angle, generally on the order of 5 to 10 degrees. When a specimen of rock is broken along the flow cleavage, the rock tends to part along one or more of the nearly parallel planes. Thus, where the rock parts along one of the planes, micas with a preferred orientation in conjugate planes of the same family appear as lines marked by subparallel mica flakes which dip into the cleavage plane at low angles. Lineation of this type is most readily recognized in rocks containing biotite and muscovite because of the strong color contrast. In rocks containing either all muscovite or all biotite, the lineation is not nearly so obvious.

Textural Lineation

Wrinkling, fluting, streaking, quartz-feldspar-epidote segregations in amphibolite, "stretched pebbles" in quartzite, and fragments in tectonic breccia are grouped as textural lineations. In interpreting lineation according to process, the first and last classes could be considered as groups induced by superposed structural features, while the remainder are the result of the first deformation.

Wrinkling and minor crenulations are common in schistose Precambrian rocks (figs. 9a and 9b). They are essentially microfolds with amplitude and wave-length dimensions seldom exceeding 5 mm. Where this feature is present in muscovitic quartzite, the mica laminae are corrugated, but the quartz interlayers are apparently undisturbed. Axes of individual crests and troughs are generally persistent across many feet of outcrop. Wherever wrinkling lineation was observed, the folded or crenulated micaceous layers contained a mineralogic or fluted lineation. In the muscovitic quartzite which crops out along the west-facing scarp of Mesa de la Jarita, there occur many segregations of clear to milky quartz. These "quartz eyes" are flattened spheroidal shapes which range in size from one to two inches up to about one foot in diameter. Small corrugations on the shells of these bodies invariably

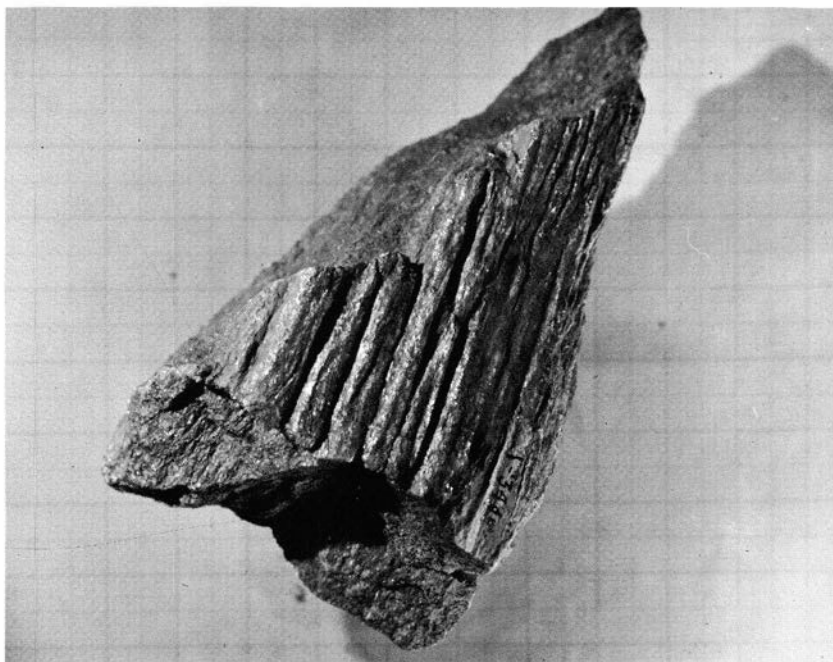


Figure 9a

CRENULATED SCHISTOSITY IN MUSCOVITIC QUARTZITE

wrap around the periphery, and consequently they have a nearly random orientation. The wrinkles are probably the result of slippage in the micaceous shell during regional deformation of the enclosing rocks. They are not recorded on the map because of their local derivation and nonsystematic relationship to similar structures in the host rocks.

Textural lineation consisting of elongate flattened swells and hollows is herein designated *fluting*. It is best developed in the dense, flinty variety of feldspathic schist and in quartzite. It is a striking feature in outcrop where it appears as prominent linears similar in style and orientation within the limits of individual exposures. It closely resembles a micromullion structure. This type of lineation is the result of mutually intersecting planes of low dihedral angle which constitute the axial-plane flow cleavage. Fluting lineation and mica lineation are consanguineous and parallel. Where these two types of lineation occur together, fluting is always megascopically dominant.

Striking lineation consists of crudely parallel, attenuated, fine-grained mineral aggregates. In quartzite, streaks of finely comminuted quartz stand out as elongate white blebs against the gray to blue-gray quartzite. Individual blebs are generally only a fraction of a millimeter

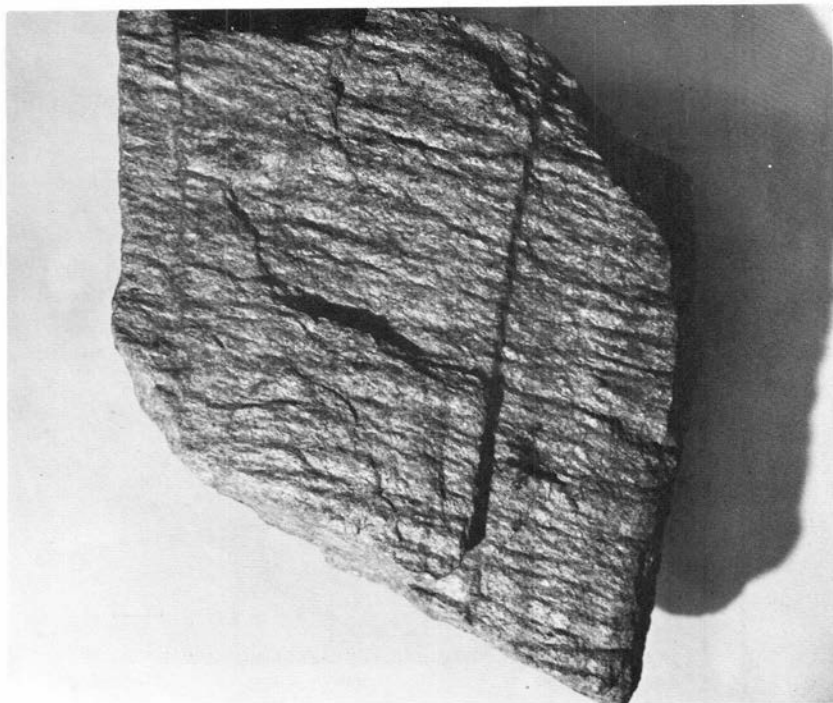


Figure 9b

WRINKLED SCHISTOSITY IN MUSCOVITIC QUARTZITE

thick and range in length from less than one centimeter up to nearly a meter. Width is also variable, but seldom exceeds one centimeter. In several quartzite outcrops, quartz streaks between two and three millimeters thick were observed on a few foliation planes. Where streaking attained this thickness, the blebs were tightly corrugated, yet the axes of the corrugations were parallel to the long axis of the streaks. In quartz-feldspar-mica rocks, streaking is generally marked by segregations of black opaques, pink quartz-feldspar masses, and pale green mica concentrations. Streaking of individual mineral concentrations is present in many outcrops of feldspathic schist in which a fluting lineation is well developed. In all outcrops where both types of lineation are pronounced, they are parallel.

Elongate quartz-feldspar-epidote segregations are a special case of streaking found only in the marginal phase of the amphibolite east of Ancones. The elongate blebs are flattened in the plane of the flow cleavage and commonly have a length-width ratio of about 10:1. In rare outcrops, individual blebs extend several feet across the planar structure, yet are less than a centimeter thick. In all outcrops contain-

ing these elongate segregations, the attitude of the long axis is parallel to the hornblende lineation.

Ellipsoidal coarse-grained xenomorphic aggregates of quartz, so-called "stretched pebbles," constitute a lineation in quartzite. Individual ellipsoids generally have an axial ratio of about 1:1:3. In some exposures, notably in the quartzite hills of the upper Vallecitos valley, the quartz aggregates are extremely attenuated and have an axial ratio of about 1:2:10. These elongate aggregates appear as a prominent lineation on the foliation plane.

Ellipsoidal fragments of fine-grained hematitic quartzite and white quartz have a preferred orientation in all outcrops of the tectonic breccia. Individual fragments are notably flattened and have an axial ratio of about 1:3:8. The matrix of the muscovitic quartzite host rock has weathered out preferentially in many exposures and there remains a forest of quartz and quartzite fragments projecting two to three inches above the surface of the outcrop and plunging steeply south-westward.

Intersecting Planes

A lineation that is the result of the intersection of two spatially and genetically distinct planes is present in many exposures of Precambrian rocks. This type of lineation is best developed in muscovitic quartzite and feldspathic schist which underlie the northern end of Mesa de la Jarita. In this area prominent flow cleavage is transected by younger fracture cleavage and slip cleavage. Micaceous layers which form the flow cleavage appear as pale green irregular lines on the fracture and slip cleavage planes.

Lineation produced by intersecting planes is very important in the reconstruction of major fold systems. It is free of the complex arguments often required to demonstrate the spatial and genetic relationship between folds and mineralogic lineation. If it can be established that rock cleavage in an area is an axial-plane feature, then the line generated by the intersection of rock cleavage and the folded planar element is parallel to fold axes.

Fluting lineation described above is a special case of lineation produced by intersecting planes. The two types of lineation may be similar in aspect, but they are genetically distinct. Fluting, as noted above, is the result of intersecting planes with a small dihedral angle. The whole family of planes which intersect at a small acute angle, taken together, constitutes a single structural element, such as flow cleavage, which reflects a single event of penetrative shear and plastic flow. Lineation produced by the intersection of axial-plane cleavage and an older planar element, however, is the result of two separate events, for example, flow cleavage cut by fracture cleavage, that are the result of deformation under the influence of widely different environments.

Boudins

The term *boudin*, as used in La Madera quadrangle, refers to elongate bodies of rock or monomineralic aggregate that are compositionally distinct from enclosing rock and that exhibit a lens or augen shape in section perpendicular to the elongation. The four types of boudins mapped are (1) epidote in amphibolite, (2) milky quartz, (3) quartzite in schist, and (4) muscovitic quartzite in amphibolite. Boudins of the first and second groups appear to be segregations of material mobilized during metamorphism, whereas boudins of groups three and four appear to be essentially fragments of metamorphic rocks isolated from more extensive masses.

Boudins composed principally of epidote with minor amounts of quartz and feldspar are common in the peripheral zone of the amphibolite exposed east of Ancones. These boudins are not nearly so elongate as the other types recognized. They closely resemble flattened spheroids, with the shortest axis normal to cleavage in the amphibolite and with the long axis essentially parallel to the hornblende lineation. Most of the boudins have an axial ratio of about 1:1.5:3, with the shortest axis ranging in length from one inch up to about one foot. Most of these structures are mineralogically homogeneous, but some exhibit a crude zoning in which an epidote-rich layer one to two inches thick surrounds a quartz-rich core. Two boudins similar in form and size to the zoned boudins discussed above but composed of an epidote-rich mantle surrounding a thulite-quartz core were found in muscovitic quartzite near the base of the west-facing scarp of Mesa de la Jarita about two miles north of Ancones.

White "milky" quartz boudins are the most common type encountered in the Precambrian of La Madera quadrangle. Most of the quartz boudins occur in quartzite, with lesser numbers in feldspathic schist and muscovitic quartzite. The greatest abundance of quartz boudins is found in the kyanite schist which crops out in the Ortega Mountains and in the sheath of sericite schist which encompasses the isolated mass of gneissic feldspathic schist supporting the elongate ridge in the northern part of Mesa de la Jarita. In these two rock types, quartz boudins generally make up an estimated 20 to 40 per cent of the outcrop area.

There are two styles of quartz boudin. Most of the first style are rodlike forms with an axial ratio of about 1:1.5+. The second style consists of elongate, flattened lenses which appear sigmoidal in a section cut normal to the long axis. The shear sense was measured in all boudins of the latter type.

The contact relationship between quartz boudins and host rock is variable. In some boudins, for both types, there is no visible parting at the boudin margin. These boudins are sharply outlined against the host rock by color contrast; yet, under a hand lens, the contact appears

diffuse and ill-defined. Most of the quartz boudins, however, are distinctly separated from the enclosing host, and where they occur on the foliation plane, it is possible to lift segments off the exposed foliation.

Where the rodlike type of quartz boudin was observed in foliated quartzite, folic of the host rock appeared to swell and flow around the individual quartz rods, whereas sigmoidal boudins truncated foliation in the quartzite. The long axes of quartz boudins parallel one of the three sets of fold axes present in the area. Most sigmoidal boudins are parallel to first deformation fold axes, and most simple rods are parallel to second and third deformation fold axes.

Boudins of gray, hematitic quartzite were observed in a single outcrop of quartz-albite-muscovite-biotite schist about 800 feet south of the center of sec. 30, T. 26 N., R. 9 E. In section normal to the long axis, these boudins have the form of flattened ellipses with a short to intermediate axial ratio of 1:2. The length of the shortest axis ranges from three inches to one foot. The boundaries of the quartzite masses are sharp and concordant with the flow cleavage of the enclosing schist. The long axes of these boudins parallel the mineralogic lineation developed in the bordering schist which bears S. 40° W. and plunges 40° S. The boudins are compositionally and structurally identical to the quartzite which underlies the Ortega Mountains.

The largest boudins in the area are composed of muscovitic quartzite and occur within the peripheral zone of the amphibolite east of Ancones. These structures are of giant proportions compared to the boudins discussed above. The longest dimension could not be determined, but the shortest axes range in length from less than one foot up to three feet. Axial ratios in the normal section range from about 1:2 to 1:3. All boudins of this type are located within a few feet of the amphibolite-muscovitic quartzite contact. In one outcrop, the boudin appeared to merge into muscovitic quartzite at one of the tapered ends. The bulk of one boudin was bounded by an attenuated drag fold of amphibolite.

Transposition of Lineation

Sander early recognized that an original layered structure could be deformed by a combination of flexure and slip to such an extent that the originally parallel layers are recognizable only in the crests and troughs of folds (Knopf and Ingerson, 1938, p. 189). He termed this process *Umfaltung*. The details of this process have recently been discussed and given deserved emphasis (Turner and Weiss, 1963, p. 92-96) in reviewing the problems encountered in recognizing true bedding. Unfortunately, the writers, concerned with the process of transposition of structural elements, largely restricted their attention specifically to planar elements and gave less emphasis to the problems raised by the transposition of linear elements.

Unequivocal evidence for the transposition of lineation contained in an older planar element has been observed in several Precambrian rock types. The best example occurs in an outcrop of feldspathic schist along the Old Petaca road east of Vallecitos. This unit contains a well-developed flow cleavage with a prominent lineation marked by fluting, segregations, and the preferred orientation of minute muscovite flakes. In one place feldspathic schist has been transected by a slip cleavage consisting of nearly parallel planes marked by mica segregations, with interplanar spacing ranging from about one millimeter to two centimeters. The older foliation is thrown into sigmoidal flexures whose axes are parallel to the flow cleavage-slip cleavage line of intersection. The zone of penetrative slip cleavage is crudely tabular and about six to eight inches thick. The boundary of the zone is gradational and is the result of the abrupt termination of the slip cleavage planes in feldspathic schist. In hand specimen, schist from the shear zone breaks along the slip cleavage plane. This plane contains two lineations; the most prominent one trends south-southwest, is marked by a faint ribbing or ruling, and is emphasized by the parallelism of small mica flakes. The northwest-trending lineation produced by the intersection of slip cleavage and flow cleavage is less obvious and is marked by the trace of alternating quartz- and muscovite-rich layers (flow cleavage) on the slip cleavage plane. The prominent lineation has been induced on the slip cleavage plane by the rotation of the older flow cleavage, containing its mineralogic and textural lineation, into the slip cleavage plane. This conclusion is also supported by the relations shown in the boundary of the shear zone, where undeformed flow cleavage enters the initial stages of rotation along incipient slip cleavage planes, for the textural lineation in the slip cleavage plane does not appear until some flexing of the flow cleavage has been accomplished. Also, when samples from the shear zone are cut parallel to the slip cleavage well within the individual layers where flexing is not severe, the transposed textural and mineralogic lineation is virtually absent.

The recognition of the existence of transposed lineation is important in the reconstruction of structural history. Inasmuch as historical inference is based upon the style, order, and orientation of small-scale elements including lineation, the correct categorization of these features is critical to the formulation of the structural hypothesis. Perhaps of even greater importance is the confusion that results if transposed lineation is identified as indicating direction of transport or "slickenslide type" of lineation. The usual result of this process is to produce two lineations that intersect at a high angle within a single cleavage plane. Because one of the lineations is parallel to the fold axis, there may be a strong tendency to equate the remaining lineation with direction of slip if its origin by transposition is not recognized. Because of the ubiquitous nature of pronounced lineation in flow cleavage and foliation and the

pervasive character of younger slip and fracture cleavages locally, it is the opinion of this writer that transposed lineation is common in the Precambrian rocks of the mapped area.

Relationship of Lineation to Mesoscopic Folds

Style and orientation are the two parameters by which lineation and folds may be compared. Such comparisons can be made directly in those outcrops where lineations occur in, or are closely associated with, small-scale folds. These structural elements may also be compared statistically by constructing equal area projections of the available data. Conclusions regarding similarities in orientation may be drawn by comparing a diagram of all lineations with a diagram of all fold axes. To compare style of lineations with preferred orientation of lineation or fold axes, it is necessary to construct partial diagrams of lineations separated according to style.

All lineations in the area were found to parallel fold axes. This conclusion is based upon the direct observation of linear elements where they occur with folds. It is also supported indirectly by affinities of style and orientation. Textural and mineralogical lineations, which are everywhere an integral part of flow cleavage and foliation, were observed to parallel the axes of compressed, isoclinal shear folds in which the planar structures constitute the axial-plane cleavage. The axes of folds of this style and orientation uniformly bear and plunge to the southwest. In outcrops exhibiting no folds, but in which there exists a well-developed flow cleavage or foliation with a prominent textural or mineralogic lineation, the lineation has a southwest trend. Because of the similarity in style and orientation, the southwest-trending lineation is believed everywhere to parallel, and be genetically related to, the southwest-trending set of isoclinal folds.

Many exposures illustrate the folding of flow cleavage and foliation about northwest-trending fold axes and, less commonly, about east-west fold axes. The axes of these folds are marked by a line generated by the intersection of axial-plane slip or fracture cleavage with the folded element; that is, flow cleavage or foliation. The mineralogic and textural lineations present in the folded element intersect the axes of the northwest and east-west trending folds at a high angle. In such exposures two lineations are present: (1) mineralogic and textural lineations lying within the folded element and intersecting the fold axes at a large angle and (2) lineation parallel to the fold axes which is generated by the intersection of axial-plane cleavage with the folded element. These two contrasting styles of lineation have a different orientation; however, the genetic relationship between the two types requires some interpretation and inference regarding the origin of lineation in the La Madera quadrangle. This topic is considered in detail in the section *Origin of Lineation*.

Lineation on axial-plane cleavage is of two types. In rocks where fracture cleavage is the axial-plane element, layering in the cleaved rock is reflected as a textural lineation parallel to fold axes. In folds where the axial-plane element is slip cleavage, there are frequently two lineations. One is parallel to the fold axis and is the direct result of intersection of cleavage with the folded element, and the second is transposed lineation derived from mineralogic and textural lineations present in the folded element.

Lower hemisphere equal-area projections of lineation (intersecting planes), lineation (mineralogic and textural), and mesoscopic folds are presented on Plate 3b, a, and c, respectively. By comparing the pattern of submaxima in the diagram of fold axes with the orientation of mineralogic and textural lineations, it is apparent that this type of lineation is preferentially oriented parallel to one set of fold axes; namely, the southwest-trending set. Lineations produced by intersecting planes, however, appear to be related in orientation to the northwest- and eastwest-trending folds. The congruence of maxima representing the preferred orientations of fold axes and lineations is *prima facie* evidence that all lineations in the Precambrian are parallel to systematic regional mesoscopic folds.

Orientation of Lineation

The spatial orientation of the various linear elements mapped in La Madera quadrangle is illustrated by means of lower hemisphere equal-area projection on Plate 3a (mineralogic and textural lineations) and 3b (intersecting planes). Mineralogic and textural lineations exhibit a high degree of preferred orientation indicated by the maximum in the southwest quadrant. This area in projection indicates an average bearing of 20° S to 30° W and an average plunge of 20° to 40° SW. The average attitude of flow cleavage and foliation is indicated by the great circle S_1 (pl. 3e). Because textural and mineralogic lineations are restricted to these planes, S_1 passes through the polar maximum of lineation.

Plate 3g represents the orientation of lineation produced by the intersection of cleavage planes formed during different periods of deformation. Submaxima are distributed along a great circle and represent the intersection of second and third deformation axial-plane cleavage with uniformly oriented first deformation flow cleavage and foliation. Other considerations which influence the size, distribution, and orientation of the submaxima shown on Plate 3a and b are discussed in the section *Structural History*.

Origin of Lineation

The origin and significance of lineation is one of the most important considerations in the reconstruction of the deformational history

in any metamorphic terrane. Unfortunately, it is at the same time the most speculative and subjective. No one has yet succeeded in reproducing the common types of mineralogic and textural lineations under controlled experimental conditions; hence, these structures have been explained by hypotheses constructed in accordance with observed field evidence. Many of these hypotheses have been fitted to data peculiar to a given area or to inadequate or superficial data. It would not serve the purpose of this report, nor is it the inclination of the writer, to attempt an analysis or evaluation of existing theory regarding the origin of linear structures in metamorphic rocks. Instead, in the discussion below, an attempt is made to analyze available structural data in the light of recognized concepts.

Insight into the origin of lineation is especially important in the Precambrian of La Madera quadrangle, for this structural element constitutes a fundamental building block in the thesis of superposed deformation. It is not a part, however, of the evidence for an east-west system of folds superposed upon a northwest-trending fold system. There is other evidence to establish this conclusion. To facilitate discussion, the term *L-lineation* is used in this section for textural and mineralogical lineations variously described as fluting, streaking, elongate segregations, and "stretched pebbles." Similarity in style and orientation as well as occurrence in the plane of flow cleavage and foliation indicate a common genesis. The origin of L-lineation, ubiquitous in the La Madera area, is a major line of evidence used in support of a regional deformation which predates the formation of the northwest fold system. Hence, the following discussion considers in detail only L-lineation developed in the flow cleavage and foliation which is itself folded by northwest-trending mesoscopic folds. The principal question to be answered is whether L-lineation formed during the growth of northwest-trending folds, or whether it was produced by an earlier episode of deformation heretofore unrecognized in this region.

The following abbreviated synopsis regarding the origin of lineation is drawn from several sources which discuss the problem fully and in great detail (Knopf and Ingerson; Cloos, 1946; Fairbairn, 1949). The reader desiring a complete and documented review of the lineation problem is referred to these texts.

A fundamental aim in studying deformed rocks is to discover the magnitude and orientation of the stresses responsible for observed permanent strain. Geologists have sought to approach this goal by acquiring all possible information about the kinematics, the effect of applied forces, of deformation. The classical approach has been to equate kinematic symmetry with fabric (in the broad sense) symmetry. It was early recognized that a close relationship exists between kinematics and the direction of movement of material during deformation. To this parameter of a structural system characterized by monoclinic differential slip, Sander gave the name *direction of slip*. *Movement*

direction and *direction of tectonic transport* are synonymous with Sander's term. It is a linear element within the slip plane normal to an axis of rotation and constitutes the kinematic *a* axis. The axis of rotation normal to *a* is kinematic *b*. The *c* axis defined kinematically is perpendicular to the *ab* plane. In present theory, there is general agreement that lineation forms parallel to or normal to fold axes and that *a* is either perpendicular to or parallel to fold axes. There is at least one example from structural petrology (Kvale, 1948, p. 27) in which *a* lies at an oblique angle to fold axes. Also, Ramsay (1960, p. 89) has shown that kinematic *a* may subtend any angle with the fold axis in shear folds. The fabric criterion for the identification of a normal to lineation is the presence of an *ac* girdle, defined by the preferred orientation of quartz *c*-axes or poles to the cleavage planes in mica, oriented perpendicular to the lineation. This relationship has been found in many studies of deformed rocks. The *a* direction is presumed to be parallel to lineation if the linear element coincides with a strong point maxima in quartz. This condition is rarely met outside of mylonites and slickensides. Anderson (1948) has taken an extreme point of view in declaring that virtually all single girdles of quartz and mica form normal to *a*. Although this view has not enjoyed general acceptance, it remains as an alternative explanation for girdle fabrics perpendicular to lineations. The presence of girdle fabrics perpendicular to lineation that parallels fold axes suggests, but does not prove, transport normal to the fold axis.

Another problem in the assessment of lineations and their origin lies in the concept of "cross" folds or "crenulate" folds. These terms refer to minor folds which occur on the flanks of major folds. Examples of these structures are known from the Caledonide fold belt in Great Britain, in the Bergsdalen area in Norway, and in California. These minor folds are generally broad undulations or crinkles in the major folded element and are thought to originate through a minor component of material transport parallel to a principal rotational axis or to converging or diverging movements on uneven thrust planes. In any event, lineation parallel to minor fold axes and normal to girdle fabrics could conceivably result from such subsidiary movement. This view is in part modified by the possibility that examples of lineation supposedly parallel to *a*, or parallel to the axes of "crenulate" folds, are drawn from areas in which the structural history is inadequately known. Nevertheless, the presence in an area of two or more sets of fold axes can not alone be considered proof of two or more episodes of deformation.

Conclusions regarding the origin of L-lineation in metamorphic rocks of La Madera quadrangle are based upon direction of transport inferred from the physical nature and fabric relations of the lineation, and more importantly upon the orientation and position of the linear element with respect to two sets of mesoscopic folds which differ in attitude and style.

Fluting and the preferred orientation of micas make up the bulk of L-lineation in the area studied. These visual manifestations of the rock fabric are the direct result of nearly equally developed intersecting cleavage planes which have a very small dihedral angle. Flow cleavage and foliation are defined by the preferred orientation of constituent mica flakes. The line of intersection shared by these planes marks the L-lineation. This lineation is parallel to relatively rare isoclinal shear fold axes which mark axes of external rotation. The fact that these planes are very close-spaced, intersect in a common axis, and have served as a locus for considerable nonaffine slip supports the contention that they are cogenetic shear planes formed as a direct result of penetrative shear. The monoclinic symmetry of this structure as observed in outcrop combined with the features mentioned above is suggestive of unrestricted transport or rotational strain normal to the lineation.

Fabric data bearing on the origin of lineation are given in the form of petrofabric diagrams in Plate 3i, j, k, and n. Sections of muscovitic quartzite and amphibolite were cut perpendicular to L-lineation, and diagrams illustrating the preferred orientation of quartz, muscovite, chlorite, and hornblende were prepared. The monoclinic symmetry of the fabrics is reflected in the preferred orientation of each mineral species. The quartz diagram (pl. 3n) is more nearly triclinic than the others because of a partial girdle which transects the peripheral girdle. The two-girdle quartz pattern was recorded by Lindholm (1963, p. 37) in all quartzite samples that he studied from the Ortega Mountains. His diagrams are triclinic with the fabric co-ordinates based upon the northwest-trending fold axes as *b*. It is interesting to note, however, that poles to the quartz girdles are always parallel to either L-lineation or the axes of northwest-trending folds. These fabrics could be explained by two deformational episodes, as well as the interpretation favored by Lindholm that they formed concurrently during formation of the northwest-trending folds. There is no question, however, about the monoclinic symmetry shown by hornblende, muscovite, and chlorite, which supports a monoclinic movement plan with rotational componental movements in the plane normal to L-lineation.

The least subjective, hence most important, data bearing on the problems under discussion are afforded by a critical field examination of L-lineation, the planar element containing it, and their relationship to mesoscopic folds. Two sets of folds, different in style and orientation, are associated with L-lineation. The northwest-trending nearly horizontal set of mesoscopic folds varies in style with attributes of flexural, shear, and flow types. These are very prominent folds, visible in many exposures, with one feature in common—the folded element is always flow cleavage or foliation which contains L-lineation. In outcrops where the fold hinge was exposed, L-lineation was observed to wrap around the nose of the folds. The lineation exposed on the flanks of these folds in most instances subtends an angle of from 60 to 70 degrees,

measured counterclockwise, with the fold axis. A second set of mesoscopic folds, of which there are fewer examples, is constant in attitude and style. These folds uniformly bear and plunge to the southwest and occupy the same geometric realm as L-lineation (pl. 3a and c). All observed folds of this set are isoclinal shear folds with attenuated limbs and thickened crests.

The observed facts presented so far are equally consistent with respect to the two propositions outlined earlier. Either (1) the southwest-trending shear folds are crenulate folds developed during the growth of the northwest fold system or (2) the southwest-trending folds represent the remnants of an older fold system which has been refolded by the northwest set of folds. A third proposition, that the southwest-trending shear folds are the result of sedimentary slumping, is considered unlikely in view of the high degree of preferred orientation of the fold axes, the coincidence of fold axes with L-lineation of metamorphic origin, the obvious metamorphic style of the folds, and the presence of these folds in granite gneiss which is most probably of igneous origin.

It is now the opinion of this writer that the southwest set of mesoscopic folds are relics of an older fold system, because the hypothesis of crenulate folds is seriously weakened, if not rendered completely untenable, by the following considerations. First, the style of the southwest-trending folds is manifestly dissimilar to the style of postulated crenulate folds which are described as "(1) large undulations which show on the maps in the sinuous arrangement of strata, and (2) crenulations and wrinkles which form the lineation in individual exposures" (Cloos, 1946, p. 26). This type of structural configuration is in keeping with the postulate of minor movement of material parallel to major fold axes during deformation, but it does not compare favorably with the style of deformation exhibited by the southwest-trending folds in La Madera quadrangle. Second, and of much greater consequence, the folded planar element in the two fold sets is not the same structural element. With crenulate folds or folds in a, the same folded element is shared by the major folds and the minor folds developed on the flanks of the major folds. In the La Madera area, however, the plane folded by the northwest-trending folds is flow cleavage and foliation containing L-lineation (fig. 10). In all the observed southwest-trending folds, flow cleavage and foliation pass through the isoclinal folds parallel to the axial plane. In the noses of the isoclinal folds, hematite layering in quartzite departs from parallelism with foliation, and defines the fold form. In these folds, the line of intersection between foliation and hematite layering is parallel to L-lineation. It is difficult to conceive of a process whereby crenulate folds could form on the flanks of a major fold system in such a way that axial-plane cleavage developed in the minor folds could be the folded planar element in the major folds. In most exposures of southwest-trending folds it was not possible to identify the axial-plane flow cleavage or foliation as a refolded ele-

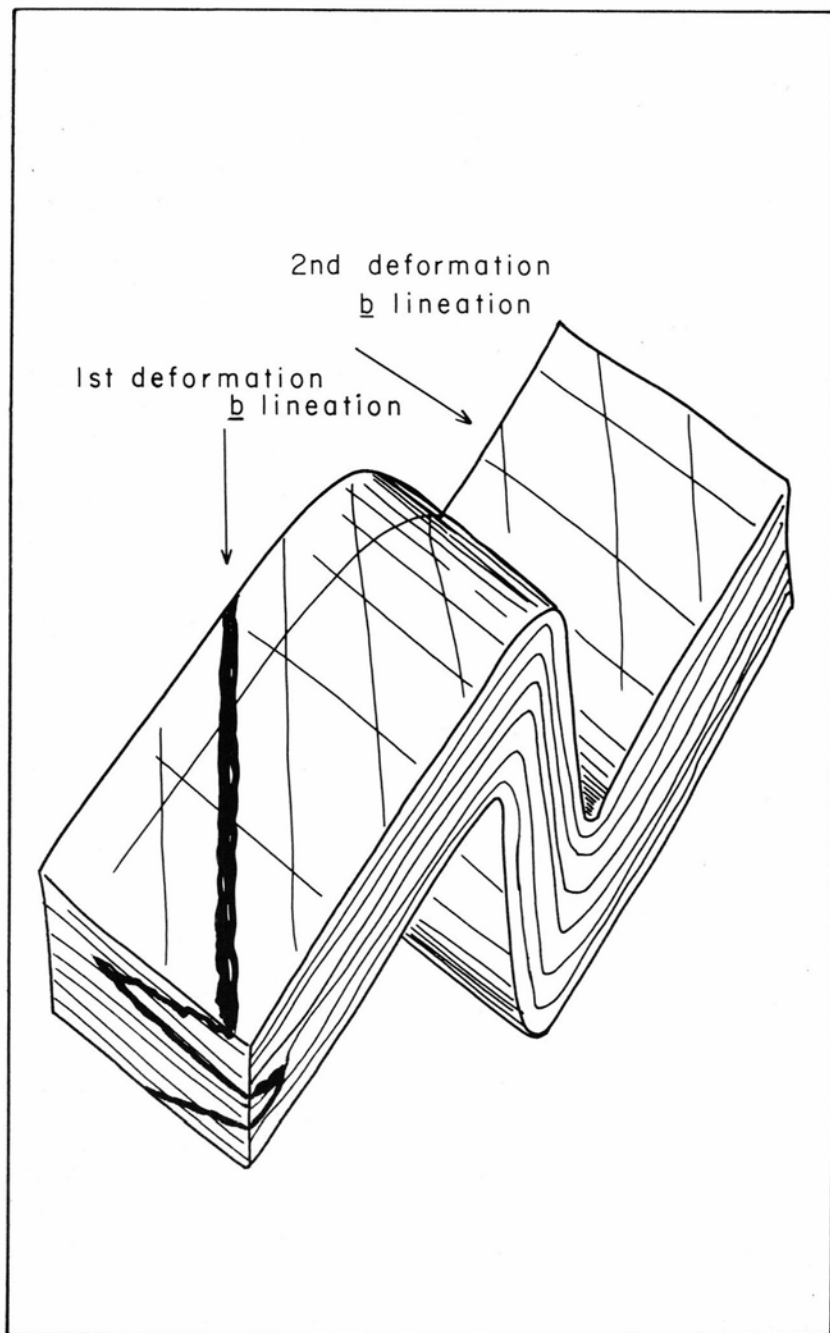


Figure 10
SECOND DEFORMATION FOLD IN WHICH L-LINEATION AND FIRST
DEFORMATION AXIAL-PLANE CLEAVAGE ARE FOLDED

ment. There are several exposures, however, where the two sets of folds are superimposed in a single exposure; for example, in quartzite on the crest of the northwest-trending ridge half a mile south of Rancho del Olguin; in muscovitic quartzite near the base of the west-facing scarp of Mesa de la Jarita, in NEIANEN sec. 2, T. 25 N., R. 8 E.; and in the amphibolite exposed in this same locality. These exposures directly confirm the relations between the folded element and two sets of fold structures.

In summary, L-lineation is parallel to the fold axes (b-lineation in the classical sense) of southwest-trending isoclinal shear folds. The folds, L-lineation, and axial-plane flow cleavage and foliation are co-genetic aspects of an interval of regional, penetrative, unrestricted flow of material. The mesoscopic and microscopic fabrics exhibit monoclinic symmetry with the deformation plane, *ac*, perpendicular to L-lineation. On the basis of symmetry, tectonic style, and superposition of structural elements in outcrop, the hypothesis of crenulate folds or folds in a to explain the southwest-trending folds is rejected and the concept of an independent orogenic event for the origin of these folds and L-lineation is favored.

Textural lineation in quartzite is emphasized in many outcrops by the presence of kyanite blades in the cleavage plane. Some of the kyanite laths are parallel to the textural lineation, but in many exposed foliation planes, much of the kyanite has a random orientation within the planar structure. The parallelism of only small percentages of kyanite in addition to its concentration within axial-plane cleavage suggests that the observed preferred orientation is the result of growth in an isotropic stress environment with the orientation of some blades controlled by a pre-existing textural lineation. Lack of an orienting process during growth is also indicated by the common occurrence of radial bursts or rosettes of kyanite in the cleavage plane, microscopically by the presence of porphyroblastic kyanite laths which have grown transverse to, and incorporate, a pre-existing cleavage, and the irregular pods of kyanite in which laths are arranged perpendicular to the pod walls. The concept of *Abbildungskristallisation* does not imply introduction of material into host rock; it is merely indicative of crystallization in an isotropic stress field.

Boudins are frequently encountered in geologic field studies and there is consequently a wealth of data regarding their form, style, and orientation. The most frequently postulated mode of origin is the tensional or "necking" hypothesis as outlined by Cloos (1947, p. 630-631). Cloos maintains that boudins arise through initial tensional fracturing of a competent layer intercalated with less competent layers. Attenuated, lenslike forms in section may be produced by continued flowage during deformation. Rast (1956, p. 402-3) has described three types of "tectonic inclusions" which occur in the metamorphic terrane of Perthshire, England:

1. Relicts of folds or fold closures
2. Contorted relicts around which the schistosity of the surrounding medium is affected
3. . . . an imperfect oval or lozenge-shaped cross section.

He considers types 1 and 2 to be the result of extreme shearing, translation along axial planes, and rotation. The first and second types are presumably of compressional origin, whereas the third is probably the result of tension and should retain the name *boudin*. Structures Rast describes bear a marked similarity to boudins mapped in the La Madera quadrangle.

Boudins, described earlier as flattened lenses, and quartzite in thinly laminated schist may be the result of separation of an originally continuous layer broken systematically by fracture cleavage. The single occurrence of quartzite boudins in schist may also be the result of a similar process because of the parallelism of their long axes with first deformation linear structures. It is equally possible, however, that these bodies represent remnants of tectonically intercalated quartzite which have become separated from the main quartzite mass through extreme attenuation and separation of fold limbs. This type of process may also account for the very large boudinlike masses of muscovitic quartzite common in the peripheral zone of the amphibolite east of Ancones. In this area, a thin isoclinal drag fold wraps around the margin of an inclusion. It is apparent that, had deformation proceeded a little farther, the hinge of the drag fold could have merged with the main amphibolite mass, leaving the body of muscovitic quartzite as a conventional-appearing boudin. The S-shaped milky quartz boudins that are ubiquitous in quartzite are similar in all respects to the "tectonic inclusions" figured by Rast. Their origin as sheared-out fold hinges is also compatible with the style of the first deformation dislocation based upon independent evidence. They have probably formed through a process similar to the one outlined by Rast.

The boudin-shaped mineralogic segregations described earlier could have been produced by several mechanisms acting separately or in combination. Perhaps the simplest explanation for the epidote concretions in amphibolite is that they represent primary concentrations of epidote in an original basic flow. The effect of thermal metamorphism on original concentrations would be merely a recrystallization of epidote accompanied by minor diffusion to produce the present form and orientation of the observed segregations. The grossly spheroidal form exhibited by the epidote segregations is anomalous, however, in view of the pronounced dislocation and flattening which occurred during the first deformation. In several outcrops of amphibolite, bulbous segregations were observed to be closely intercalated with first deformation isoclinal folds. It seems unlikely that the form of the segregation could have been preserved during the type of deformation indicated by the

style of pervasive folding. The process of metamorphic differentiation during dynamo-thermal metamorphism appears to offer an explanation in closer accord with field observation. The mineral assemblage hornblende-plagioclase-epidote exhibited by denser, more homogeneous phases of the amphibolite is believed to represent an equilibrium assemblage developed during dynamo-thermal metamorphism of regional extent. It was noted in an earlier section that near the margin of the amphibolite east of Ancones, the mineralogy changes to alternating layers of hornblende-plagioclase and epidote-quartz intercalated with muscovitic quartzite. It was also concluded that this was the result of chemical mobility during the folding stage. It is possible that the epidote segregations are a manifestation of this same process in which epidote derived from the breakdown of calcic plagioclase is concentrated into spindle-shaped zones whose long axes are parallel to the axis of rotation. The discontinuous globules of epidote-rich rock may have been produced by thinning of rodlike zones, in a manner similar to the formation of extensional boudins. The shape of the segregations may also be the result of continued epidote growth after the cessation of deformation, with the form and distribution controlled by a process of "concretionary growth" (Turner, p. 138-139).

These postulations are obviously of a speculative nature and are cited merely as possible explanations. In the absence of positive criteria, the origin of the epidote segregations must remain tenuous.

Elongate fragments of white quartz and fine-grained hematitic quartzite constitute a prominent linear element in the tectonic breccia. The preferred south-southwest orientation of the elongate fragments is due to pronounced translation along intersecting cogenetic shear planes which are parallel to the axial planes of first deformation folds. The attitude of this lineation is concordant with first deformation L-lineation recorded elsewhere in the map area.

The origin of lineation produced by mutually intersecting planar elements is self evident. Wherever a pre-existing set of planes is transected by a new set of planes having a different orientation, the family of lines produced constitutes a lineation whose orientation can be measured in either the primary plane or the secondary plane.

FOLDS

The Precambrian rocks within La Madera quadrangle display numerous folds. These structures vary considerably in style, orientation, size, and degree of development. Systematic analysis of fold structures is based largely upon the measurement of orientation and shear sense. Assuming that folds in individual outcrops are congruent with the major folds in the area, it is possible to re-create, with varying degrees of success, the trend and distribution of major folds.

To discuss folds and folding unambiguously, it is necessary to es-

establish a terminology based in part upon scale. In this report, the terms recommended by Turner and Weiss (p. 15) are employed. Four groups are recognized: (1) *submicroscopic*, includes bodies of rock too small or too fine-grained to be resolved under the microscope; (2) *microscopic*, fields amenable to microscopic analysis; (3) *mesoscopic*, ranges in scale from hand specimen to the limits of individual outcrops; and (4) *macroscopic*, includes features of regional aspect which appear on maps. Microscopic structures are usually studied with petrofabric methods, whereas mesoscopic structures are the responsibility of the field geologist.

The term *mesoscopic fold* is applied in this report to the more familiar term *drag fold* which implies rotation of layers on a small scale as a result of interlayer shear during regional folding. This phenomenon is restricted to concentric folding; hence, the analogy can not validly be extended to shear folds which are a part of major fold structures. In reviewing this problem, De Sitter (1957, p. 57) has suggested the term *parasitic folds* for minor folds on the flanks of shear folds. By replacing the terms *drag fold* and *parasitic fold* in this report with the expression *mesoscopic fold*, the descriptive data of style and orientation can be presented free of genetic implication.

The classifications and terminology used in this paper are briefly reviewed here in order to avoid confusion arising from the use of terms with several connotations. Three descriptive classifications based on (1) fold form in normal section (a section perpendicular to the fold axis), (2) attitude of axial plane in normal section, and (3) the geometric relationship between fold axis and axial plane are used herein. The familiar terms *anticline* and *syncline* have been used for many years in the first classification. However, since these terms lead to conclusions regarding the relative age of folded layers, they are replaced by the terms *antiform* and *synform* to refer to folds that close upward and downward, respectively, and in which the age relations of the folded layers are not known (Turner and Weiss, p. 106). In folds with nearly vertical axes or horizontal axial planes, the criterion of closing "upward" or "downward" is ambiguous. In these situations, the frame of reference becomes geographic; that is, *synforms* close westward and *antiforms* close eastward.

The second classification is based upon the attitude of the axial surface as it appears in normal section and includes folds which may be symmetric, asymmetric, overturned, isoclinal, and recumbent. These terms are not defined here because of their wide usage and acceptance.

The third classification is based upon the geometric properties of a fold grouped according to the relationship between the fold axis and axial surface (Turner and Weiss). The axis of any fold is geometrically either rectilinear, planar curvilinear, or nonplanar curvilinear. The axial surface of any fold may be planar, cylindrical curvilinear, or non-cylindrical curvilinear. By combining these parameters, folds are

grouped as (1) plane cylindrical (planar, rectilinear; the first term refers to the form of the axial surface, the second term refers to the form of the fold axis), (2) plane noncylindrical (planar, planar curvilinear), (3) nonplane cylindrical (cylindrical curvilinear, rectilinear), or (4) nonplane noncylindrical (axial surface cylindrical curvilinear or noncylindrical curvilinear with a nonplanar curvilinear axis). It is important to note that the application of a name in this system 'is contingent upon the specification of scale. Obviously, folds do not remain constant in form for an indefinite distance along their axes. A fold which is plane cylindrical in a given outcrop may be nonplane cylindrical in a neighboring outcrop. Also a plane cylindrical fold in a 7 1/2-minute quadrangle may be nonplane cylindrical in a 15-minute or 30-minute quadrangle which encloses the smaller sector. These statements follow from the concept of the statistically homogeneous area or domain (Turner and Weiss, p. 20) as applied to the analysis of folds. The value of this somewhat esoteric classification is that the three-dimensional form of a fold must be considered in order to apply a name. Also, it is a purely descriptive classification, unlike the genetic classification of folds which requires kinematic inferences often difficult to establish.

The genetic classification of folds is based on the identification of form as a function of process. It is this attribute of fold form which is commonly referred to as *style*. Concentric folding, for example, is considered a structural style associated with elastic or brittle behavior of rock under low confining pressure. Similar and disharmonic folds, on the other hand, correspond to a style of deformation in which penetrative shear and unrestricted transport constitute the dominant strain mechanisms. Thus, the application of these names implies either direct or indirect knowledge of the rheologic and kinematic parameters of a system during rock deformation. There is, however, only meager knowledge at the present time concerning the effect of stress difference, total stress, composition, chemical environment, and time on total strain. Consequently, the identification of categories in this classification is invariably subjective and often highly speculative. The genetic terms used in this report are (1) *concentric* (parallel) *folds*, the radius of curvature of the fold changes along the directrix which is defined as the intersection of the axial surface and the normal section; (2) *similar folds*, radius of curvature of the fold remains constant along the directrix; (3) *disharmonic* (flow) *folds*, form of individual layers varies within a single fold; (4) *chevron folds*, a special case of similar folds characterized by planar limbs and sharp closures, generally in the hinge area of macroscopic folds; (5) *conjugate folds*, "closely associated folds of identical style, occurring in pairs with mutually inclined approximately conjugate axial surfaces" (Turner and Weiss, p. 114-115); and (6) *intrafolial folds*, "isolated closure or pair of opposing closures in a

disrupted portion of a layer now 'floating' as a tectonic inclusion in relatively unfolded foliation" (Turner and Weiss, p. 117).

Mesoscopic Folds

Folds are widely distributed in all Precambrian rock types in La Madera quadrangle. They occur most frequently in the quartzite underlying the Ortega Mountains and in the northwest-trending belt of exposed Precambrian on the eastern flank of Mesa de la Jarita. In the latter area, mesoscopic folds are frequently encountered west of Sunnyside mine in the SW1/4SW1/4 sec. 25, T. 26 N., R. 8 E. and in a narrow tract along the contact between the tectonic breccia phase of muscovitic quartzite and normal muscovitic quartzite in the SW1/4 NE1/4 sec. 15, T. 26 N., R. 8 E.

Mesoscopic folds occur in a variety of styles, shapes, and orientations. By ordering or grouping folds on the basis of orientation and relative age based on order of superposition, the variation within groups is much reduced. These considerations serve as the basis for classifying folds according to the period of deformation in which they developed and, as such, constitutes a separation based in part on inference. The description of folds as they occur in this genetic framework is consequently reserved for the section *Structural History*.

There are three broad groups of mesoscopic folds based on a separation according to style in the La Madera area.

Most observed folds are plane to nonplane cylindrical, nearly isoclinal, and disharmonic to similar folds. They have a WL:A (wavelength to amplitude ratio) which ranges from 1:1 to about 1:3, with an average of 1:2. Most folds of this type are asymmetric, but in the vicinity of macroscopic axial surfaces they tend to be symmetrical and isoclinal and exhibit the minimum WL:A of the group. Folds of this group are ubiquitous and well exposed in the quartzite of the Ortega Mountains. In this area, the folded elements are hematite layering and "pebble beds" which parallel foliation in most outcrops. Folds with the greatest attenuation occur in quartz-feldspar-muscovite-biotite schist on the east flank of Mesa de la Jarita, and chevron folds are largely restricted to feldspathic schist and biotite-muscovite-microcline granite in the Cribbenville district. Nonaffine deformation and flowage of material are common features of this group of folds, as indicated by the usual partly disharmonic form.

A less numerous group of folds is classified as plane cylindrical, symmetric, and nearly concentric. This group could perhaps best be described as simple flexures. WL:A ranges from 3:1 to 1:1, with an average of 2:1. Folds of this type are uniformly distributed in the Precambrian rocks and are best exposed a few hundred feet west of Sunnyside mine, in the kyanite schist intercalations present within the Ortega Moun-

tains, and in muscovitic quartzite at the site of the White mine. The folded element is generally flow cleavage or foliation, but at the White and Sunnyside mines and at the south end of the prominent ridge in the NE1/4 sec. 15, T. 26 N., R. 8 E., the folded element is slip cleavage. Many folds of this type were found at the margins of pegmatite dikes and tabular quartz veins.

Plane cylindrical isoclinal similar folds are the rarest type of mesoscopic fold mapped in the La Madera quadrangle. Nevertheless, they are widely distributed and occur in every major metamorphic rock type with the exception of quartz-feldspar-muscovite-biotite schist. They are characterized by extreme attenuation with a WL:A from 1:3 to 1:10. In some folds of this type it is difficult to establish this parameter because of the presence of only one fold nose. In all instances, the folded element is transected by flow cleavage and foliation in the fold noses and is parallel to these cleavages in the isoclinal limbs. In quartzite, the folded element is hematite layering; in feldspathic schist and amphibolite, it is a crude, poorly defined compositional layering. Well-defined folds of this type are best exposed in feldspathic schist at the junction of the Petaca road and the Globe district road in feldspathic schist along the Old Petaca road in the SW1/4 NW1/4 sec. 15, T. 26 N., R. 8 E.; in quartzite exposed along the crest of the ridge half a mile southwest of Rancho del Olguin; and in the amphibolite east of Ancones.

There is some overlap between first and second deformation folds, for where the folds of the second deformation are more isoclinal, they appear much like the folds of the first deformation. There is also some overlap between second and third deformation folds in that the more symmetrical similar folds of the second deformation are like in appearance to third deformation folds. Little similarity exists, however, between first and third deformation folds. (*See* figs. 15, 17, and 20.)

Several examples from La Madera quadrangle would seem to indicate that, in general, axial-plane cleavage forms rather late in the development of a particular fold form. Figure 11 a is an illustration of a plane cylindrical symmetric chevron fold in which the folded element is flow cleavage marked by biotite and parallel hematite-rich layers. The fold is cut by an incipient axial-plane fracture cleavage composed of several wide-spaced fracture planes. In this example, the rotation of flow cleavage has obviously not been accomplished by translation along the fracture cleavage planes, and it is concluded that the fracture cleavage originated after the form of the fold had been established. Figure 11 b is an illustration of a sample in which axial-plane cleavage is pervasive in the rock. In this sample, there are no criteria to establish the time of cleavage formation with respect to the time of formation of the fold form. It is equally possible that the fold is the result of translation along the cleavage or that the cleavage has been induced by the folding process. It seems more probable, however, that the fold form has been

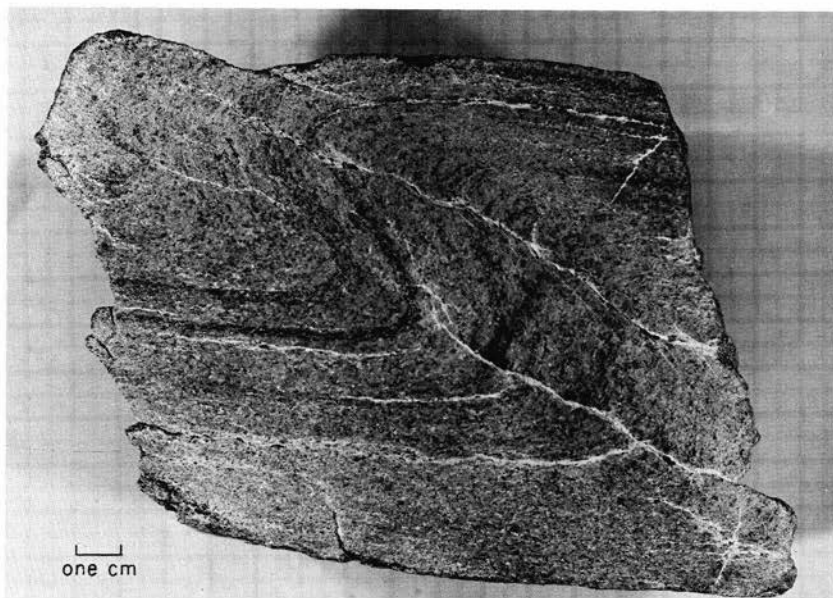


Figure 11a

FOLDED FLOW CLEAVAGE WITH INCIPIENT FRACTURE CLEAVAGE DEVELOPED
PARALLEL TO THE AXIAL PLANE

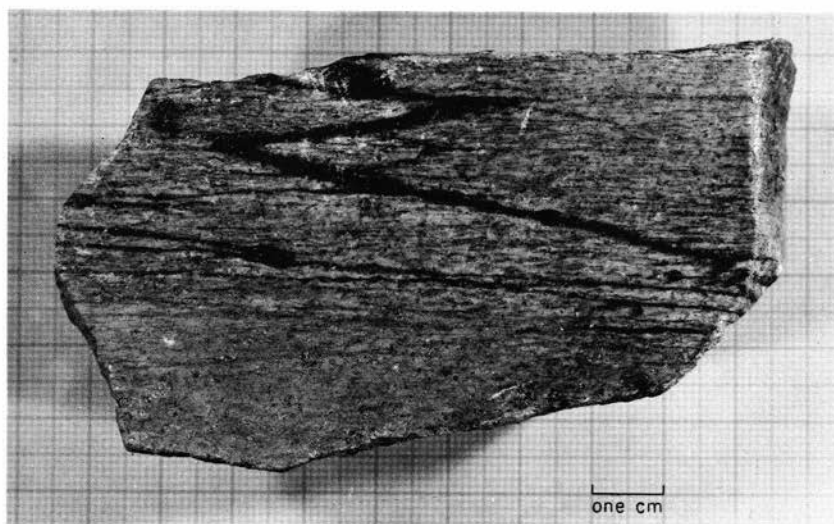


Figure 11b

FOLDED HEMATITE LAYER IN FELDSPATHIC SCHIST

strongly emphasized by shear movements along the axial-plane cleavage. It is the opinion of this writer that the mesoscopic fold forms exhibited in La Madera quadrangle are the result of a process whose initial stages include minor flexing and rotation of some planar element, and that shearing movements that occur late in the development of the fold and parallel to the developing axial-plane cleavage serve to increase the WL:A and in general contribute to the development of isoclinal and extremely attenuated fold forms.

Macroscopic Folds

The trend and distribution of macroscopic folds is deduced from the orientation, distribution, and shear sense of mesoscopic folds. As earlier indicated, this reconstruction is based upon the assumption that mesoscopic folds are similar in style and trend to macroscopic folds. In areas of superposed fold systems distinct in space and time, the reconstruction is also based upon a history formulated from the superposition of mesoscopic structures. For this reason, the salient features of macroscopic structures are discussed in the section *Structural History*. The macroscopic structure outlined by amphibolite east of Ancones, however, is the result of outcrop configuration and internal structural features and consequently is not inferred.

The amphibolite east of Ancones crops out on the west-facing faceted scarp of Mesa de la Jarita. The northern outcrop part lies within sec. 35, T. 26 N., R. 8 E. and the southern part lies in sec. 2, T. 25 N., R. 8 E. The map unit has an average thickness of about 35 feet measured normal to its contacts with muscovitic quartzite which entirely encloses it. Where the tabular amphibolite crops out in steep-fronted west-facing spurs, the outcrop area widens to form crescent-shaped extensions from the main amphibolite body. The continuity of this thin unit is well established except in the southeastern areas, where slope wash and scree conceal most of the bed rock and along the Vallecitos fault zone where a part of the amphibolite has been truncated by faulting. Detailed mapping of the well-exposed northern area reveals flanking mesoscopic nearly isoclinal folds of amphibolite in muscovitic quartzite. Folds of the same type are exposed in the valley walls of Vallecitos Creek where it crosses the southern limit of sec. 35, T. 26 N., R. 8 E., and along the southwest flank of the southernmost exposures. The axes of all these folds bear and plunge to the southwest parallel to the hornblende lineation within the amphibolite.

Structurally, the amphibolite is believed to represent an alternation of synform-antiform-synform, with the synforms closing to the south. This pattern of folds is based upon the following relationships. The two westernmost amphibolite layers at the north end of the amphibolite outcrop area form an appressed U open to the south. The right-handed shear sense of the left limb and the left-handed shear sense of

the right limb (looking down the fold plunge) are consistent with a southwest-plunging antiform. By assuming continuity of this form with the U-shaped traces opening north, as exposed to the south and southeast, these latter forms must be the flanking structures to the antiform; that is, synforms. This interpretation is strengthened by the pattern of left-handed mesoscopic folds which make up most of the southernmost part of the amphibolite. The outcrop pattern as it would appear on a horizontal datum plane, assuming outcrop continuity, is shown in Figure 12. The argument against including the macroscopic fold pattern illustrated by the amphibolite as related to and an integral part of the second deformation northwest-trending fold system is presented in the section *Structural History*.

RELICT STRUCTURES

Structural features preserved in the metamorphic rocks of the La Madera quadrangle which originated prior to the last regional folding deformation are considered relict structures. This definition obviously includes many small-scale structural features associated with folding, but these elements have been discussed elsewhere. The present discussion is reserved for original sedimentary structures and relict structural features that grossly resemble sedimentary structures. The nature and significance of cross-bedding, pseudocross-bedding, and pseudoconglomerates (tectonic breccia) are discussed below.

It was earlier indicated that several writers have cited the presence of cross-bedding in the Precambrian quartzite of north-central New Mexico. Only Lindholm has attempted a systematic study of cross-bedding, and he encountered considerable difficulty in distinguishing true cross-bedding from structural features having the general appearance of cross-bedding.

One occurrence of small-scale, festoon type of cross-bedding was observed by the writer. It is in quartzite at the crest of the quartzite ridge in the SW1/4 sec. 12, T. 25 N., R. 8 W. Sharply curved arcuate layers marked by hematite-rich laminae occur with clusters of relict clastic fragments up to three millimeters in diameter. The form of the arcuate layers, the relict clastic texture, and the close similarity to festoon cross-bedding suggest a sedimentary origin for this structure. It is also similar in all respects to the feature in the quartzite that Lindholm (p. 13) held to be cross-bedding. It is not unusual for small islands of relatively undisturbed primary structures to occur in highly deformed rocks, as noted by Engel (1949, p. 771). The scarcity of the structure described above is consistent with such conditions.

The commonly occurring structures in quartzite generally regarded as cross-bedding are markedly dissimilar in form from those discussed above. Reference is made here to the sweeping arcuate layers of hematitic quartzite which occur in sets bounded by hematite layers parallel

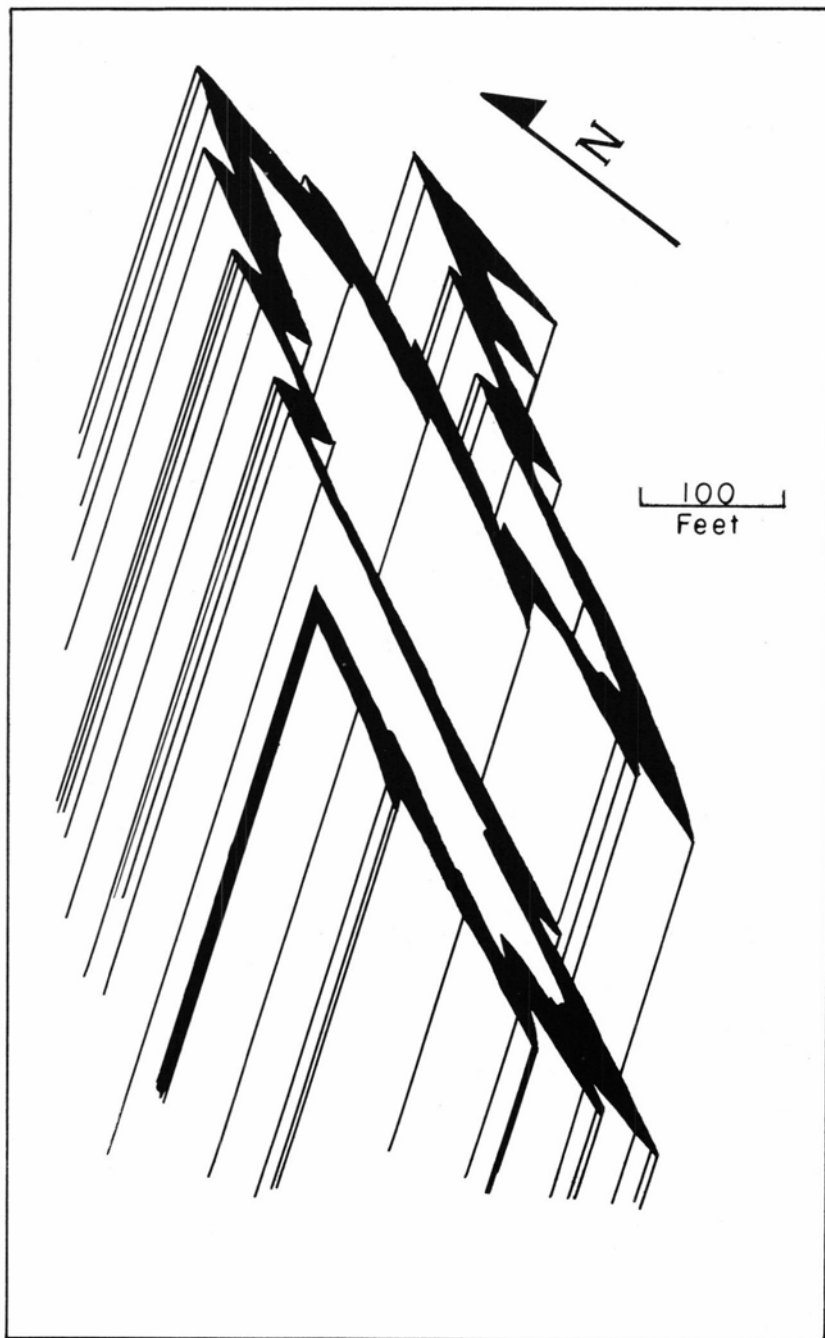


Figure 12

INFERRED CONTINUITY OF AMPHIBOLITE LAYER SHOWN IN PERSPECTIVE

to relict fracture cleavage. This structure was described in the section on bedding and is considered by this writer to be of tectonic origin and is herein termed *pseudocross-bedding*. Several lines of evidence support this conclusion. First, in outcrops where first deformation isoclinal folds are exposed, the flanks of the folds are identical in form to the arcuate layers. Axial-plane cleavage transects the arcuate layers in the same manner as it transects the flanks of nearly isoclinal folds. In folds, the line of intersection shared by axial-plane cleavage and hematite layering is parallel to the fold axis, and in isolated arcuate layers, the line of intersection is parallel to fluting and kyanite lineation, both of which have the same regional trend as the first deformation fold axes. Also, as described earlier, the transition from sigmoidal hematite layers to smooth arcuate forms can be observed in one continuous exposure of quartzite (fig. 6). Second, it seems highly unlikely that smoothly curving layers representing original cross-bedding could be preserved in rock which has undergone intense shearing, flowage, and flattening, as evidenced by the form of first deformation folds and the nature of the fabric. Rather, such structures are more likely the result of these pervasive metamorphic processes. Third, the efficacy of the shearing process to produce truncated arcuate layers is illustrated in a sample of hematitic quartzite (fig. 13). The prominent black band represents a set boundary and is parallel to axial-plane cleavage that is pervasive in the sample. Dark curved streaks near the center of the set sweep downward and become tangential to foliation. Where the sharply curved layers meet the cleavage plane at the center of the set, they are slightly recurved. The axis of curvature of these hematite layers and the line of intersection between relict fracture cleavage and the curved layers are parallel to textural lineation on the cleavage plane which bounds the hand specimen. One and one-half inches of translation along the cleavage halfway between the set boundaries can be established by direct measurement. The resultant structure bears an obvious similarity to cross-bedding, and had dislocation proceeded further, the arcuate layers in this specimen would be virtually indistinguishable from most of what has been termed cross-bedding in the Ortega Mountains.

Two conditions serve as the basis for the contention that the arcuate layers represent relict cross-bedding. First, there is an undeniable similarity in form between the arcuate layers and true cross-bedding. Second, most of the arcuate layers are concave downward in the Ortega Mountains. This suggests that the quartzite layers are overturned—a conclusion substantiated by the shear sense of northwest-trending mesoscopic folds. For the first premise, the identification of cross-bedding by analogy is, in this writer's opinion, very speculative and not a reliable criterion in metamorphic rocks. The second premise, that of overturning, is weakened by the following considerations. Although it is true that most arcuate layers are concave downward, some are concave up-

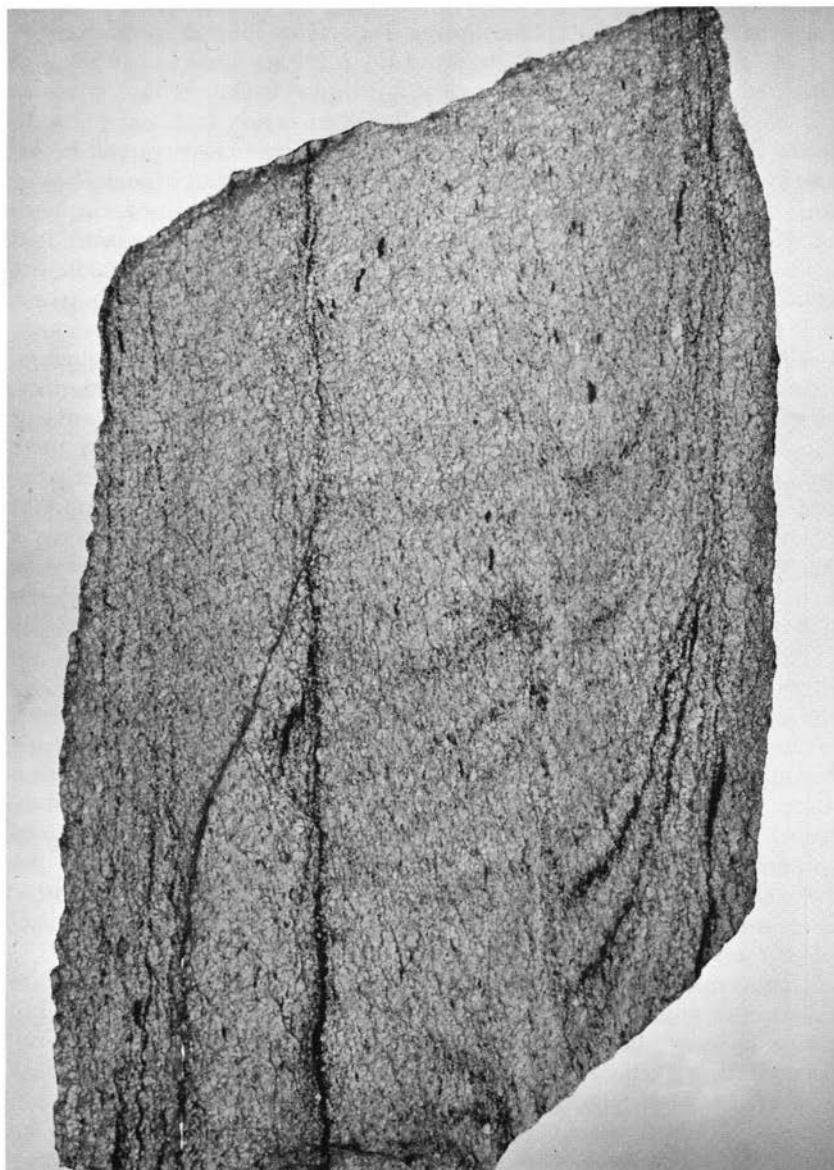


Figure 13
PSEUDOCROSS-BEDDING IN SHEARED QUARTZITE

ward. If the first deformation is assumed nonexistent, and if all the hematite layering represents undisturbed bedding, it must follow that some cross-bed layers formed in an inverted position within a considerable thickness of quartzite which "youngs" eastward across the Ortega Mountains. If, on the other hand, the first deformation is included in the working hypothesis, the concave upward arcuate layers represent remnants of similar folds that, for the most part have been destroyed by intense shearing and translation during deformation. Green (1931, p. 529) and Whitten (1959, p. 32) have emphasized the tendency for one limb to be preferentially destroyed during intense regional shearing.

Admittedly, the evidence presented for the tectonic origin of the arcuate hematite layers in the quartzite of La Madera quadrangle is largely suggestive. But in view of the first deformation established by structural evidence and its probable effect on an essentially monomineralic mass of quartzite, the relationship of relict fracture cleavage to the arcuate layers, and the assumed primary sedimentary origin of hematite layers based on analogy, it is this writer's opinion that the arcuate hematite layers are of tectonic origin. If so, then the proposition that these structures have originated through intense nonaffine translation along axial-plane cleavage and that they represent the remnant flanks of nearly isoclinal similar folds seems best to fit the available evidence.

Flat S-shaped segments of foliation in quartzite also resemble cross-bedding (fig. 14). This structure is produced by the development of wide-spaced (3 to 6 inches) fracture cleavage planes which transect foliation. The fact that the sigmoidal layers are an early structural plane separated by an axial-plane cleavage serves to distinguish this feature from relict cross-bedding. King and Rast (1955, p. 205) describe an identical feature found in the Moine Series.

The tectonic breccia phase of muscovitic quartzite superficially resembles metamorphic stretched conglomerate. The appearance of this unit is not due to original clastic textures but instead is the result of the superposition of second deformation planar structures on a first deformation linear element. Since a concise statement of this process with relevant evidence requires an integration of first and second deformation processes, the discussion of the origin of this breccia is presented in the section *Structural History*.

The Precambrian structural history given below is a synthesis of available structural evidence into a single hypothesis of geologic history. It is subjective, interpretative, and in part speculative. No further description of structural parameters is introduced, but rather that which has previously been discussed serves here as the basis of the structural interpretation. The reconstruction is in reality a summary of conclusions with a review of pertinent evidence.

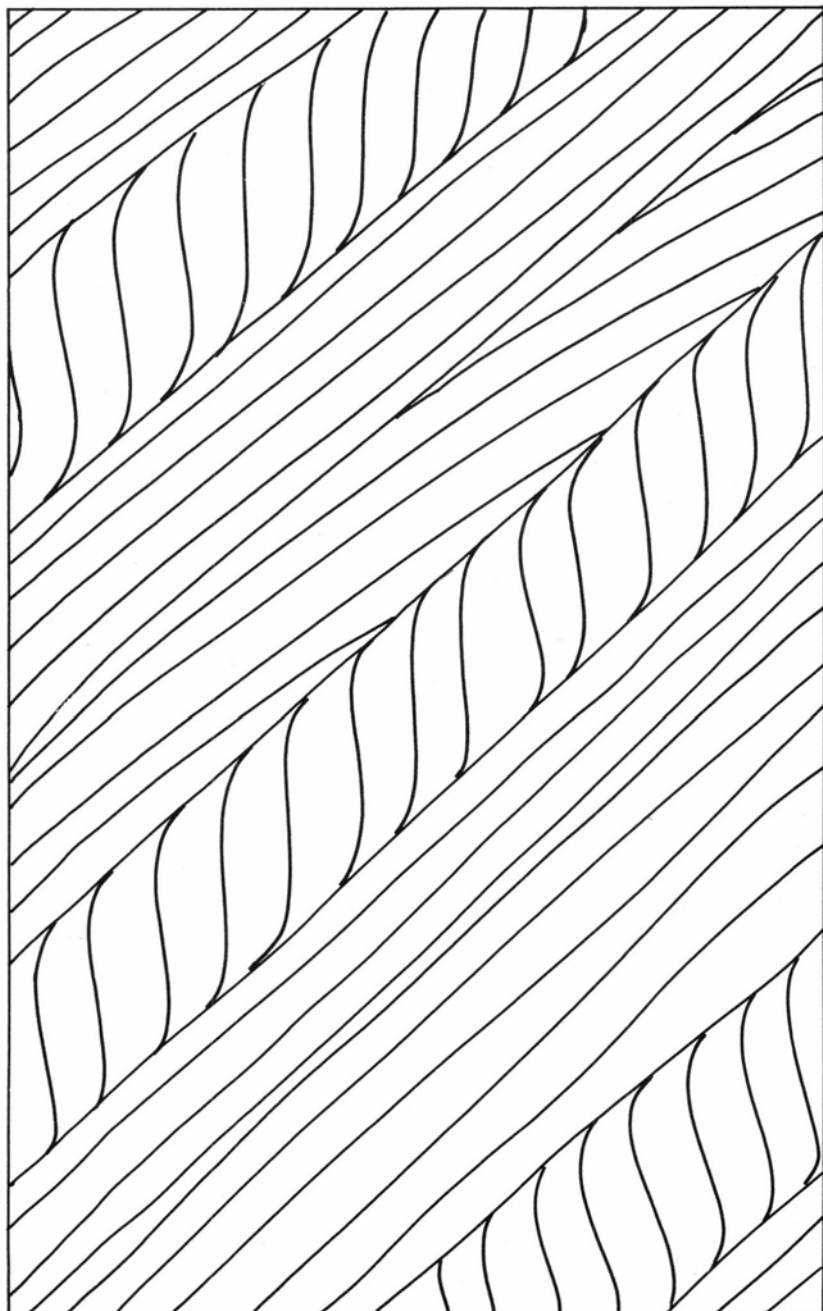


Figure 14

SIGMOIDAL SEGMENTS OF AN OLDER PLANAR ELEMENT TRUNCATED BY
FRACTURE CLEAVAGE

STRUCTURAL HISTORY

The expression *first deformation* is used throughout this report in referring to genetically related structural features such as folds, cleavage, and lineation that have been deformed by later structural events. The recognition of these features as belonging to a "first" event in any area of metamorphic rocks is a function of the tectonic history. It is entirely possible that in polymetamorphic areas the effects of deformation imposed upon older structural features could well destroy any readily recognizable evidence of an old orogenic event. In La Madera quadrangle, the oldest recognizable structural features are grouped within the expression *first deformation*. This term always should be considered synonymous with *first recognizable deformation* and means only that no evidence predating such first deformation structural features has been found.

The problem of descriptive as opposed to genetic terminology for structural features was discussed in the section *Planar Structures*. It was concluded that terms such as *flow* and *fracture cleavage* were of greater utility for the descriptive phase of this report than the Sander terminology of *S-planes*. The symbolic terminology of *S*, *L*, and *F* for planar, linear, and fold structures does have utility in reducing excess wordiness. The genetic connotation imposed by assigning subscripts indicative of temporal arrangement is not disadvantageous in this section, for the statements that follow are admittedly genetic and interpretative. This symbolic terminology is now adopted in order to more concisely develop the structural history. In this classification, *S* refers to the planar element folded by first deformation folds. *S*₁ is first deformation axial-plane cleavage; that is, relict fracture cleavage in quartzite and flow cleavage in micaceous rocks. *L*₁ indicates the B-lineation (kinematic axis of external rotation) within *S*₁ and marked by fluting, dimensional parallelism of elongate and platy minerals, elongate mineral segregations, and "clasts" in tectonic breccia. *F*₁ refers to first deformation mesoscopic folds. Second deformation axial-plane cleavage, consisting of fracture cleavage and slip cleavage which grades into flow cleavage, is designated *S*₂. Planar intersections of *S*₂ and *S*₁ are referred to as *L*₂. Second deformation B-lineation *L*₂ is parallel to second deformation fold axes, *F*₂. Axial-plane slip and fracture cleavage, planar intersections, and fold axes of the third deformation are designated *S*₃, *L*₃, and *F*₃ respectively. The assignment of small-scale structural features to this classification is summarized in Table 2.

FIRST DEFORMATION STRUCTURAL FEATURES

The effects of the first deformation in La Madera quadrangle are more profound and of greater geologic consequence than any other single structural event. However, the identification and establishment

of this event presents one of the most difficult tasks in the entire structural hypothesis. This earliest epoch of deformation, characterized by extreme dislocation and material transport, has resulted in the complete transposition of an earlier planar element (bedding ?), and is the mechanism which has produced the uniformly layered structural homogeneity of the metamorphic complex. These very processes have removed nearly all the obvious criteria of this folding. Most geologists have a mental picture of complexly deformed areas in which a vast number of folds are exhibited in individual outcrops. Unfortunately, the usual result of pervasive and penetrative unrestricted transport is a uniform layering which has a deceptively superficial resemblance to bedding.

Mesoscopic Structures

First deformation mesoscopic folds are rare but have a wide geographic distribution. They have been observed most often in quartzite and amphibolite and less frequently in feldspathic schist and muscovitic quartzite.

About thirty F_1 folds have been identified on the basis of style and/or orientation. They are characteristically plane cylindrical, nearly isoclinal to isoclinal, similar folds. They consist of highly attenuated limbs and thickened crests and troughs as viewed in normal section. Most folds of this generation are intrafolial folds. WL:A ratio is generally about 1:6-8, but folds with a ratio of 1:10 have been observed.

TABLE 2. STRUCTURAL ELEMENTS

| <i>Sequence</i> | <i>Planar Structures</i> | <i>Linear Structures</i> |
|--------------------|--|---|
| Primary | Bedding (S_1). Includes some hematite layering in quartzite, and some contacts between map units. | No evidence of sedimentary lineation. |
| First deformation | Axial-plane cleavage (S_1). Includes relict fracture cleavage in quartzite and flow cleavage in other metamorphic units. Isoclinal folding has transposed S parallel S_1 except in crests and troughs of mesoscopic folds (F_1) which fold S . | B -lineation (L_1) in S_1 . Includes fluting, dimensional parallelism of hornblende, kyanite, specular hematite, and micas, streaking, elongate segregations, boudins, and fragments in tectonic breccia. Mesoscopic folds (F_1) with axial-plane cleavage (S_1); axes are parallel L_1 . |
| Second deformation | Axial-plane cleavage (S_2). Includes fracture and slip cleavage which cuts S_1 . | B -lineation (L_2) in S_2 . Line of intersection between S_2 and S_1 . Mesoscopic folds (F_2) with axial-plane cleavage (S_2), axes are parallel L_2 . |
| Third deformation | Axial-plane cleavage (S_3). Includes fracture and slip cleavage which cuts S_2 and S_1 . | B -lineation (L_3) in S_3 . Line of intersection between S_3 and S_2 or S_1 . Mesoscopic folds (F_3) with axial-plane cleavage (S_3), axes are parallel L_3 . |

The folded element (S) is transposed by the isoclinal folding so that it is nearly everywhere subparallel to S_1 . In quartzite, the folded element is hematite layering; in amphibolite, it is alternating light- and dark-colored layers; in feldspathic schist, it is a crude alternation of quartzose and feldspathic layers. Severe attenuation has resulted in the shearing out of many mesoscopic similar folds, the remnants of which form gently sweeping arcuate layers that strongly resemble cross-bedding. The style of first deformation folds is shown in Figure 15.

Planar structures associated with the first deformation are relict fracture cleavage in quartzite and flow cleavage in all other rock types. These structures are parallel to the axial planes of F_1 folds, hence, constitute axial-plane cleavage. This S_1 cleavage is ubiquitous and well developed in La Madera quadrangle. It is parallel to the contacts of all major metamorphic units and, together with parallel compositional layering, constitutes the prominent planar feature present in every outcrop of Precambrian rocks.

Textural and mineralogic lineation (L_1) in the plane of S_1 is a conspicuous feature in all outcrops. It consists of intersecting cogenetic nearly parallel shear planes that mark axial-plane cleavage, parallel alignment of dimensionally elongate minerals, and the intersection of S_1 with S. It is designated a B-lineation because it is parallel to F_1 and is normal to girdles in quartz and mica. L_1 is presumably the result of penetrative componental movement during unrestricted transport. Textural lineation, particularly fluting in quartzite, has been enhanced by a tendency for the growth of kyanite to take place along this pre-existing fabric element.

By plotting the strike and dip of planar features and the bearing and plunge of linear elements in equal-area lower-hemisphere projection, it is possible to obtain a visual measure of the orientation and degree of preferred orientation of various structural features. First deformation structural elements are illustrated on Plates 3a, c, f, and e. Diagrams f and e on Plate 3 are π -S of relict fracture cleavage and flow cleavage; that is, the poles to the cleavage planes are plotted. The similarity of these diagrams attests to the similar orientation of these two structural features in La Madera quadrangle. It also supports the conclusion that fracture cleavage and flow cleavage are structural analogs derived from the same process that differs in effect on rocks of different composition. The tightly grouped contours forming the polar maximums are a reflection of the uniform strike and dip of S_1 throughout the area. The average strike of N. 30° W. and average dip of 60° W is marked by the trace of S_1 . This regional disposition is the result of rotation by later folding and does not represent the attitude of S_1 as it was originally formed. The change in trend of S_1 from a northwesterly strike over the bulk of the exposed Precambrian to an east-west trend is marked by the extended one per cent contours in the north-central part of Plate 3f. L_1 exhibits a high degree of preferred orienta-



Figure 15
FIRST DEFORMATION MESOSCOPIC FOLDS

tion marked by the polar maxima in the southwest quadrant of Plate 3a. The fact that L_1 lies within S_1 is indicated by the trace of S_1 which passes through the L_1 concentration (pl. 3h). The plot of mesoscopic fold axes illustrated on Plate 3c contains a girdle which follows the trace of S_1 . The weak submaxima in the southwest quadrant at a position corresponding to an average bearing and plunge of S. 25° W. and 30° S is in the same position as the L_1 maximum on Plate 3a and indicates the parallelism of these two first deformation linear elements. The F_1 submaximum is weak compared to concentrations in other parts of the girdle on Plate 3c because the pronounced shearing and dislocation of the first deformation has destroyed most of the mesoscopic folds formed during that deformational episode.

Macroscopic Structures

Only one macroscopic fold form, the synform-antiform-synform complex outlined by amphibolite east of Ancones, can be delineated with any certainty on the geologic map (pl. 1). Other map features which may be the result of folding about a south-southwest-plunging axis are (1) the isolated layers of quartz-kyanite schist in the Ortega Mountains, in particular the attenuated V-shaped mass east of Canada del Rancho; (2) the large-scale intercalated layers of feldspathic schist and muscovitic quartzite crudely exposed in the Cribbenville district; and (3) the digitate, wedge-shaped mass of feldspathic schist in the upper reaches of Canon de los Alamos. The tectonic breccia phase of the muscovitic quartzite which underlies the eastern margin of Mesa de la Jarita is a product of the first deformation, although in part it owes its existence to second deformation processes. The tight isoclinal folding associated with the first deformation has resulted in structural intercalation of thin layers along the margins of many map units. Among the finest examples are the interlayered lithologies along the amphibolite margin east of Ancones, in many outcrops of muscovitic quartzite and feldspathic schist on the west-facing scarp bordering Mesa de la Jarita in the upper Vallecitos valley, and at the quartzite-muscovitic quartzite boundary zone exposed in the cliff along the west bank of the Rio Tulas in SD/4SE1 sec. 18, T. 25 S., R. 9 E.

The scarcity of macroscopic fold forms is a characteristic feature of the first deformation. This orogenic event is indicated for the most part by the distribution, style, and orientation of mesoscopic features. The paucity of macroscopic structures is a direct result of the nature of the deforming process. Unrestricted penetrative transport of material is not conducive to the preservation of large-scale fold structures, the magnitude of which is suggested by the form of the folded amphibolite discussed above. Consequently, little positive evidence for the first deformation is afforded by outcrop pattern on the geologic map.

Summary of Evidence

The prominent planar element in the Precambrian of La Madera quadrangle is relict fracture cleavage and flow cleavage which contains a conspicuous lineation. This planar element uniformly strikes N. 30° W. and dips 60° W. The linear element has an average bearing of S. 25° W. with a plunge of 30° SW. Plane cylindrical isoclinal similar folds exist in which the planar elements indicated above parallel the axial planes and the linear element parallels fold axes. Relict fracture cleavage and flow cleavage containing the prominent lineation are exhibited in northwest-trending folds that are later than the element they fold. Since the folded surface in northwest-trending folds is axial-plane cleavage to south-southwest trending folds, the latter can not be crenulate folds formed during growth of the northwest-trending folds. Girdle fabrics of mica, hornblende, and quartz normal to textural and mineralogic lineation (L_1) suggest that this lineation and the planar element which contains it formed by rotational componental movements about L_1 rather than by mimetic recrystallization.

The fold form exhibited by the amphibolite east of Ancones is not consistent with the pattern of macroscopic folds developed in the second deformation fold system and therefore must predate it. Also mesoscopic folds developed on the periphery of the amphibolite have axial trends which bear and plunge to the south-southwest, concordant with L_2 marked by hornblende lineation within the amphibolite. The disharmony between the amphibolite fold complex of synform-antiform-synform, as described earlier, and the northwest-trending second deformation structure is indicated by the flanking mesoscopic folds and by the closure present in the east-trending arroyo wall. Yet this structure occurs within a domain of left-handed northwest-trending mesoscopic nonplane cylindrical similar folds that extends from the western margin of the Ortega Mountains across the Vallecitos valley to the eastern margin of Mesa de la Jarita (fig. 14). This domain of left-handed folds (looking north along the axes) indicates a single overturned limb of an overturned antiform. The fold closure marked by amphibolite, and the right-handed character of the amphibolite layer considered in its entirety, is inconsistent within the overturned anti-formal limb. Rather, the congruence of the folded amphibolite with flanking mesoscopic folds and mineralogic lineation with south-southwest trend indicates that the fold form marked by amphibolite is a first deformation macroscopic fold.

Effect Upon Original Stratigraphic Relations

The first deformation has effectively transposed original bedding into a new position essentially parallel to axial-plane cleavage. Attenuation and extreme dislocation with concomitant juxtaposition of contrasting lithologies on a mesoscopic scale strongly suggests the presence

of similar conditions on a macroscopic scale. These effects imply several conditions that are of primary importance in recounting the geologic history of the Precambrian in this area. First, original stratigraphic continuity has been destroyed, and it follows from this that the position of map units as they now appear do not bear any obvious relationship to original superposition or stratigraphic contiguity. Uncomfortable as this may be to the geologist who seeks to unravel Precambrian stratigraphy and sedimentology, it is nonetheless true. Second, the intense and pervasive metamorphic processes of the first deformation have resulted in a layered sequence that has been refolded into well-defined antiforms and synforms of regional aspect. The acceptance of these structures as anticlines and synclines by previous workers in this area has led to conclusions regarding the relative age of layers within the tectonically induced sequence. If the conclusions of this writer are correct regarding an early phase of isoclinal folding prior to the formation of northwest-trending folds, the stratigraphic succession and implied relative age of metamorphic rock units is of no value and should be disregarded. It also follows from the above discussion that statements regarding the original thickness of metamorphic units, particularly the quartzite, are unfounded. The estimate of quartzite thickness ranging from 10,000 to 20,000 feet, based on sections measured normal to first deformation axial-plane cleavage, could well be the result of duplication by folding and flowage of material; it is entirely conceivable that a sandstone layer a few hundred feet thick may more accurately represent original stratigraphic thickness.

SECOND DEFORMATION STRUCTURAL FEATURES

The second deformation has profoundly affected Precambrian rocks of La Madera quadrangle. It has resulted in a readily recognizable fold system of regional significance. Structural features such as folds, rock cleavage, and lineation genetically associated on the basis of similarity in style and orientation, and which deform pre-existing structural elements are considered part of the second deformation. The fold system produced during this orogenic event is the most obvious structural feature of the area and its physical features and effects have been recognized by other workers studying the Precambrian of north-central New Mexico (Just; Jahns; Barker; Muehlberger, 1960b, p. 103; Lindholm). It is commonly referred to in this report and elsewhere as the *northwest-trending fold system*.

Mesosopic Structures

Mesosopic folds constitute the most prominent feature of the second deformation. Style and orientation are the criteria which serve to identify folds of this generation. Mesosopic folds are widely distributed but are most frequently encountered and best developed in the

quartzite mass of the Ortega Mountains. Most of the folds are non-plane cylindrical, asymmetric, and overturned to the northeast. There is some variation, however, for plane cylindrical, symmetric overturned folds have been observed in a few outcrops. The similar to disharmonic style of this generation of folds is consistent throughout the map area. Also, the overturned position of the axial planes is characteristic of all observed folds, although the dip of the axial planes ranges from about 10 to 60 degrees to the west. The style of second deformation mesoscopic folds is shown in Figure 16.

F2 axes trend N. 20° - 30° W. The plunge of fold axes, however, ranges from about 10° SE through horizontal to about 30° NW. The attitude of F2 axes, and their preferred orientation in space, is illustrated on Plate 3c and h. It is apparent from Plate 3c that, statistically, more F2 axes plunge to the northwest than to the southeast; hence, the axial trend of the second deformation fold system is best represented as gently northwest-trending.

Mesoscopic folds of this system define geographic domains based on the criterion of shear sense (fig. 17). The largest domain, spanning the bulk of the Ortega Mountains and including all but the east flank of Mesa de la Jarita, consists of folds with a left-handed shear sense, when the observer is looking northward. Designation of relative shear sense depends upon whether the observer views the fold down or up the fold plunge. Several southeast-trending folds in this domain have a right-handed shear sense because the sense of shear was always recorded when the observer viewed a fold down the plunge. When the southeast-trending folds are viewed up the plunge, that is, northwestward, they have a left-handed shear sense congruent with nearby associated mesoscopic folds. Two other domains of left-handed folds lie to the northeast of Mesa de la Jarita. These domains of left-handed mesoscopic folds alternate with narrow domains of right-handed folds. Only part of one of these domains is present at the southwest margin of the Ortega Mountains.

Second deformation fracture cleavage and slip cleavage are well developed. Where these planar structures are present in outcrops with F2 mesoscopic folds, they are parallel or nearly parallel to fold axial surfaces. In exposures devoid of folds, planar structures are identified with the second deformation system if they transect S_1 and if their orientation is similar to the regional orientation of axial-plane cleavage in F2 folds. Form and style of this generation of cleavage are in some places an aid to its identification. In many outcrops, particularly of feldspathic schist and muscovitic quartzite, unequivocal S2 slip cleavage is penetrative and consists of very close-spaced planes between which S_1 flow cleavage planes are sharply flexed. This feature is so rarely observed in third deformation structures that it serves to distinguish S2 from S3.

Plate 3f illustrates the preferred orientation of second deformation

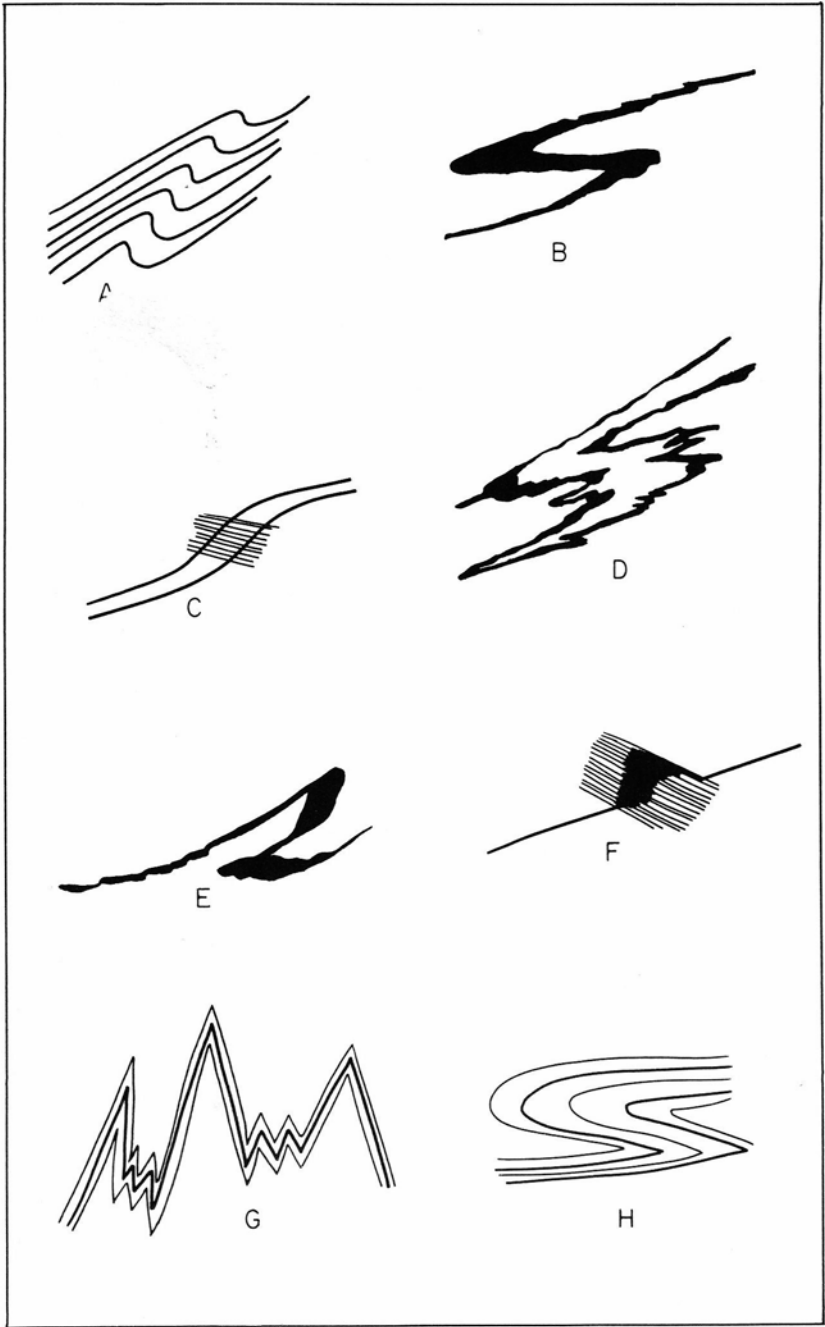


Figure 16
SECOND DEFORMATION MESOSCOPIC FOLDS

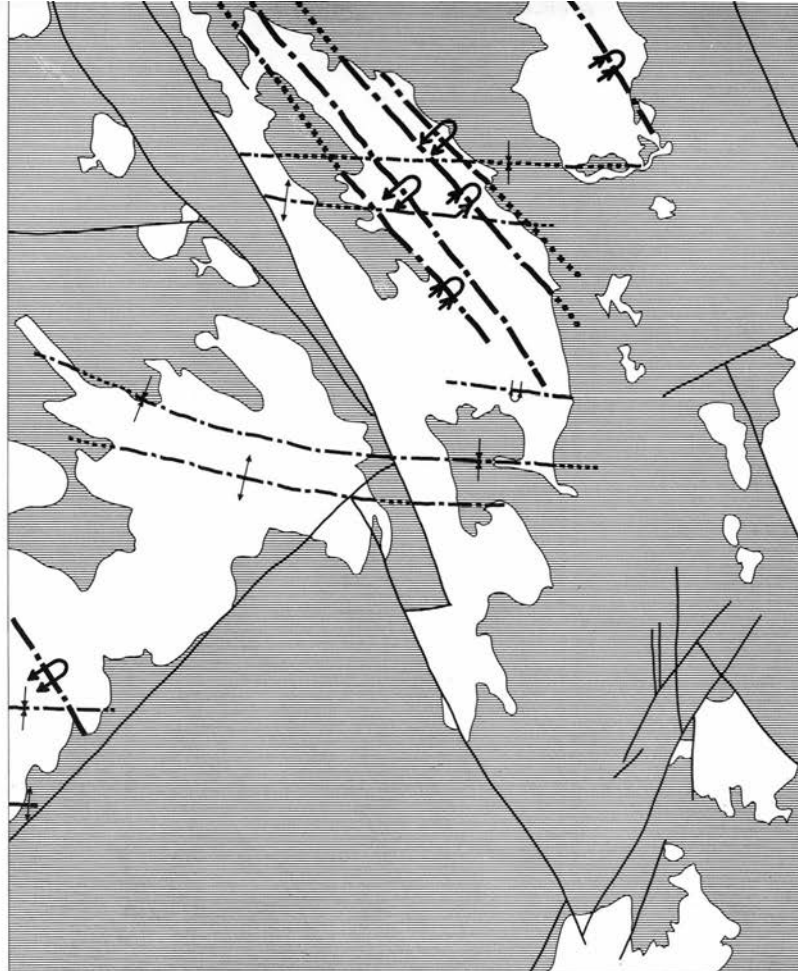
fracture and slip cleavage. These planes have an average strike of about N. 30° W. and dip from 30° to 40° W, as indicated by the polar maximum in the northeast quadrant. This maximum represents the preferred orientation of poles to cleavage and is therefore 90 degrees removed from the trace of **S**₂.

Lination related to the second deformation is largely the result of the intersection between **S**₂ and an earlier planar element. It is confined to exposures in which **S**₂ is well developed and is generally measured in **S**₁ because slabs of rock tend to weather off this better-developed planar element. Because of the mode of origin of **L**₂, it is parallel to second deformation fold axes by definition. The parallelism of **L**₂ with **F**₂ is reaffirmed by measuring and plotting each element independently. On Plate 3b and c the submaxima in the northwest quadrants occupy similar positions. This relationship demonstrates the parallelism between **L**₂ and **F**₂ independent of definition.

Macroscopic Structures

Following Pumpelly's Rule, the bearing and plunge of second deformation macroscopic folds are assumed to be congruent with the bearing and plunge of genetically related mesoscopic folds. In the absence of direct evidence, it is also assumed that the style, WL:A ratio, and degree of overturning exemplified by the mesoscopic folds corresponds directly to the same parameters of the macroscopic folds. The domains of left-handed and right-handed mesoscopic folds shown on Figure 17 represent alternate limbs of macroscopic synforms and antiforms. The heavy dash-dot lines which separate domains represent the trace of macroscopic axial planes on the present surface. The orientation and shear sense of mesoscopic folds indicate a sequence of overturned folds composed of, from southwest to northeast, antiform-synform- antiform -synform- antiform-synform, or three antiform-synform pairs. It is obvious from the spacing of the fold axial traces, however, that the fold of greatest magnitude is represented by the overturned limb of the antiform underlying most of the Ortega Mountains. The tectonic style in normal section of the macroscopic second deformation is illustrated in Figure 18. The overturned form of these folds suggests material transport from southwest and northeast. However, since these folds have a style that implies considerable flow and nonaffine translation along axial-plane cleavage, the direction of transport (kinematic a) may not be normal to fold axes (Ramsay, 1960, p. 89). In Figure 18, a lithologic profile along the normal section is superimposed on the fold form in order to illustrate the lack of conformity between the outcrop pattern of metamorphic map units and the juxtaposed limbs of macroscopic folds.

The axial trends of second deformation folds remain constant in the map area north of a line drawn from the southwest to northeast



EXPLANATION

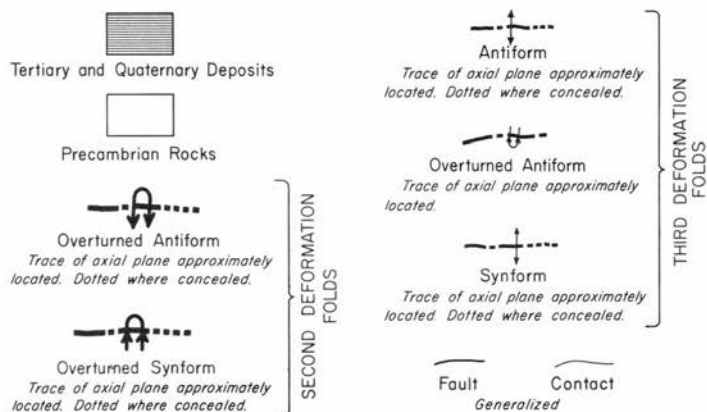


Figure 17

DOMAINS OF SECOND AND THIRD DEFORMATION FOLDS

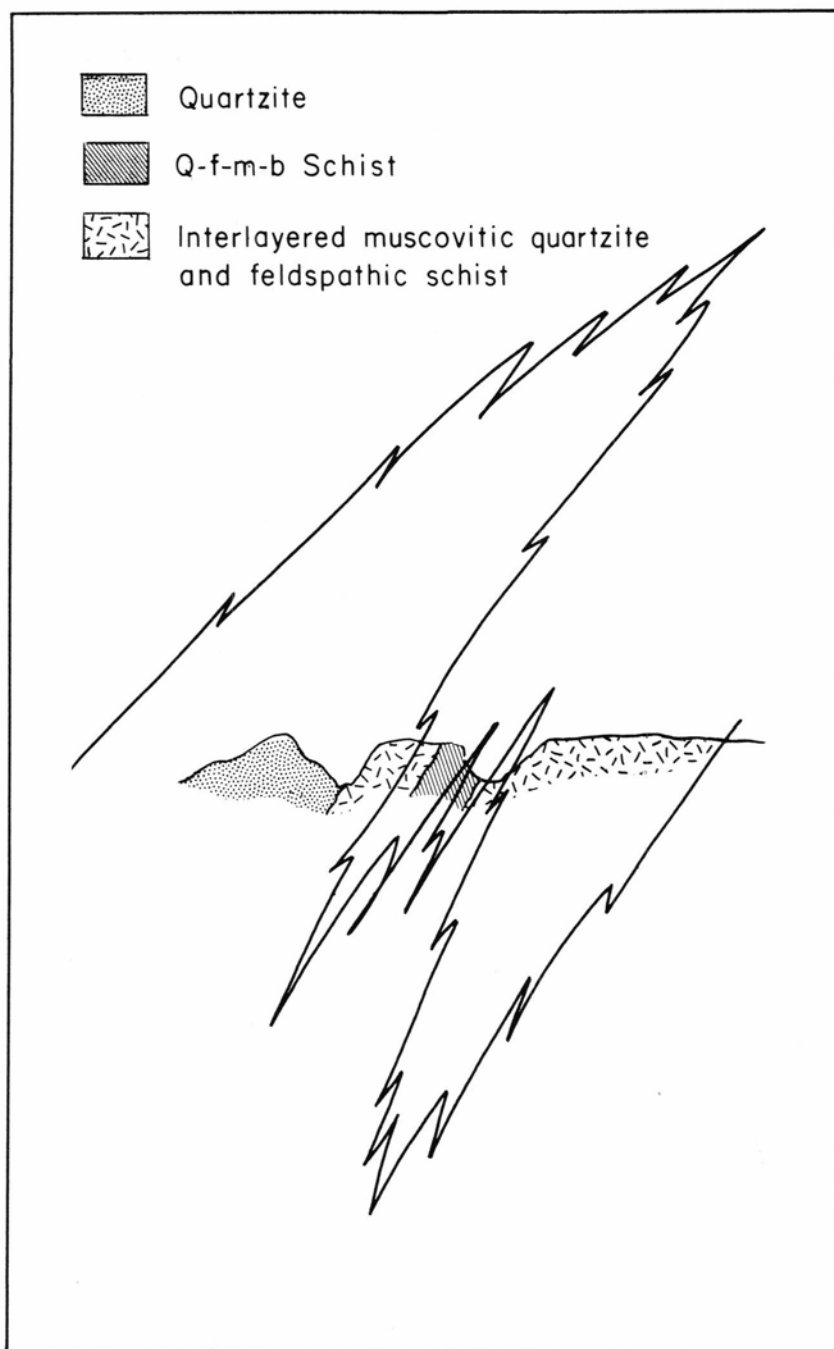


Figure 18
TECTONIC STYLE OF SECOND DEFORMATION FOLD SYSTEM

corners of La Madera quadrangle. In this area, **F2** macroscopic folds are plane noncylindrical. Southeast of this diagonal boundary, however, there is a prominent change in strike of second deformation structural features and lithologic contacts to a dominantly east-west direction (pl. 1). The arbitrary diagonal across the quadrangle marks the approximate hinge line of this arcuate form which is convex to the southwest. For ease of description, this macroscopic form is hereinafter referred to as the *Petaca arc*, named for a town through which the hinge line passes. A similar change in strike of structure and lithology occurs in the Las Tablas quadrangle to the north (Barker) and in the Chama quadrangle to the northwest of Las Tablas quadrangle (Muehlberger, 1960b). Since the origin of the Petaca arc involves consideration of third deformation structures, discussion of this problem is reserved for a later section. Suffice it to say here that no single hypothesis would seem to offer a completely satisfactory explanation of this structure.

Second deformation structures, in particular the uniform strike and dip of planar elements, have imparted a prominent northwest "grain" to the Precambrian within La Madera quadrangle. The northwest "grain" is in part the result of fault-controlled topography. Fault trends, however, may also owe their origin in part to northwest-trending structures established by the first and second deformations.

Summary of Evidence

The presence of the second deformation fold system is indicated by widely distributed mesoscopic folds consistent in style and orientation. The fact that these folds occur in discrete domains based upon shear sense indicates their relationship to a regional fold system. These features serve to distinguish second deformation folds from incongruous folds or fold forms originating from sedimentologic processes. Axial-plane fracture and slip cleavage consanguineous with second deformation folds are also well developed and widely distributed. The uniform attitude of these planar elements also indicates a pervasive tectonic event. All geologists who have worked in this area have noted the presence of northwest-trending fold structures, although none has studied their regional continuity or relationship to the Precambrian structural history within La Madera quadrangle.

Superposition of structural elements is evidenced by **F2** folds in which the folded element is S_1 , and by the intersection of **S2** fracture and slip cleavage which transects S_1 flow cleavage and foliation.

Effect Upon Older Structures

Second deformation folding has rotated all structural elements of the first deformation. S_1 now strikes northwest and dips uniformly west because of nearly isoclinal folding about **F2**. The preferred orientation of L_1 with a south-southwest bearing and plunge is shown on Plate 3a.

The concentration of L_1 within a polar maximum is the result of several independent variables. The processes and conditions which control the locus of a deformed linear element are (1) the angle between the plane of deformation and the linear element, (2) the rotation of lineation in a great circle path in similar or shear folds or a small circle path in concentric folds, (3) the degree of parallelism between opposing fold limbs, (4) the asymmetry of folds which introduces a sampling bias into the frequency of linear orientation directions, and (5) homogeneous versus heterogeneous domains. The absence of a girdle pattern in L_1 lineations is the result of strongly asymmetric isoclinal similar folds. These conditions have resulted in a well-defined polar maximum almost bisected by S_1 . The broad area of the maximum is due partly to the slightly heterogeneous nature of La Madera quadrangle, considered as a single domain with respect to L_1 , and partly to a skewness between the plane of deformation of **F2**, defined for want of better evidence by *ac* quartz girdles, and the original orientation of L_1 . This last condition is inferred from minor divergence of L_1 on opposing flanks of **F2** folds, but it is obscured by the presence of transposed L_1 , in turn masked by a growth fabric of kyanite and mica. No direct evidence is available to determine the direction of tectonic transport for **F2** folds. Ramsay has described a technique for determining kinematic *a* by constructing the line of intersection between axial-plane cleavage and the locus of deformed lineation. Inasmuch as L_1 lineation is not disposed in a girdle, this technique is not applicable to the resolution of second deformation kinematic *a*.

The tectonic breccia phase of muscovitic quartzite exposed along the eastern flank of Mesa de la Jarita is the result of superposition of **S2** upon L_1 structures where the rock consists of thinly laminated muscovitic quartzite, hematitic quartzite, and monomineralic quartz rods. The principal rock type of this phase is muscovitic quartzite with the content of interlayered quartz and hematitic quartzite ranging from about 10 per cent to about 70 per cent. These layers are parallel to S_1 and contain L_1 fluting and mineralogic lineation. Many of the thin layers are discontinuous in S_1 and form rodlike or flattened cylindrical bodies parallel to L_1 . The layering and elongate fragments are presumably the result of penetrative slip along S_1 during the first deformation. Separation of the elongate rods into flattened ellipsoidal fragments has been induced by left-handed slip (looking north) along **S2**. The length of individual quartz and quartzite fragments parallel to L_1 ranges from less than one inch to about six inches. Nonaffine slip along **S2** has resulted in a staggered array of ellipsoidal fragments when they are viewed in the plane of **S2**. Figure 19 consists of four schematic sketches of the relations shown in exposures which strike east-west in NW1/4 sec. 23, T. 26 N., R. 8 E. These sketches illustrate the progressive development of the salient features exhibited by the tectonic breccia.

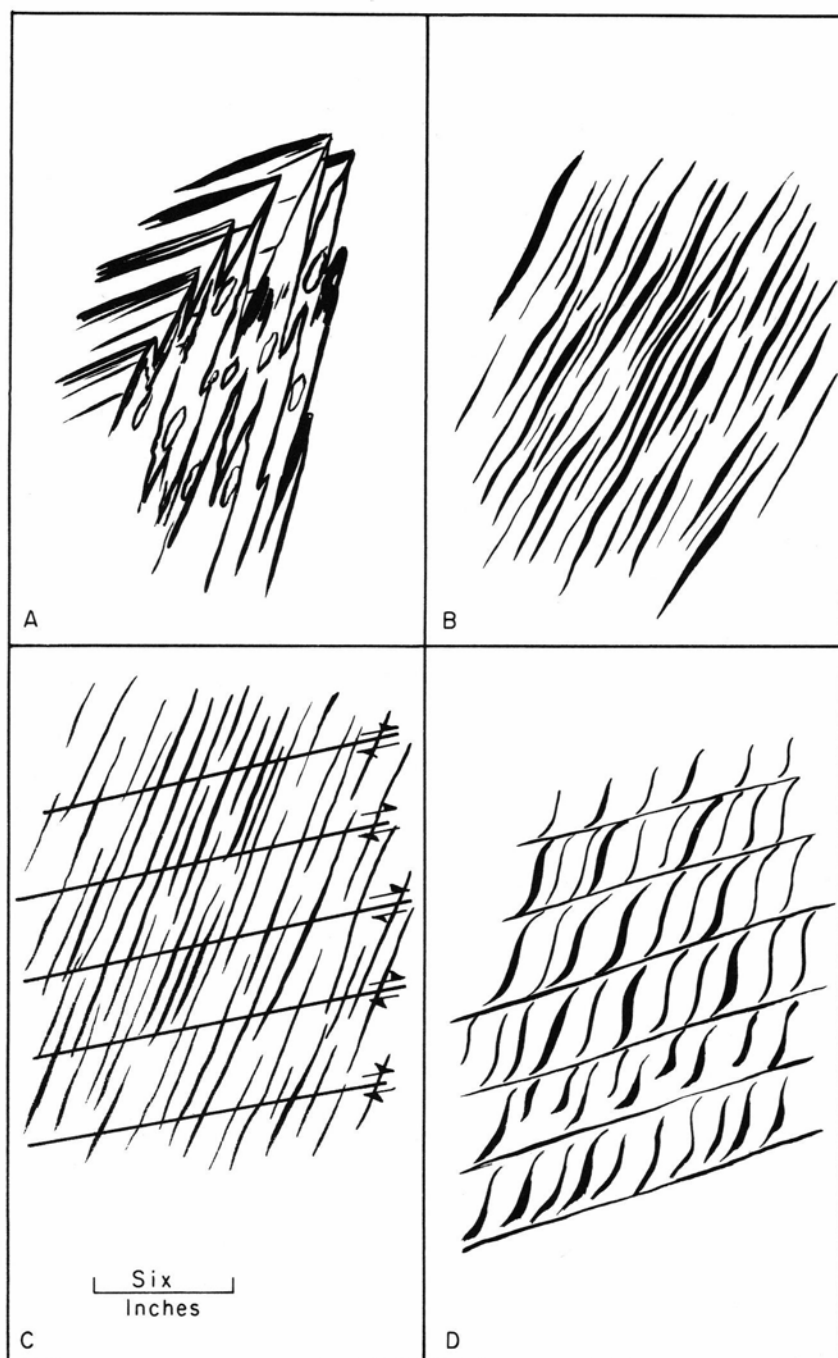


Figure 19. EVOLUTION OF TECTONIC BRECCIA

THIRD DEFORMATION STRUCTURAL FEATURES

The third deformation is characterized by a west-trending set of structural features that are mostly cataclastic in nature, minor flowage of material being rare. The trend is marked by nearly vertical axial-plane cleavage that cuts across older planar elements. Minor folds and warps are largely confined to the margin of the west-trending shear planes. Paired antiforms and synforms are wide-spaced and appear to represent a series of step folds from north to south across La Madera quadrangle. Pegmatite dikes and tabular quartz veins are similar in orientation and localized along some of the axial-plane cleavage surfaces.

Mesoscopic Structures

Third deformation mesoscopic folds are widely distributed throughout La Madera quadrangle but are best developed in muscovitic quartzite west of the Sunnyside mine and in kyanite schist within the Ortega Mountains. There is considerable variation in form ranging from open asymmetric nearly concentric folds to appressed chevron folds. Nearly symmetrical, open similar folds are the most common type encountered. Many of the folds are simple flexures developed along the margin of widely spaced axial-plane slip cleavage. Figure 20 illustrates the common forms of third deformation folds. The style of folds illustrated is typical of folding accomplished by intercrystalline displacements with little neocrystallization involved in the deforming process.

Unlike second deformation structures, planar structures of the third deformation occur more commonly than **F3** folds. Where **S3** fracture and slip cleavages occur in **F3** folds, they are parallel to fold axial surfaces. In exposures where **S3** occurs without genetically related folds, the planar elements are identified by the fact that they transect first and second deformation structural elements. The preferred orientation of **S3** is shown on Plate 3f and h. Poles to **S3** form submaxima localized about the north-central and south-central sections of the projection sphere. The diffuse nature of these submaxima is largely the result of relatively few measurements and considerable variation in strike of **S3**. **S3** ranges in strike from N. 70° W. to S. 70° W. and ranges in dip from about 60° N to 60° S. A few third deformation shear planes are nearly horizontal.

The orientation of fold axes and lineation produced by the intersection of axial-plane cleavage (**S3**) with **S1** and **S2** is highly variable. On Plate 3b, which shows lineation produced by intersecting planes, the two submaxima arranged along **S1** represent **L3**, which bears to the west and plunges between 30 and 60 degrees west. Because **S3** has a broad range in strike and dip, the submaxima percentage values are considerably reduced. Plate 3d indicates the probable projection domain for **L3** and **F3** as limited by variation in axial-plane orientation and

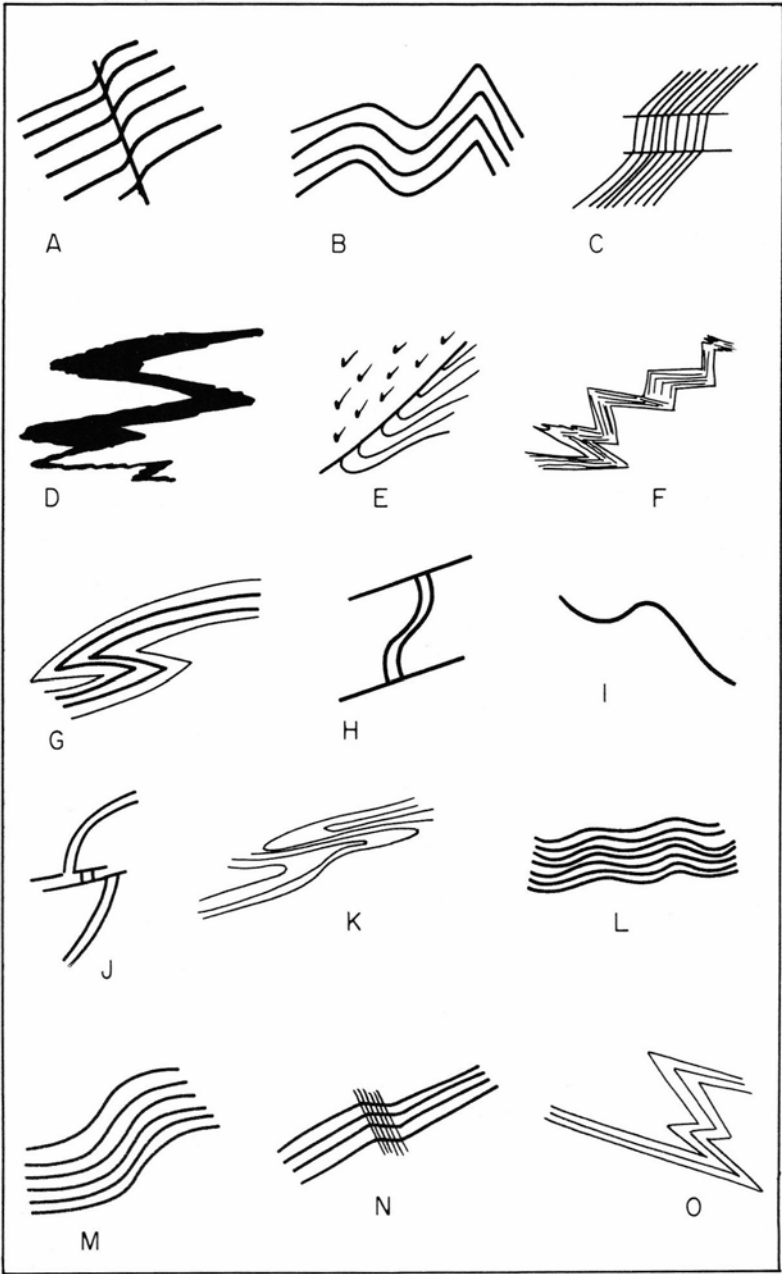


Figure 20
THIRD DEFORMATION MESOSCOPIC FOLDS

orientation of the older planar element. Inasmuch as most of the displacement of rock during the third deformation has been accomplished by slip along wide-spaced slip cleavage, **F3** folds may exhibit axes of external rotation that do not necessarily parallel axes of internal rotation or lie perpendicular to the deformation plane.

Rotation of Earlier Structural Elements

There exists no direct evidence to establish major rotation of earlier structural elements by the third deformation fold system. Rotation can be observed on a minor scale in outcrop where the flexures flanking axial-plane cleavage have warped and bent pre-existing rock cleavage. This rotation is insignificant macroscopically. Considerable rotation has taken place in the zone of relatively intense east-west folding east of Sunnyside mine. However, this is a very local area and, again, is of little importance on a regional scale. The only indirect evidence which could be construed to indicate major rotation of earlier structural elements lies in the present gently doubly plunging nature of **F2** fold axes. It is equally possible, however, that **F2** axes were formed with this orientation and that they have not undergone any significant rotation since their inception. In general, the wide-spaced minor warps and slip planes produced by the third deformation seem to this author to constitute a very ineffective means for widespread rotation of earlier elements.

Macroscopic Structures

Third deformation synforms and antiforms of regional extent are not marked by the distribution of metamorphic rock units in La Madera quadrangle. Like second deformation macroscopic structures, they are defined by domains of mesoscopic folds with a similar shear sense. **F3** folds consist of paired synforms and antiforms which appear alternately close-spaced and wide-spaced in north-south profile and are plane cylindrical within the confines of La Madera quadrangle. Figure 17 illustrates the trace of the axial planes on the present surface. From the distribution of wide-spaced paired synforms and antiforms, it is inferred that the third deformation fold system is composed of a series of three "step" folds in which the southern limbs of antiforms have been raised relative to an arbitrary, gently inclined reference plane that represents uniformly dipping S_1 . The inferred relations as they would appear in a north-south section are shown in Figure 21. The available data are insufficient to determine the amount of relative displacement along the axial-plane slip surfaces. The structural picture is also complicated by the variable dip exhibited by axial-plane cleavage and the variable plunge of **F3**. The amount of deformation is greater in the vicinity of the Sunnyside mine, for in that area mesoscopic folds are nearly isoclinal with axial planes overturned to the south and nearly

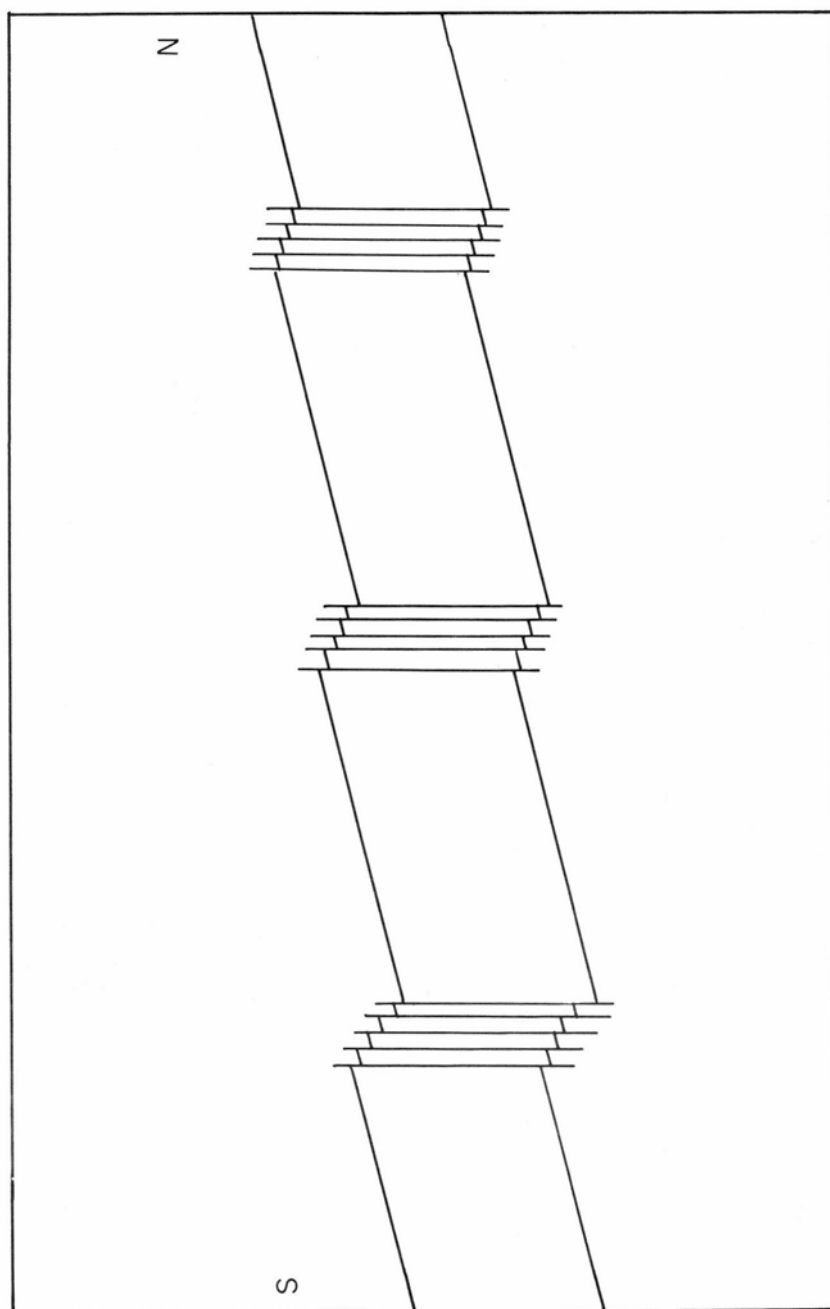


Figure 21
SCHEMATIC CROSS SECTION OF THIRD DEFORMATION FOLD SYSTEM

horizontal. The traces of these folds could not be carried for more than a few thousand feet. The writer is able to offer no well-documented explanation for the relatively prominent effects of the third deformation in this local area.

The style and form of the third deformation strongly resemble a conjugate fold system in the Caledonides, as defined by Johnson (1956, p. 347). He states that

The fold systems consist of paired reversed folds that are controlled by a pair of symmetrically arranged slip planes which are inclined towards one another and intersect parallel to the eastward plunging fold axes. The slip planes are parallel to the axial planes of the reversed folds and cut the median limbs of the folds. . . . Some conjugate fold systems have formed from monoclinial steps in the parting planes which evolve into overturned z folds. . . . The tectonic style suggests brittle deformation.

There are obvious similarities between the fold system described by Johnson and third deformation features of La Madera quadrangle. The symmetrical relationship of two sets of S3 planes and the style of folding are the most obvious. A striking dissimilarity exists in the scale of the structures, for Johnson states that "The scale is important; the conjugate folds are usually about 1-3 feet across"; in La Madera quadrangle, however, no folds of this type were observed on a mesoscopic scale. Although it is possible that the third deformation fold system represents a conjugate fold system developed on a regional scale, there is insufficient evidence to warrant strongly favoring this conclusion.

Summary of Evidence

Four lines of direct evidence for a third episode of regional dislocation exist. First, numerous examples of fracture and slip cleavage with a west trend transect older first and second deformation structures. The orientation of these planar structures is spatially distinct from similar-appearing second deformation rock cleavage; hence, their origin during the waning stages of the second deformation seems unlikely. Second, mesoscopic folds with a westerly trend and plunge can be observed in several outcrops to fold cleavage banding, which is the result of S2 transecting S1. Third, both the folds and planar structures of the third deformation are of distinctly different style. Fourth, examples of S3 slip cleavage transecting S2 slip cleavage have been found (fig. 7b). First and second deformation structures exhibit features indicative of solid flow, unrestricted transport, and syntectonic mineralogic reconstitution. Third deformation structures differ from earlier structures in that they exhibit a brittle and cataclastic style.

PROBLEM OF THE PETACA ARC

The Petaca arc was defined earlier as the change in strike exhibited by mapped metamorphic units from a northwest trend in the northwest part of the quadrangle to a west trend in the southeast part of the quadrangle.

The change in trend of map units is shown in several areas. The boundary between amphibolite and muscovitic quartzite east of Ancones marks the most prominent change in strike. The curvature is emphasized by the combination of dip of the amphibolite layers and erosion on the west-facing scarp. The quartzite-muscovitic quartzite contact in the same area also changes strike across the summit of the southern margin of Mesa de la Jarita, substantiating the true change in strike. Similar deflections from the "normal" northwest trend are indicated by the amphibolite bridging Palomas Canyon and Canon de los Alamos in secs. 17 and 18, T. 25 N., R. 9 E., by the feldspathic schist in isolated hills in Precambrian rock bordering the Petaca road in sec. 5, T. 25 N., R. 9 E. and sec. 32, T. 26 N., R. 9 E., and by quartzite in granitic gneiss within the isolated outcrop of Precambrian rock in sec. 19, T. 26 N., R. 9 E., although in this latter locality the arcuate structure is convex northeastward. Thin layers of quartz-kyanite-andalusite schist in La Madera Mountain strike west, whereas similar layers in the quartzite ridge northwest of Vallecitos strike northwest. These dissimilar trends of identical rock layers in isolated exposures are believed to be an expression of the Petaca arc.

East-striking foliation continues through the Ojo Caliente quadrangle (Muehlberger, personal communication) and across the Rio Grande through the Picuris Range (Montgomery). The generalized strike of foliation and schistosity changes from northwest to west in Las Tablas quadrangle (Barker) and is west-trending in the Brazos River area (Muehlberger, 1960b).

The Petaca arc also includes the structural elements S_1 and S_2 , which change trend across the quadrangle. However, S_1 , which is generally parallel to lithologic layering, changes trend more sharply than S_2 , and consequently S_2 truncates lithologic layering within the realm of the Petaca arc. The most noticeable divergence from the general northwest trend of S_1 and S_2 is in La Madera Mountain where foliation strikes on the average about 20 degrees farther west. Schistosity in rocks along the Petaca road, noted above, strikes north and may be anomalous because of considerable faulting in this area. The essential relationship between planar structures and map pattern is that, in general, S_2 transects lithologic contacts at an acute angle within the Petaca arc, implying that S_2 has been imposed upon the arcuate trend of lithologic layering after the arc has formed.

Third deformation structures bear no genetic relationship to the Petaca arc despite the fact that the ends of the arc parallel the regional

trends of second and third deformation fold systems. Where **F3** folds are best developed, there is no change in trend of lithologic layering, and conversely, where the change in strike is most pronounced, **S3** is neither more close-spaced nor more pervasively developed.

One explanation that fits the above evidence is that the Petaca arc is the result of sinuous lithologic trends developed during the first deformation. In the absence of well-defined macroscopic first deformation folds, no direct evidence for this conclusion can be offered. An alternative is that the truncation of **S1** and **S2** implying superposition is more apparent than real. If this is true, the Petaca arc may represent an undulating axial surface in second deformation macroscopic folds. This would correspond closely to what has generally been considered folds *in a*.

A similar macroscopic arcuate structure, the Schiehallion Twist, has been described by King and Rast (p. 264) from the Moines and Dalradian of Scotland.

Although two directions of folding strongly predominate, and commonly remain distinct, on a small scale, the distribution of formations on a regional scale often display a gradual swing from one direction to another. Indeed, on this scale, the folds themselves show a corresponding arcuate pattern.

The explanation offered by the authors is that this structure "originated as an accommodation structure by the simultaneous operation of locally intense cross-folding, and the main Caledonian overfolding." It is interesting to note, however, that arcuate structures may form during one episode of folding, as evidenced by the salients and recesses along the western front of the Appalachian Valley and Ridge System.

The geometric classification of the first and second fold systems in La Madera quadrangle is dependent upon the interpretation of the Petaca arc. If the arcuate outcrop pattern of metamorphic units formed during the first deformation, then the **F1** macroscopic folds were non-plane cylindrical prior to the formation of **F2** folds. After superposition of **F2** folds, **F1** folds would be nonplane noncylindrical and **F2** folds would be nonplane cylindrical. If, alternatively, the Petaca arc represents curved second deformation axial planes, or crenulate folds, then **F1** folds were plane cylindrical prior to the second deformation, and nonplane noncylindrical **F2** folds have transformed **F1** folds into non-plane noncylindrical folds. In either event, **F1** folds are now nonplane noncylindrical because of superposed folding, but the geometry of the two fold systems during the history of their development hinges upon the origin of the Petaca arc.

The writer considers the origin of the Petaca arc largely unresolved. It is possible that a detailed structural study along the entire sinuous

trace of metamorphic units from the Brazos River area into the La Madera area may provide evidence requisite for a satisfactory solution of this problem.

SUMMARY

Three episodes of regional, pervasive deformation are recognized in the Precambrian rocks of La Madera quadrangle. The total effect of these events has been to produce a metamorphic complex containing a variety of structural elements that vary in style, orientation, and order of superposition.

The earliest deformation for which evidence now exists—the first deformation—involved major transport of material. Unrestricted flow, accompanied in later stages by flattening and penetrative shearing movements, resulted in the formation of isoclinal folds. These folds were probably recumbent and their axes were oriented southwest-northeast. Most of these folds were destroyed during the terminal phases of deformation by axial-plane shearing. These processes transposed an earlier planar element, probably bedding, into parallelism with the fold axial planes. Shearing movements, internal rotation, and contemporaneous recrystallization resulted in well-defined axial-plane flow and fracture cleavage which contain prominent textural and mineralogical b-lineation. The mode and intensity of deformation resulted in the destruction of original stratigraphic continuity and contiguity. The end result of the first deformation process was a regularly interlayered sequence of mixed lithologies.

The second deformation resulted in the formation of a readily recognizable macroscopic fold system of generally nonplane cylindrical, asymmetric, nearly isoclinal, similar folds. The axial planes of these folds are overturned to the northeast. Fold axes trend northwest-southeast and are gently doubly plunging with a slight preferred orientation of axes plunging to the northwest. Congruent mesoscopic folds, similar in style in all rock types, indicate that Precambrian rocks behaved as a plastic or viscous medium during deformation. Earlier planar and linear structures were rotated nearly parallel with second deformation axial planes by the folding, and this process combined with the overturned attitude of the folds has produced the homoclinal, southwest-dipping layered sequence now exposed. Fracture and slip cleavages parallel to fold axial planes developed during the later stages of deformation and constitute a prominent structural parameter of the fold system. The form and attitude of this fold system are responsible for the prominent northwest structural "grain" exhibited by exposed Precambrian rocks in the map area. Transport of material from southwest to northeast is suggested by the uniform eastward overturning of synforms and antiforms.

The third deformation consists largely of wide-spaced axial-plane fracture and slip cleavage ranging in strike from N. 70° W. to S. 70° W. and in dip from 60° S to 60° N. The variation in strike and dip of axial-plane cleavage, combined with uniformly west-dipping older planar elements has produced variable fold axial trends. Mesoscopic folds are sparsely developed, yet widely distributed. The disposition of minor flexures in narrow, widely spaced zones suggests that the disposition of macroscopic plane cylindrical folds form a step-fold pattern with broad southerly flanks raised relative to steep northerly flanks. The low amplitude warps associated with this fold system have not effectively rotated earlier planar elements.

A synoptic diagram (pl. 3h) containing the structural elements of all three deformations summarizes the orientation of all parameters discussed above.

The temporal relationships of the deformational history constitute the most speculative aspect of this structural study. Superposition has been documented, but the amount of elapsed time between the generation of one set of structural elements and the penetrative development of a second set of structural elements is obscure. The only direct evidence that might answer this question consists of radiogenic dates. A detailed radiogenic analysis of rocks in La Madera quadrangle has been initiated, but the results will not be available for some time (L. E. Long, personal communication, 1963). Even this technique may not satisfactorily date all periods of deformation because of isotopic modification induced by reconstitution of component minerals during dynamo-thermal metamorphism, thermal metamorphism, or conversely the possible lack of isotopic modification during purely dislocation or cataclastic metamorphism.

Variation in style and orientation within the immense framework of Precambrian time is the only available evidence which can be construed to indicate that the three periods of deformation are temporally distinct. It is merely a hypothesis that these events are widely separated in time. Thus, it seems more likely that deformation accomplished by flow of rock should be separated by a considerable length of time from an epoch of brittle failure than the alternative that such distinctly different rheologic conditions would be closely associated in time. Even the traditional example of orogenic pulses separated by hundreds of millions of years in post-Precambrian time is being challenged; hence, it does not serve as a useful analogy. Clearly, the suggestive evidence of structural style is of little value, for it is dependent upon many independent variables. There is no question but that the temporal framework in Precambrian structural history is a tenuous and speculative subject. In the writer's opinion, the three stages of deformation represented in the Precambrian complex of La Madera quadrangle are probably separated by many millions of years, but there should be no

doubt in the reader's mind that this conclusion is merely an intuitive supposition.

ANOMALOUS STRUCTURAL TRENDS

Several folds and planar structures have been observed in the Precambrian of La Madera quadrangle which can not be readily integrated into the structural history. Open concentric folds that are largely gentle swells in S2 occur in granitic gneiss along the eastern quadrangle boundary in the NE $\frac{1}{4}$ sec. 29, T. 26 N., R. 9 E. A single mesoscopic antiform with a WL:A of about 5:1 exposed in this area bears S. 20° W. and plunges between 5° and 10° S. A similar type of fold is exposed in the north face of Canada de Los Tangues in the SW $\frac{1}{4}$ sec. 7, T. 26 N., R. 9 E. Here, flow cleavage in granitic gneiss is broadly folded about an axis that trends north-south and plunges about 60° S. Other evidence for a minor set of mesoscopic folds is illustrated by the concentration of fold axes in the southwest quadrant of Plate 3c. The axial trend of these broad warps is similar to F1 and L1 trends, but the distinctly different style and the fact that they fold S2 structures distinguish them from first deformation folds.

A set of vertical joint planes trends N. 20° E. and bears an approximate axial-plane relationship to the south- to southwest-trending structures. None of these planes is found in the minor flexures, and consequently there is no direct evidence they represent axial-plane fracture cleavage. It has been noted in the field that many of the north-northeast-trending joints are in fact extension joints, rendering their origin as fracture cleavage untenable.

Several possible explanations are proffered for the structures discussed above, but in the absence of definitive evidence, their origin remains speculative. The similarity in style between the minor warps and F3 folds suggests that the former may be the result of the third deformation with aberrant orientation resulting from the range in orientation exhibited by S3 axial-plane cleavage imposed upon S2 divergent from its otherwise uniform regional trend. They may also be the result of locally skewed stress distribution during the third deformation.

An entirely different interpretation is that the folds are the result of drag effects along major normal faults in the area. The absence of like folds in Tertiary rocks cut by the major faults, and the absence of any obvious association between the geographic distribution of faults and the south-southwest-trending folds makes this hypothesis untenable. It is also possible that the metamorphic rocks have been modified by regional compression postdating the third deformation, but the relative rarity of these minor folds tends to preclude this hypothesis.

PRECAMBRIAN STRUCTURAL TRENDS IN NEW MEXICO

Geologic study of exposed Precambrian rocks in New Mexico, with only a few exceptions, has consisted largely of reconnaissance surveys. The principal result of such surveys to date has been to outline the gross distribution and lithology of metamorphic units. The status of structural studies is even less satisfactory. Most reports devote only a few sentences or paragraphs to structural features and ignore the distribution and origin of structural parameters necessary for the elucidation of structural history.

The available evidence of structural trends, though generally meager, does not conflict with the structural systems resolved in La Madera quadrangle:

"On La Jarita Mesa . . . the axial planes of all the folds strike about N30°W and dip about 40°SW." (Barker, p. 65)

"These strata were compressed during Precambrian time into two large overturned folds that trend and plunge northwest." (Barker, p. 1)

"The axes of these slightly asymmetric open wrinkles have an average trend of N76°W and an average plunge of 39°WNW." (Corey, p. 26)

"The foliated metamorphic rocks of the Sandia—Manzanita—Manzano zone have a general northeasterly trend; that is, the foliation has this trend." (Fitzsimmons, 1962, p. 94)

. . . the outcrop pattern outlines a broad fold . . . ; the axial plane of this fold strikes about N30°E and dips northwest." (Hewitt, 1959, p. 98)

"Small asymmetric folds . . . occur in quartz feldspar gneiss. . . . The axial planes are parallel, strike north, and are vertical; the axes of the folds plunge 30°S." (Hewitt, p. 98)

. . . the attitude of foliation suggests a synclinal structure, the axial plane of which strikes N10°E and is vertical. In this general area and to the south the regional northeast trend is locally disturbed by folds and contortions. . . ." (Hewitt, p. 98)

"Locally these rocks . . . have a lineation which deviates very little from a mode of N63°E, 51°NE, bearing and plunge, respectively." (Kuellmer, 1954, p. 6)

"Precambrian rocks were folded along N70°E and N20°W axes." (McKinlay, 1957, p. 14)

"Precambrian rocks were folded along a N70°E and a N20°W axis [sic]." (McKinlay, 1956, p. 20)

"Along the west front of the Sangre de Cristo Mountains, south of Little Latir Creek, the metamorphic rocks are exposed in folds which trend N.20°W. to due

north. The change in structure from a northeast trend to a northwest trend probably represents a second folding of the Precambrian rocks. Additional evidence of two periods of Precambrian deformation at about right angles is shown in an outcrop of biotite gneiss on the lower Cabresto Creek. In this exposure, a series of tight folds, 6 inches to 1 foot across, trend N.60°E. These folds, in turn, are folded along a N.40°W. axis that plunges 10-20 degrees to the south-east." (McKinlay, 1956, p. 22)

"Great pressure along a north-south direction has produced a system of tightly compressed east-west trending folds, the axial planes and limbs of which are essentially parallel, are overturned slightly to the north, and dip southward at an average inclination of 60° to 70°." (Montgomery, p. 54)

"A broad view of the structural picture is of major northwest-plunging folds." (Muehlberger, 1960a, p. 47)

"East-trending fracture cleavage has been noted in quartzite south of the Brazos Box in Rio Arriba County." (Muehlberger, personal communication, 1963)

"With negligible exception the axes of the drag folds approximately parallel the direction of dip of the schistosity. . . . A south-southeast dip of 50° to 80° characterizes both schistosity and bedding, nearly throughout the area mapped." (Reiche, 1949, p. 1196)

"This thick series shares a remarkable persistency in strike and dip directions, averaging N20°E and dip of 45°W." (Stark and Dapples, 1946, p. 1157)

"In the thicker zones of schist, there is much distortion, indicating more than a single period of deformation." (Stark and Dapples, p. 1157)

"The axial plane [of a large syncline] strikes N30°E [dip ranges from 60° to 85° SE]. . . . The syncline has an average plunge of not more than 5° or 6° to the southwest." (Stark, 1956, p. 30)

"The Sais quartzite and Blue Springs schist . . . contain folds that cross the regional trend of the central syncline. An anticline, syncline, and anticline occur in an outcrop less than a mile wide. The folds trend northwest and plunge in the same direction." (Stark, p. 31)

It is interesting to note that all the trends correspond to one or more of those recognized in La Madera quadrangle. No writer has reported the presence of three fold trends in any part of New Mexico, but significantly, where superposition has been recognized, the relative order of superposition is, in every instance, the same as that established in the area of this report. Such evidence alone is not sufficient to confirm the presence of three spatially distinct fold systems in La Madera quadrangle, but neither does it contradict this writer's historical hypothesis and hence is considered substantiating evidence.

PRECAMBRIAN GEOLOGIC HISTORY

The earliest recognizable geologic process represented in the Precambrian rocks of La Madera quadrangle is sedimentation. Sands and shales accumulated in some primordial basin. The prevalence of quartzite and siliceous pelites suggests a littoral-neritic accumulation, and the high silica content of the quartzite indicates that the original sandstone body or bodies were mature sediments. Deposition of clastic material was interrupted from time to time by the sudden influx of siliceous volcanic clastics, pyroclastics, or flow rock. Basic flows may have accompanied deposition or have been intruded as dikes and sills in the sedimentary mass. Prior to profound orogenesis, the accumulated sediments were intruded by granite which was accompanied by widespread peripheral metasomatism.

This accumulated assemblage of siliceous and pelitic sediments, siliceous and basic volcanics, and granite was intensely deformed and metamorphosed during an episode of regional metamorphism. Deformation was uniformly distributed and was accomplished by pervasive, penetrative componental movement during mineralogic reconstitution. These events resulted in a northeast-trending belt of isoclinal folds, which by analogy with post-Precambrian mobile belts was probably marked by a chain of mountains. Crystallization of equilibrium mineral assemblages during regional metamorphism took place in a pressure-temperature environment near the greenschist-almundine amphibolite boundary. Phyllites (phyllonites?), schists, and schistose gneisses were the characteristic products of this major event. The metamorphism was nearly isochemical with mobility of ions occupying a restricted range from a few inches to a few feet.

At some later time these rocks were again subjected to regional compression which resulted in the formation of a northwest-trending system of nearly isoclinal folds uniformly overturned to the northeast. This deformation resulted in local flowage of material, reorientation of mineral components in the cores of individual folds, and the transposition of older structural features. Small-scale structural features remained as relicts throughout most of the area and may have in part been emphasized by neocrystallization.

A regional episode of metamorphism accompanied by minor local metasomatism occurred after the second deformation. The principal result of this process was the hydration of pre-existing kyanite. It may also have contributed to the formation of kaolinite at the expense of muscovite and regrowth of kyanite, quartz, mica, and albite that formed as aggregates of randomly oriented individuals which poikiloblastically include the first deformation fabric. Pyritization of chlorite schist and solution of portions of feldspathic schist with concomitant introduction of manganese may have been local effects of a hydrothermal stage. Polymorphic conversion of kyanite and dehydration of kaolinite to form

andalusite appear to be local effects confined to sheared breccia zones in quartzite. The dehydration of kaolinite possibly heralded a period of increasing temperature that led to the formation of sillimanite in quartzite and garnet in feldspathic schist and chlorite schist. The formation of specularite and associated rutile and/or sphene probably occurred at about this same time and indicates a relatively high partial pressure of oxygen accompanying a general increase in thermochemical activity. The high temperature event in this area may have been consanguineous with the later metamorphism or much later in time.

After widespread neocrystallization, the rocks were subjected to a relatively weak, largely cataclastic deformation. The formation of broad folds with wide-spaced axial-plane cleavage was the principal effect of this event. The generally west-trending, nearly vertical axial-plane cleavage suggests compression along a north-south line. Shear folds formed locally and in one area third deformation slip cleavage is gradational into flow cleavage.

Pegmatite intrusion and local alkali metasomatism is the last major geologic event recorded within the Precambrian. Most of the pegmatite dikes were intruded along third deformation axial-plane cleavage and a few along second deformation axial-plane cleavage. In the larger metasomatic aureoles surrounding some of the pegmatites, alkali metasomatism has resulted in the formation of microcline and albite in quartzite, regrowth of muscovite in schists, and the conversion of chlorite and hornblende to biotite in otherwise potassium-deficient hornblende-chlorite schist. In one small area, tourmaline-bearing schist is closely related to tourmaline-rich pegmatites and probably represents boron metasomatism as a minor variety of pegmatitic metasomatism.

A synopsis of the tectonic and thermal history of the map area, as interpreted by the writer, is presented in schematic form in Figure 22. The relative order is believed to be correct, but the relative spacing is arbitrary and has no significance with respect to elapsed time between events.

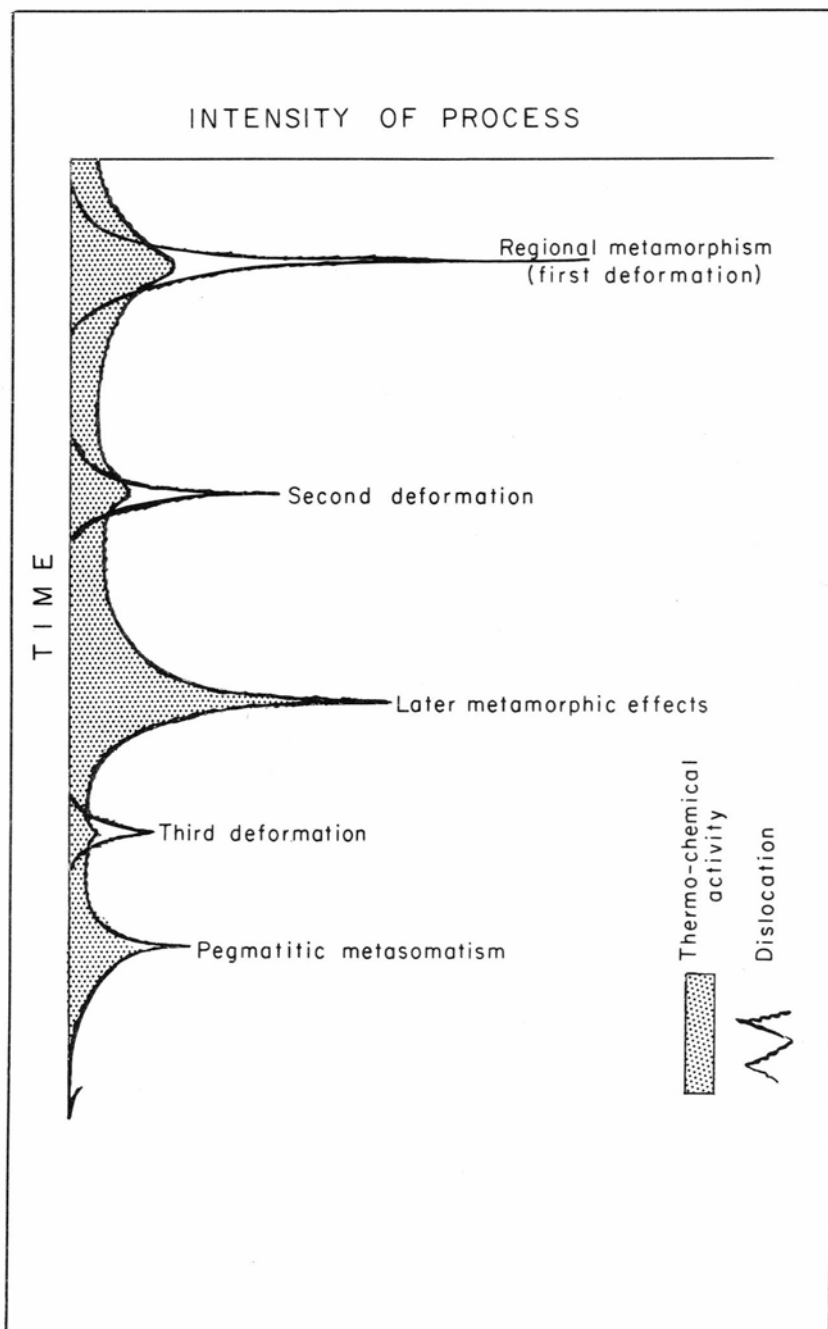


Figure 22
SCHEMATIC DIAGRAM ILLUSTRATING PRECAMBRIAN GEOLOGIC HISTORY IN LA MADERA QUADRANGLE

References

- Anderson, E. M. (1948) *On lineation and petrofabric structure and the shearing movement by which they have been produced*, Quart. Jour. Geol. Soc. London, v. 104, p. 99-132.
- Atwood, W. W., and Mather, K. F. (1932) *Physiography and Quaternary geology of the San Juan Mountains, Colorado*, US. Geol. Surv., Prof. Paper 166, 176 p.
- Barker, Fred (1958) *Precambrian and Tertiary geology of Las Tablas quadrangle, New Mexico*, N. Mex. Inst. Min. and Tech., State Bur. Mines and Mineral Res., Bull. 45, 104 p.
- Butler, A. P. (1946) *Tertiary and Quaternary geology of the Tusas—Tres Piedras area, New Mexico*, unpub. Ph.D. thesis, Harvard Univ.
- Cloos, Ernst (1946) *Lineation: A critical review and annotated bibliography*, Geol. Soc. Am., Mem. 18, 122 p.
- (1947) *Boudinage*, Am. Geophys. Union Trans., v. 28, n. 4, p. 626-632.
- Corey, A. F. (1960) *Kyanite occurrences in the Petaca district, Rio Arriba County, New Mexico*, N. Mex. Inst. Min. and Tech., State Bur. Mines and Mineral Res., Bull. 47, 70 p.
- De Sitter, L. U. (1957) *Cleavage folding in relation to sedimentary structure*, Twentieth Internat. Geol. Cong., Mexico, Section V, p. 53-64.
- Engel, A. E. J. (1949) *Studies of cleavage in the meta-sedimentary rocks of the northwest Adirondack Mountains, New York*, Am. Geophys. Union Trans., v. 30, n. 5, p. 767-784.
- Fairbairn, H. W. (1949) *Structural petrology of deformed rocks*, Cambridge, Mass.: Addison-Wesley Pub. Co., 344 p.
- Fitzsimmons, J. P. (1962) *Precambrian rocks of the Albuquerque country, N. Mex.* Geol. Soc., Guidebook, Twelfth field conference, The Albuquerque country, p. 90-96.
- Fyfe, W. S., Turner, F. J., and Verhoogen, J. (1958) *Metamorphic reactions and metamorphic facies*, Geol. Soc. Am., Mem. 73, 259 p.
- Gilluly, James (1934) *Mineral orientation in some rocks of the Shuswap terrane as a clue to their metamorphism*, Am. Jour. Sci., ser. 5, v. 28, n. 165, p. 182-201.
- Green, J. R. W. (1931) *The south-west Highland sequence*, Quart. Jour. Geol. Soc. London, v. 87, p. 513-550.
- Hewitt, C. H. (1959) *Geology and mineral deposits of the northern Big Burro Mountains—Redrock area, Grant County, New Mexico*, N. Mex. Inst. Min. and Tech., State Bur. Mines and Mineral Res., Bull. 60.
- Jahns, R. H. (1946) *Mica deposits of the Petaca district, Rio Arriba County, New Mexico*, N. Mex. Inst. Min. and Tech., State Bur. Mines and Mineral Res., Bull. 25, 294 p.
- Johnson, M. R. W. (1956) *Conjugate fold systems in the Moine thrust zone in the Lochcarron and Coulin Forest areas of Wester Ross*, Geol. Mag., v. 93, n. 4, p. 345-350.
- Just, Evan (1937) *Geology and economic features of the pegmatites of Taos and Rio Arriba counties, New Mexico*, N. Mex. Inst. Min. and Tech., State Bur. Mines and Mineral Res., Bull. 13, 73 p.
- King, B. C., and Rast, N. (1955) *Tectonic styles in the Dalradians and Moines of parts of the central Highlands of Scotland*, Proc. Geol. Assoc., v. 66, p. 243-269.
- Knopf, E. B., and Ingerson, E. (1938) *Structural petrology*, Geol. Soc. Am., Mem. 6, 270 p.

- Kuelimer, F. J. (1954) *Geologic section of the Black Range at Kingston, New Mexico*, N. Mex. Inst. Min. and Tech., State Bur. Mines and Mineral Res., Bull. 33.
- Kvale, A. (1948) *Petrologic and structural studies in the Bergsdalen quadrangle, Western Norway*, Part II, Structural Geology, Bergen Museums Arbok 1946 og 1947, 255 p.
- Leith, C. K. (1905) *Rock cleavage*, US. Geol. Surv., Bull. 239, 216 p.
- Lindholm, R. (1963) *Structural petrology of the Ortega quartzite, Ortega Mountains, Rio Arriba County, New Mexico*, unpub. M. S. thesis, Univ. Texas, 43 p.
- McKinlay, P. F. (1956) *Geology of Costilla and Latir Peak quadrangles, Taos County, New Mexico*, N. Mex. Inst. Min. and Tech., State Bur. Mines and Mineral Res., Bull. 42.
- (1957) *Geology of Questa quadrangle, Taos County, New Mexico*, N. Mex. Inst. Min. and Tech., State Bur. Mines and Mineral Res., Bull. 53.
- Montgomery, Arthur (1953) *Pre-Cambrian geology of the Picuris Range, north-central New Mexico*, N. Mex. Inst. Min. and Tech., State Bur. Mines and Mineral Res., Bull. 30, 89 p.
- Muehlberger, W. R. (1960a) *Precambrian rocks of the Tusas Mountains, Rio Arriba County, New Mexico*, N. Mex. Geol. Soc., Guidebook, Eleventh field conference, Rio Chama country, p. 45-47.
- (1960b) *Structure of the central Chama platform, northern Rio Arriba County, New Mexico*, N. Mex. Geol. Soc., Guidebook, Eleventh field conference, Rio Chama Country, p. 103-109.
- Nelson, B. W., and Roy, R. (1958) *Synthesis of the chlorites and their structural and chemical composition*, Am. Mineralogist, v. 43, p. 707-725.
- Ramsay, J. G. (1960) *The deformation of early linear structures in areas of repeated folding*, Jour. Geol., v. 68, n. 1, p. 75-93.
- Rast, N. (1956) *The origin and significance of boudinage*, Geol. Mag., v. 93, n. 5, p. 401-408.
- Reiche, Parry (1949) *Geology of the Manzanita and North Manzano Mountains, New Mexico*, Geol. Soc. Am. Bull., v. 60, p. 1183-1212.
- Sander, B. (1930) *Gefügekinde der Gesteine*, Vienna: Springer, 352 p.
- Smith, H. T. U. (1938) *Tertiary geology of the Abiquiu quadrangle, New Mexico*, Jour. Geol., v. 46, p. 933-965.
- Stark, J. J. (1956) *Geology of the South Manzano Mountains, New Mexico*, N. Mex. Inst. Min. and Tech., State Bur. Mines and Mineral Res., Bull. 34.
- , and Dapples, E. C. (1946) *Geology of the Los Pinos Mountains, New Mexico*, Geol. Soc. Am. Bull., v. 57, p. 1121-1172.
- Sterrett, D. B. (1913) *Mica in Rio Arriba County, New Mexico*, US. Geol. Surv., Bull. 530, 15 p.
- (1923) *Mica deposits of the United States*, US. Geol. Surv., Bull. 740, 342 p.
- Turner, F. J. (1948) *Mineralogical and structural evolution of the metamorphic rocks*, Geol. Soc. Am., Mem. 30, 342 p.
- , and Verhoogen, J. (1960) *Igneous and metamorphic petrology*, New York: McGraw-Hill Book Company, Inc. (2nd ed.), 694 p.
- , and Weiss, L. E. (1963) *Structural analysis of metamorphic tectonites*, New York: McGraw-Hill Book Company, Inc., 545 p.
- White, W. S. (1949) *Cleavage in east-central Vermont*, Am. Geophys. Union Trans., v. 30, n. 4, p. 587-594.
- Whitten, E. H. T. (1959) *A study of two directions of folding: The structural geology of the Monadliath and Mid-Strathspey*, Jour. Geol., v. 67, n. 1, p. 14-47.

Index

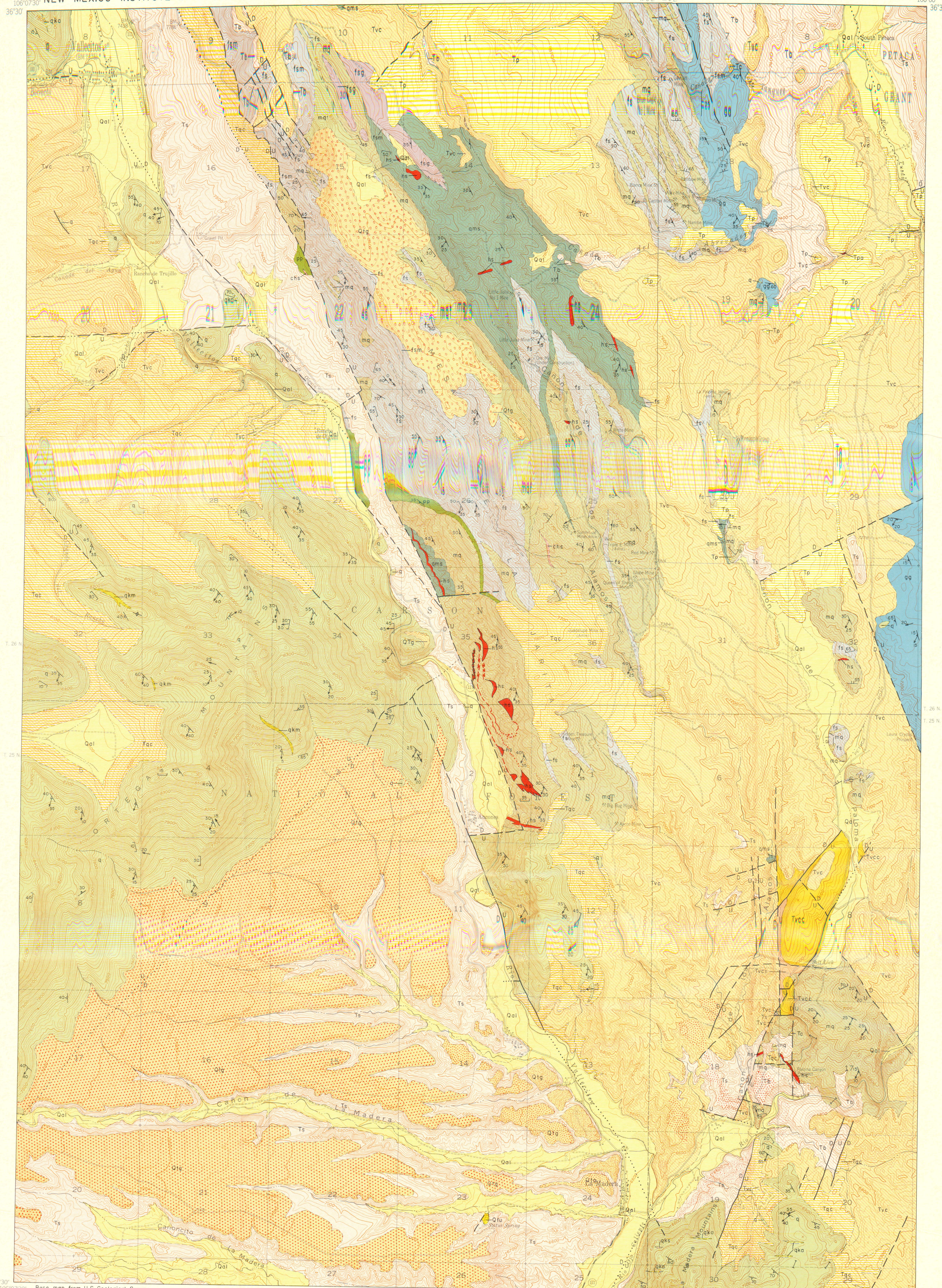
Numbers in **boldface** indicate main sections

- Abbildungskristallisation*, 82
 Abiquiu tuff, 13
 Albite, 17, 34, 35, 36, 43
 Almandine, 1, 44, 45
 Alumino-silicate minerals, 19, 47
 Aluminous schist, 23, 24
 Aluminum, 48
 Amphibolite, 1, 11, 17, 44, 45, 63, 66, 79, 83, 92, 98, 101, 102, 117
 Ancones (N. Mex.), 4, 5, 19, 21, 30, 36, 40, 42, 54, 57, 59, 63, 66, 70, 72, 83, 88, 90, 101, 117
 Andalusite, 1, 23, 47, 50
 Andesine, 40, 46
 Andesite, 9, 15; porphyry, 12, 15
 Anticline, 85
 Antiform, 85, 101, 102, 112, 114
 Apatite, 40, 41
 Appalachian Valley and Ridge System, 118
 Arkosic sandstone, 7, 9, 12, 14, 16, 35
 Augén, 19, 22, 33, 57
 Basalt, 9, 11, 12, 13, 14-15, 42; amygdaloidal, 11, 15; vesicular, 15
 Basic flow rock, 1
 Bedding, 54-59, 91, 93, 102
 Biotite, 17, 27, 29, 33, 36, 37, 38, 40, 41, 44, 47, 50, 54, 59, 67; schist, 1, 41, 51
 Biscara Member, 11, 13
 Böhm lamellae, 21, 27
 Boudins, 22, 72-73, 82, 83
 Brazos River, 117, 119
 Burned Mountain Metarhyolite, 29
 Canada de los Tangles, 11, 121
 Canada del Rancho, 101
 Canon del Agua, 4
 Canon de la Madera, 4
 Canon de la Paloma, 5, 13, 26, 51, 117
 Canon de los Alamos, 5, 14, 16, 21, 30, 36, 39, 41, 51, 101, 117
 Chama quadrangle, 109
 Chlorite, 27, 36, 39, 40, 41, 42, 44, 46, 49, 50, 51, 59, 66, 79; phyllite, 45; schist, 18, 43-44, 45, 49, 50
 Chloritoid, 6, 27
 Clabaugh, Dr. S. E., 6
 Claystone, 14
 Cleavage, 1
 axial-plane, 1, 18, 19, 20, 36, 44, 45, 47, 53, 54, 59, 65, 76, 80, 81, 88, 93, 97, 99, 102, 109, 112
 flow, 27, 35, 59, 67, 71, 74, 75, 76, 79, 89, 97, 99, 102
 fracture, 1, 18, 21, 23, 24, 37, 47, 50, 59-63, 64, 71, 76, 89, 93, 96, 97, 104, 112, 119
 relict, 61, 97, 99, 102
 slip, 1, 18, 27, 59-63, 71, 74, 76, 97, 104, 109, 112, 116, 119
 Clinozoisite, 43, 49
 Conglomerate, 9-11, 15; basal, 13; cobble to boulder, 12; quartzite, 9, 11-12, 13; pebble, 28; volcanic, 9, 11, 12-13, 14, 15
 Cordito Member, 13, 14
 Cribbenville district, 4, 26, 30, 34, 37, 38, 52, 87, 101
 Dacite, 29
 Dalradian, 118
 Dikes, pegmatite, 1, 44, 112; quartz, 44
 Elk Mountain area, 2
 El Rito Formation, 11
 El Rito (N. Mex.), 4
 Epidote, 22, 27, 33, 36, 38, 40, 41, 42, 44, 66, 67, 68, 70, 72, 83, 84
 Erosion surfaces, 7; high-level, 5
 Esquibel Member, 13
 Faults, 16, 20
 Feldspar, 1, 29, 30, 34, 35, 68, 70, 72; potassium, 27, 29, 32, 33, 34, 48, 63; quartz, 57
 Feldspathic gneiss, 26
 Feldspathic schist, 1, 11, 17, 18, 26, 28, 29-36, 37, 38, 41, 42, 46, 48, 49, 59, 61, 62, 63, 64, 66, 67, 69, 71, 88, 89, 98, 104, 117
 gneissic, 30, 33, 35, 36, 72
 leucocratic, 30, 33, 34
 melanocratic, 30, 33
 Festoon cross-beds, 14, 91
 First deformation, 27, 52, 59, 76, 97-103, 110, 119; fabric, 45 (*see* Folds)
 Fluting, 68, 69, 74, 93, 110
 Folds, 1, 18, 53, 65, 77, 80, 84-91, 104, 106, 109, 110, 112, 114, 116, 118
 chevron, 86, 87, 88, 112
 concentric, 86, 112, 121

- conjugate, 86
 "crenulate," 78, 80, 118
 "cross," 78
 disharmonic, 86, 87
 drag, 65, 83, 85
 first deformation, 1, 81, 93, 99
 intrafolial, 86
 isoclinal shear, 75, 79, 80, 87, 88, 93, 98, 102, 119
 macroscopic, 85, 90-91, 106, 109, 114
 mesoscopic, 75-76, 79, 80, 85, 87-90, 91, 97, 98, 100, 102, 103, 105, 112, 113, 114
 microscopic, 85
 nonplane cylindrical, 86, 87, 104
 nonplane noncylindrical, 86
 parasitic, 85
 plane cylindrical, 86, 87, 88, 98, 102
 plane noncylindrical, 86
 second deformation, 1, 81, 106, 107, 108, 109
 similar, 86, 87, 88, 98, 102, 112
 submicroscopic, 85
 third deformation, 1, 44, 107, 112, 113, 115
 Foliation, 19, 20, 33, 54, 76, 79
- Garnet, 22, 27, 33, 39, 43, 44, 50, 51
 Garnetiferous-muscovite schist, 38
 Globe district, 4, 88
 Gneiss, 1, 2, 30; feldspathic, 26; granitic, 1, 17, 19, 20, 21, 25, 26, 27, 34, 37-39, 45, 46, 52, 54, 59, 121
 Granite, 1, 18, 27, 37; Tres Piedras, 37, 39; Tusas, 52
 Granitic gneiss, 1, 17, 19, 20, 21, 25, 26, 27, 34, 37-39, 45, 46, 52, 54, 59, 121; pegmatites, 18, 41
 Greenschist, 1, 44, 45, 46
- Hartschiefer*, 30, 55
 Hematite, 30, 42, 43, 48, 50, 57, 58, 89, 95; laminae, 22, 36; layering, 19, 20, 21, 36, 61, 88, 99; specular, 19, 20, 21, 54, 68
 Hornblende, 1, 17, 39, 40, 46, 47, 49, 50, 59, 66, 71, 79, 84, 90, 102; -biotite schist, 41; -chlorite schist, 1, 17, 39-42, 45, 51
 Hornfels, 17
- Igneous rocks, 9, 14-16
 Illite, 27, 47
 Intertonguing, 12
 Iron, 48
- Jarita basalt, 15
 Joints, 63-65, 121
- Kaolinite, 1, 6, 22, 23, 47, 48
 Kiawa Mountain Formation, 40
 Kyanite, 1, 2, 17, 19, 20, 21, 22, 23, 24, 25, 44, 47, 48, 49, 50, 61, 67, 82, 93, 99; -muscovite schist, 24-25; schist, 72, 87, 112
- La Madera Mountain, 5, 7, 11, 12, 14, 16, 17, 19, 20, 22, 23, 24, 47, 48, 50, 117
 La Madera (N. Mex.), 4, 5, 7, 17, 119
 Las Tablas quadrangle, 2, 12, 18, 29, 37, 52, 109, 117
 Latite, 15; porphyry, 12; pyroclastic, 9; quartz, 29
 Lentil, 12, 13
 Leucoxene, 44
 Limonite, 63
 Lineation, 1, 18, 23, 26, 30, 36, 37, 40, 45, 47, 66-71, 73-84, 90, 93, 97, 99, 106, 110; L-, 77, 79, 80, 81, 82
 Los Pinos Formation, 11, 13, 14, 15
- McBride, Dr. E. F., 6
 Manganese, 48
 Mesa de la Jarita, 4, 5, 7, 8, 11, 15, 17, 19, 21, 25, 26, 27, 28, 30, 31, 36, 39, 41, 42, 43, 49, 50, 52, 57, 68, 71, 72, 82, 87, 90, 101, 102, 110, 117
 Metamorphic rocks, 5, 9, 11, 12, 13, 29, 44, 91
 Metamorphism, 44-53, 120
 Metarhyolite, 29, 35
 Micaceous quartzite, 11
 Mica, 25, 29, 33, 38, 50, 102; mill, 13; schist, 19, 25, 27
 Microcline, 33, 34, 35, 37, 38; antiperthite, 33, 34, 38; micropertite, 37, 38; patch perthite, 32, 33, 34, 35, 38; perthite, 33, 34, 38, 67
 Microfolds, 68
 Microfractures, 21
 Miocene, 14, 16
 Moines, 118
 Muehlberger, Dr. W. R., 6
 Muscovite, 1, 17, 22, 23, 24, 26, 27, 29, 32, 33, 34, 36, 37, 38, 42, 51, 59, 63, 79, 87
 Muscovitic quartzite, 1, 11, 12, 17, 21, 25-28, 29, 30, 33, 35, 36, 37, 38, 40, 42, 43, 46, 49, 50, 51, 52, 59, 61, 68, 69, 70, 71, 72, 73, 79, 82, 83, 88, 90, 95, 98, 101, 104, 110, 112, 117

- Mylonite, 33, 47
 Myrmekite, 39
 New Zealand, 54
 Ojo Caliente (N. Mex.), 2
 Ojo Caliente quadrangle, 2, 13, 117
 Old Petaca road, 4, 14, 15, 34, 63, 67, 74, 88
 Ortega Mountains, 4, 7, 8, 11, 14, 16, 17, 19, 20, 24, 36, 57, 72, 79, 87-88, 101, 102, 104, 112
 Ortega Quartzite, 2, 19, 20, 25
 Otago schist, 54
 Paragonite, 41
 Pegmatites, 1, 2, 51, 52; dikes, 1, 44, 112; granitic, 18, 41; La Jarita, 52
 Perennial streams, 5
 Perlitic vitrophyre agglomerate, 15
 Perthite, 34, 35
 Petaca
 arc, 109, 117-119
 area, 2
 aureole, 52-53
 district, 50
 road, 30, 31, 88, 117
 Schist, 2, 25
 Petrology, 9-16, 17-53; metamorphic, 18
 Phyllite, 1, 51
 Picuris basalts, 40
 Picuris Range, 18, 19, 29, 117
 Piedmontite, 31, 48
 Plagioclase, 17, 27, 32, 33, 35, 36, 37, 38, 39, 41, 42, 46, 49, 51, 66, 84; -chlorite phyllite, 42-43
 Pliocene, 14, 16
 Porphyroblasts, 1, 27, 43
 Porphyry, andesite, 12; latite, 12; pyroclastic, 12; rhyolite, 9, 12, 15, 34
 Potassium feldspar, 27, 29, 32, 33, 34, 48, 63
 Precambrian, 4, 5, 11, 17, 19, 25, 30, 44, 53, 59, 95, 102, 103, 109, 122-126; geology, 17-126; quartzite, 7, 16, 91; rocks, 1, 2, 5, 7, 9, 12, 15, 18, 26, 44, 87, 103, 117, 119, 122, 123, 124
 Pyrite, 43, 50
 Pyroclastic, latite, 9; porphyry, 12; rock, 15; unit, 15-16
 Pyrophyllite, 1, 6, 17, 44, 47, 48
 Quaternary geology, 7-8
 Quartz, 11, 17, 18, 20, 21, 23, 24, 25, 26, 27, 28, 29, 30, 32, 33, 34, 35, 36, 37, 38, 39, 40, 41, 42, 48, 49, 57, 63, 68, 70, 72, 79, 84, 102, 110
 boudins, 73, 83
 dikes, 44
 feldspar, 57
 latite, 29
 sandstone, 1, 19
 superindividuals, 26, 27, 30, 34
 veins, 112
 Quartz-albite-muscovite-biotite schist, 17, 30, 35, 36-37, 39-40, 45, 46, 61, 63, 66, 67, 73
 Quartz-feldspar-muscovite-biotite schist, 87, 88
 Quartzite, 1, 2, 4, 11, 16, 17, 18, 19-25, 26, 28, 30, 36, 39, 44, 46, 47, 48, 50, 52, 56, 58, 61, 66, 67, 69, 71, 72, 73, 82, 84, 87, 91, 94, 97, 98, 99, 110, 117
 conglomerate, 9
 micaceous, 11
 muscovitic, 1, 11, 12, 17, 18, 21, 25-28, 29, 30, 33, 35, 36, 37, 38, 39, 40, 42, 43, 46, 49, 50, 51, 52, 59, 61, 68, 69, 70, 71, 72, 73, 79, 82, 83, 87, 88, 90, 95, 98, 101, 104, 110, 112, 117
 Ortega, 2, 19, 20
 Precambrian, 7, 16, 91
 Quartz-kyanite-andalusite schist, 117
 Quartz-kyanite schist, 17, 19, 101
 Quartz muscovite schist, 11, 35
 Rancho del Olguin, 4, 19, 42, 82, 88
 Recent deposits, 8
 Relic bedding, 25, 55
 Relict
 cross-bedding, 19, 93
 fracture cleavage, 61, 97, 99, 102
 pebble beds, 20, 57
 phenocrysts, 29
 structures, 91-96
 textures, 39
 Rhyolite, 12, 14, 15; porphyry, 9, 15, 34
 Rio Arriba County, 2
 Rio Grande, 117; graben, 4
 Rio Ojo Caliente, 5
 Rio Tusas, 5, 7, 14, 15, 21, 101
 Rio Vallecitos, 4, 7, 12, 14, 19, 20
 Ritito Conglomerate, 12
 Rocks
 basic flow, 1
 igneous, 9, 14-16
 metamorphic, 5, 9, 11, 12, 13, 29, 44, 91
 Precambrian, 1, 2, 5, 7, 9, 12, 15, 18, 26, 44, 87, 103, 117, 119, 122, 123, 124

- pyroclastic, 15
- schistose, 45
- sedimentary, 7, 9
- silicic, 1
- Tertiary, 4, 7, 9, 36
- volcanic, 1, 7, 14
- Rutile, 17, 19, 21, 24, 41, 48
- Salt Lick Spring, 51
- Sandstone, 12, 20; arkosic, 7, 9, 12, 35; quartz, 1, 19; tuffaceous quartz, 12
- Sanidine, 15
- San Juan Basin, 4
- San Juan Mountains, 4
- Santa Fe Formation, 14
- Schist, 1, 2, 48
 - aluminous, 23
 - biotite, 1, 41, 51
 - chlorite, 18, 43-44, 45, 49, 50
 - feldspathic, 1, 11, 17, 18, 26, 28, 29-36, 37, 38, 41, 42, 46, 48, 49, 59, 61, 62, 63, 64, 66, 67, 69, 71, 88, 89, 98, 104, 117
 - gneissic, 30, 33, 35, 36, 72
 - leucocratic, 30, 33, 34
 - melanocratic, 30, 33
 - garnetiferous-muscovite, 38
 - green, 1, 44, 45, 46
 - hornblende-biotite, 41
 - hornblende-chlorite, 1, 17, 39-42, 45, 51
 - kyanite, 72, 87, 112
 - kyanite-muscovite, 24-25
 - mica, 19, 25, 27
 - Otago, 54
 - Petaca, 2, 25
 - quartz-albite-muscovite-biotite, 17, 30, 35, 36-37, 39-40, 45, 46, 61, 63, 66, 67, 73
 - quartz-feldspar-muscovite-biotite, 87, 88
 - quartz-kyanite, 17, 19, 101
 - andalusite, 117
 - quartz-muscovite, 11, 35
 - sericite, 72
 - specularite, 24
- Schistose rocks, 45
- Schistosity, 30, 32, 36, 37, 43, 47, 55, 62, 69
- Scotland, 118
- Second deformation, 47, 76, 97, 103-111, 114, 119 (*see* Folds)
- Sedimentary rocks, 7, 9
- Sericite, 41, 59; schist, 72
- Sets, 55, 57
- Shale, 1
- Silicic volcanic rock, 1
- Silicon, 48
- Sillimanite, 17, 19, 22, 23, 24, 50, 61
- Sills, 1
- Siltstone, 14
- Socorro, N. Mex., 5
- Sodium-oligoclase, 32, 33, 46
- South Petaca (N. Mex.), 4, 5, 9, 11, 13, 14, 15, 17, 21, 25, 30
- Specularite, 17, 22, 23, 27, 33, 34, 36, 39, 40, 43, 50; schist, 24
- Sphene, 17, 19, 21
- S-plane, 60, 97
- Streams:
 - consequent, 4, 7
 - insequent, 4
 - intermittent, 5
 - perennial, 5
- Stream terraces, 4
- Sunnyside mine, 49, 50, 87, 112, 114
- Syncline, 85
- Synform, 85, 101, 112, 114
- Tectonic breccia phase, 28-29, 87, 95, 101, 110
- Tertiary, 5, 9, 10, 14, 16, 19, 30, 42; geology, 9-16; rocks, 4, 7, 9, 36; sequence, 9
- Third deformation, 50, 53, 76, 112-116, 120 (*see* Folds)
- Thompson, A. J., 6
- Titanium, 48
- Tourmaline, 42, 43, 50, 51
- Tres Piedras granite, 37, 39
- Tuffaceous quartz sandstone, 12
- Tuff beds, 14
- Twinning, 32, 34
- Umfaltung*, 73
- Vallecitos
 - Creek, 90
 - fault zone, 16, 20, 47, 90
 - rhyolites, 29
 - valley, 16, 19, 22, 36, 42, 101, 102
- Vallecitos (N. Mex.), 4, 14, 15, 17, 19, 23, 26, 47, 63, 74, 117
- Volcanic rock, 1, 7, 14
- White mine, 88
- Willard, Max E., 6
- Xenoliths, 15
- Zircon, 21, 55



EXPLANATION

Qal
Alluvium

Unconsolidated deposits of gravel, sand, and silt in stream beds. Present in local depressions at higher elevations within the quadrangle.

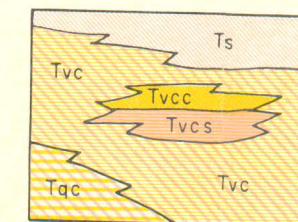
Qlt
Calicheous tufa at Statue Spring

Calicheous tufa at Statue Spring

Qlg
Terrace gravel

Unconsolidated gravel of volcanic and metamorphic rock fragments.

UNCONFORMITY



Volcanic epiclastic units

Ts - Arkosic sandstone-Pink to yellowish pink fine-grained arkosic sandstone, locally part well-cemented and intertongued with volcanic conglomerate. Upper part unconsolidated and prominently cross-bedded.

Tvc - Volcanic conglomerate-Gray conglomerate and coarse sandstone of volcanic and metamorphic rock fragments. Locally well-cemented portions are prominent cliff-formers.

Tvcv - Red volcanic conglom-

erite conglomerate-Dominant clast - red quartz latite porphyry.

Tvcs - Tuffaceous quartz sandstone-lower part of lens with volcanic conglomerate. Poorly cemented, pink to pinkish white sandstone with unusually high content of detrital quartz bipyramids.

Tac - Quartzite conglomerate-Gray to pinkish gray largely unconsolidated conglomerate of quartzite fragments.

Tb
Basalt

Sequence of four basalt flow units. Top flow unit is brown, unaltered, vesicular basalt. Underlying units range in color from green to purple, are amygdaloidal, and highly altered.

Tc
Conglomerate

Well-cemented conglomerate of subangular to rounded metamorphic rock fragments. Matrix of quartz sand ranges in color from gray to pinkish gray.

UNCONFORMITY

Note: Prefix Pe omitted from symbols

Q Dense, vitreous, hematite-layered gray quartzite.
Qkm Blue-black, kyanite-muscovite schist.
Qka Reddish brown, mylonitic, kyanite-andalusite-sillimanite schist.
Qks Black to greenish black, quartz-kyanite-specularite-rutile schist.

mq
Muscovitic Quartzite

mq - Greenish white to grayish white, schistose, muscovite-rich quartzite.

mat
Biotite-muscovite quartzite

mat - Biotite-muscovite quartzite.

fs
Feldspathic Schist

fs - Fine-grained matrix of quartz, k-feldspar and muscovite, containing prominent quartz blebs and large euhedral pink feldspar grains.

fsm - Leucocratic, fine-grained, compact to flinty, pink to grayish white schist.

fsg - Melanocratic, biotite-bearing feldspathic schist.

fsg - Gneissic phase of feldspathic schist.

qms
Quartz-Albite-Muscovite-Biotite Schist

qms - Grayish brown to greenish brown homogeneous fine grained schist. Hematite layering present locally.

gg
Granitic Gneiss

gg - Yellowish brown to grayish brown, crystalloblastic gneiss of granitic composition. Muscovite and biotite content highly variable.

hcs
Hornblende-Chlorite Schist

hcs - Greenish black to grayish green, generally hard and compact schist. Locally gneissic and porphyroblastic.

pcp
Plagioclase-Chlorite-Phyllite

pcp - Bluish gray to greenish gray phyllite. Some parts compact and flinty. Locally rich in tourmaline.

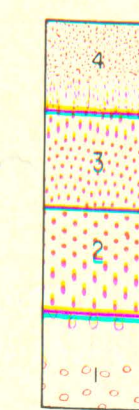
chs
Chlorite Schist

chs - Green to greenish black porphyroblastic schist. Hematite pseudomorphs after pyrite and large garnet dodecahedra prominent locally.

QUATERNARY

TERTIARY

PRECAMBRIAN



4 - Terrace developed in the vicinity of La Madera at an elevation of 6600 feet.

3 - Terrace developed in the vicinity of La Madera at an elevation of 6800 feet.

2 - Terrace extensively developed west of La Madera and south of the Ortega Mountains. Nearly everywhere capped by 20 to 40 feet of unconsolidated gravel composed principally of metamorphic rock fragments. Gravel composed wholly of quartzite clasts along the southern front of the Ortega Mountains.

1 - Erosion surface capping Mesa de la Jorita. Covered by gravel composed principally of hematitic quartzite. Gravel is locally slumped and mixed with colluvium along the edge of Mesa de la Jorita.

Contact

Dashed where approximately located.

Fault

Dashed where approximately located or inferred; dotted where buried. U and D indicate upthrown and downthrown side respectively.

Bearing and Plunge of Mesoscopic Fold Axes

Horizontal Mesoscopic Fold Axes

Strike and Dip of Flow Cleavage

Dart indicates bearing and plunge of lineation in plane of flow cleavage.

Strike and Dip of Fracture Cleavage

Dart indicates bearing and plunge of lineation in plane of fracture cleavage.

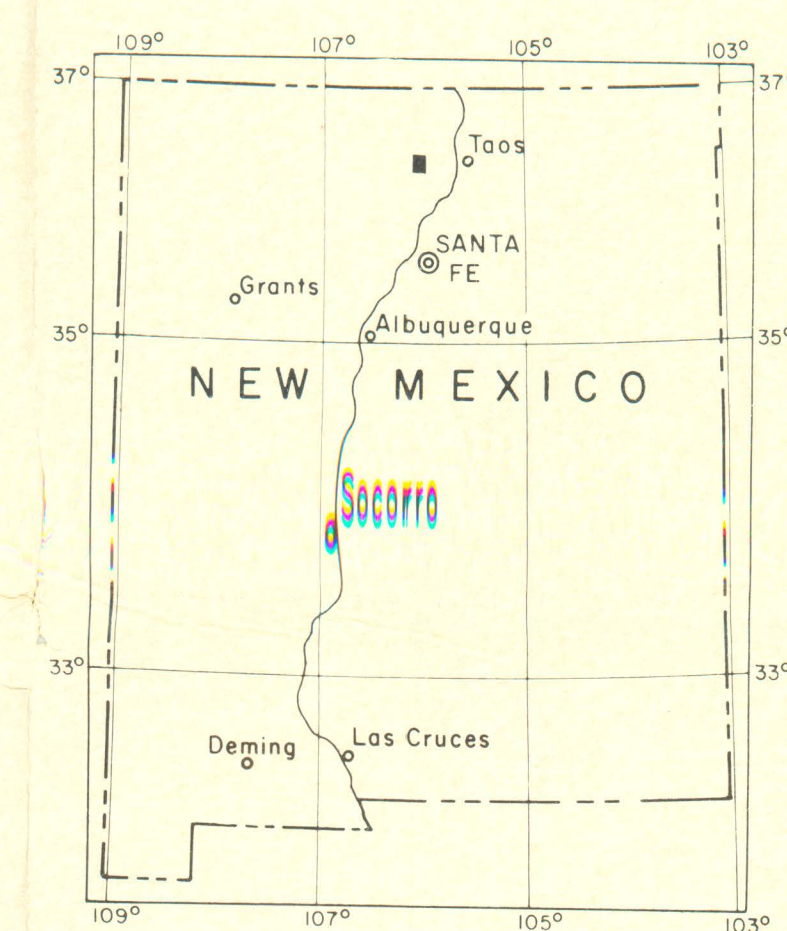
Strike and Dip of Slip Cleavage

Dart indicates bearing and plunge of lineation in plane of slip cleavage.

Mines

Prospects

Portal of Adit



INDEX MAP OF NEW MEXICO

TRUE NORTH
MAGNETIC NORTH

Approximate Mean Declination, 1953

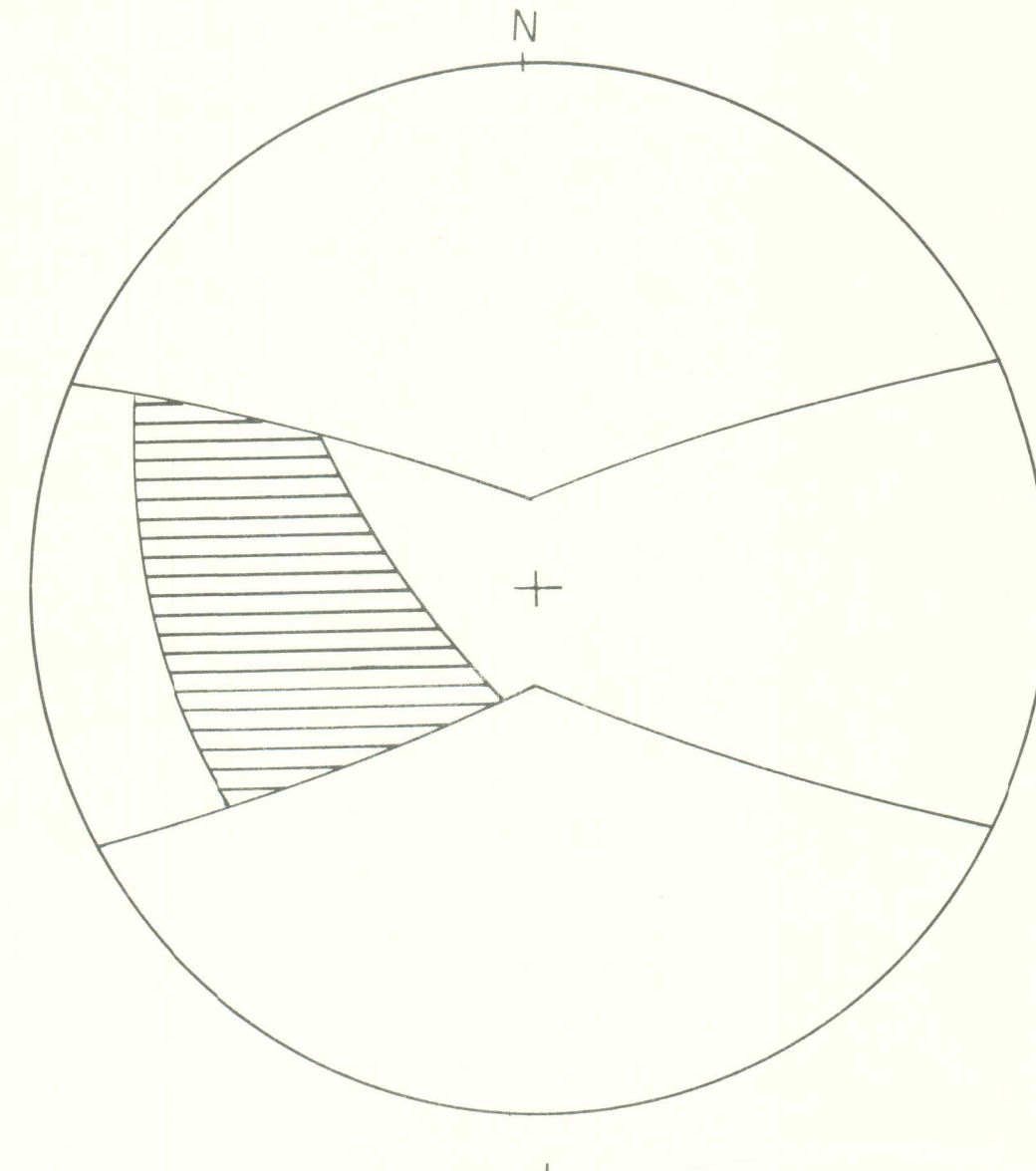
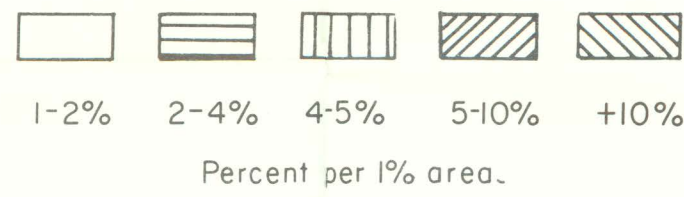
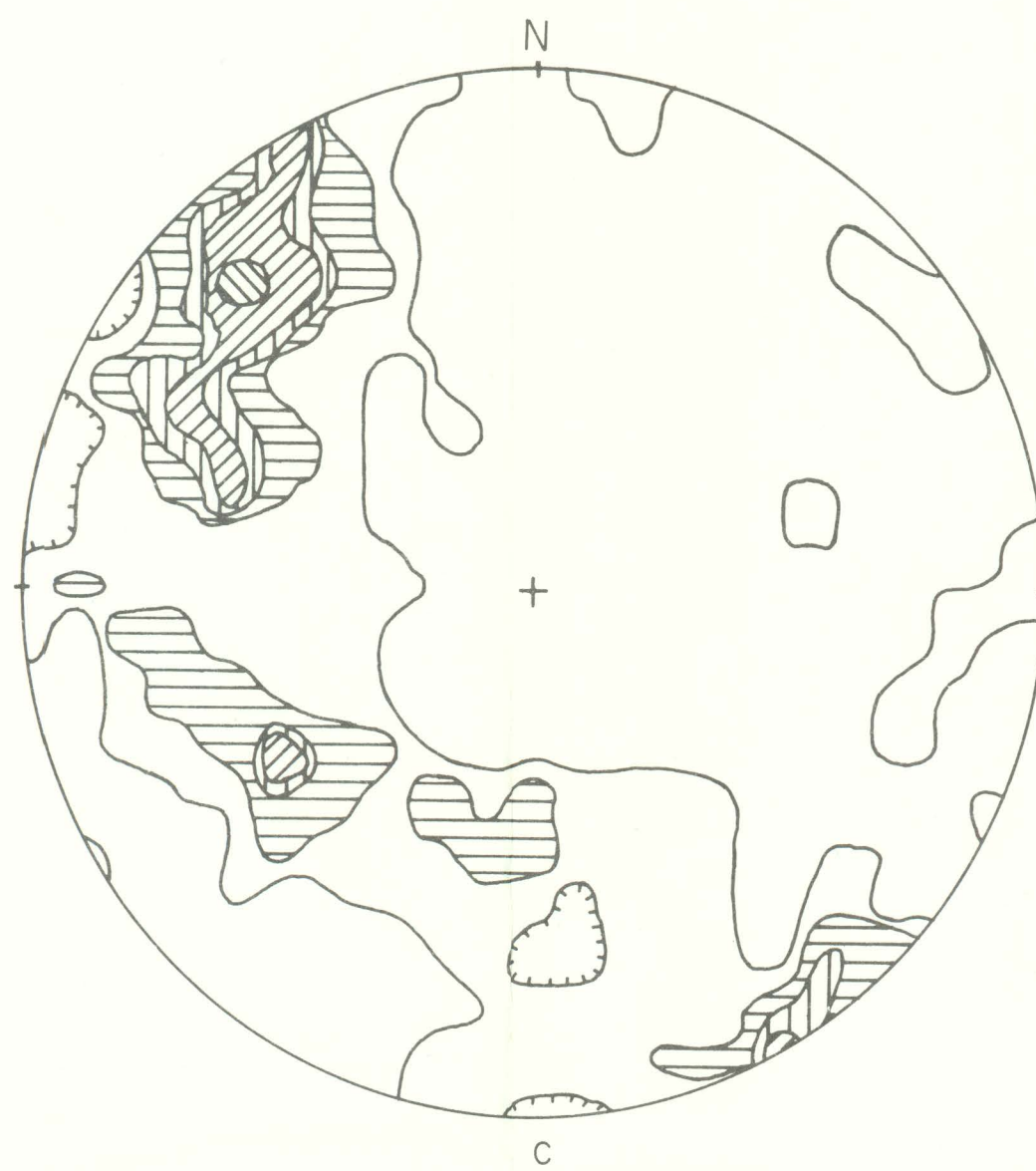
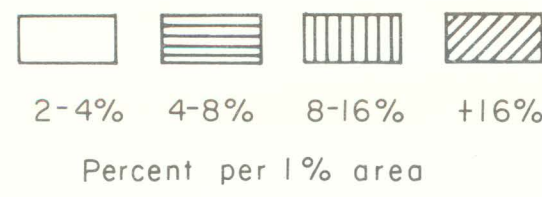
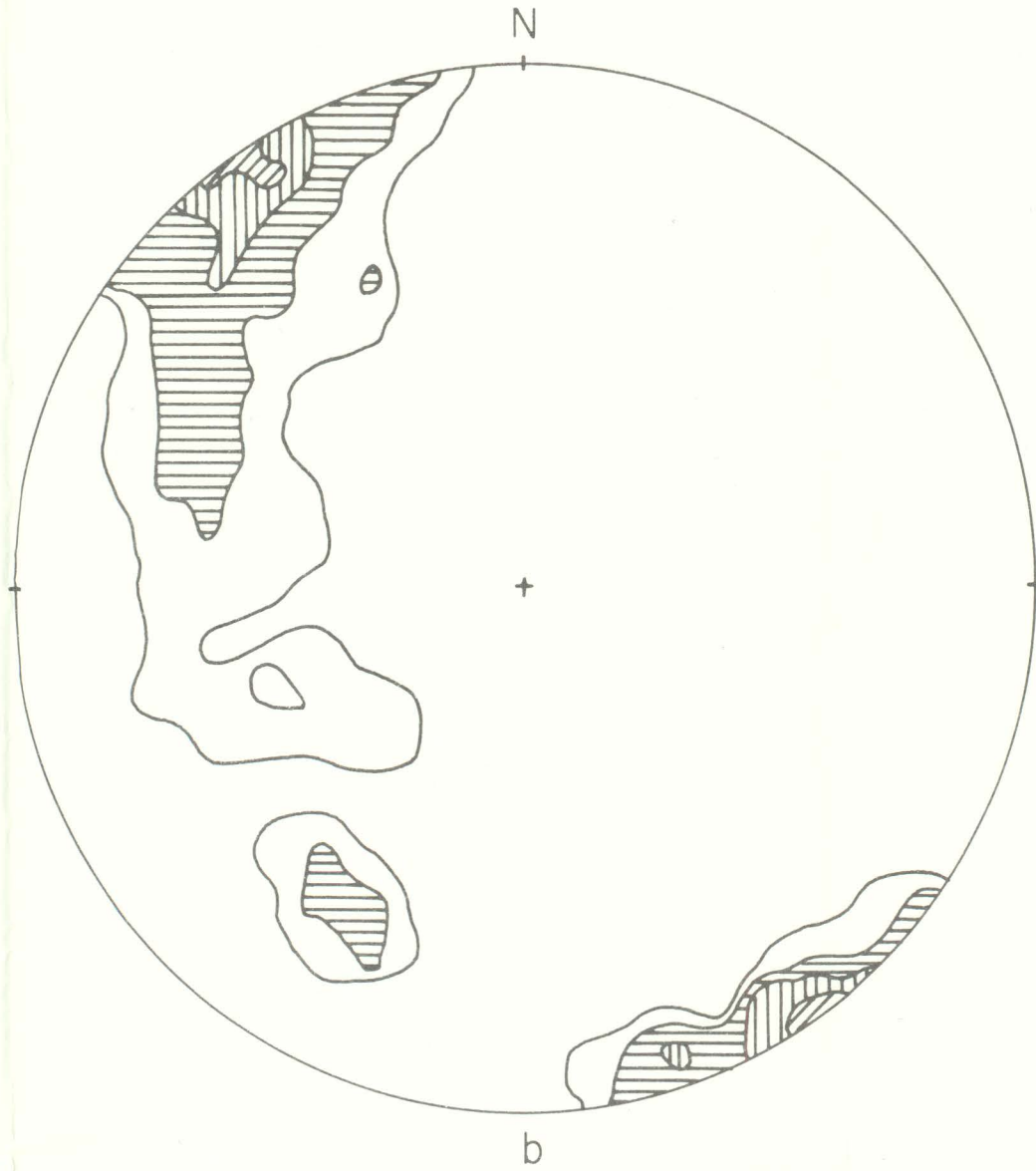
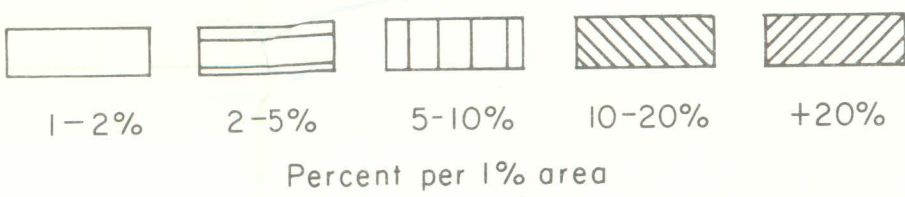
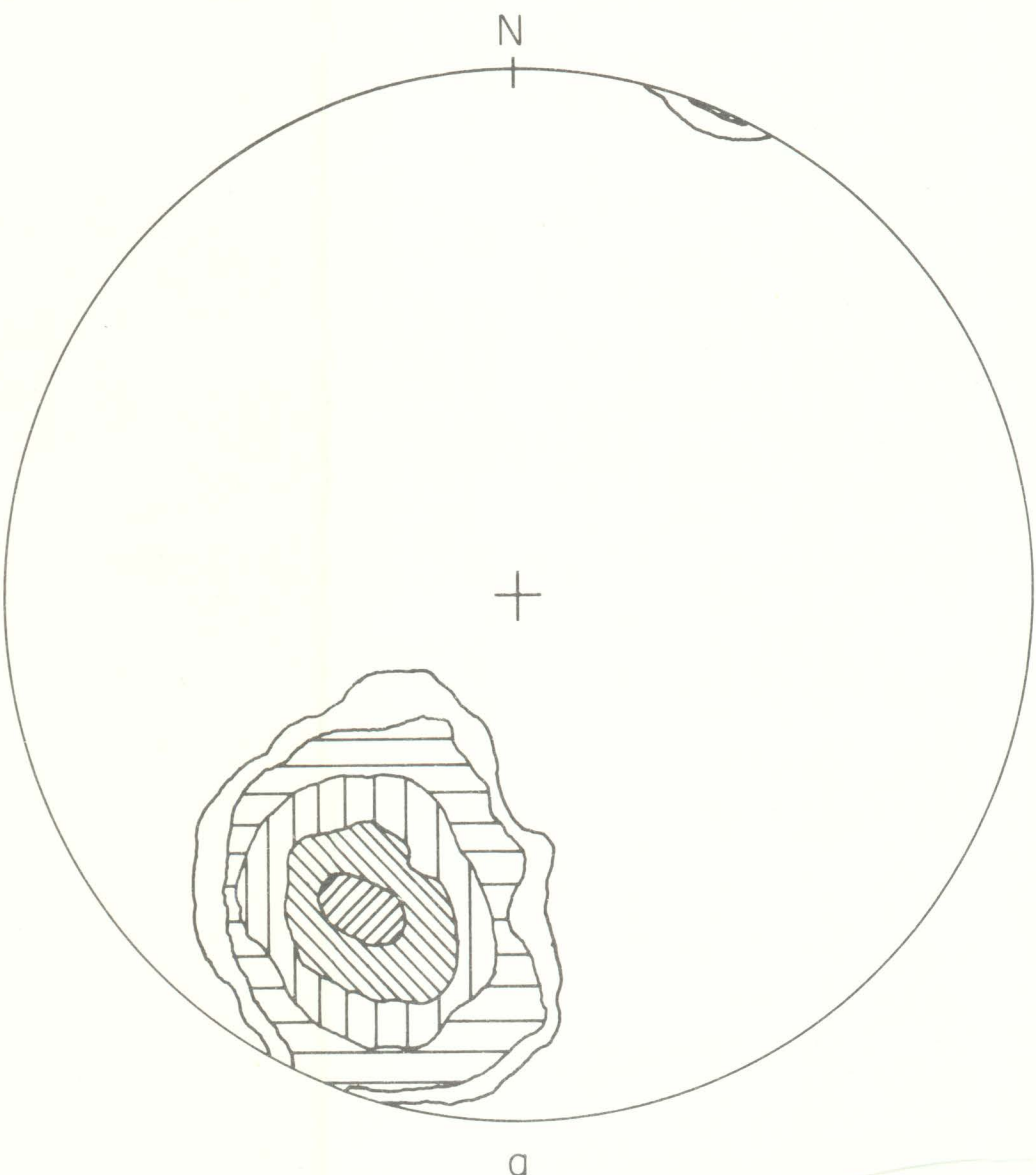
SCALE 1:24,000

CONTOUR INTERVAL 20 FEET
DATUM IS MEAN SEA LEVEL

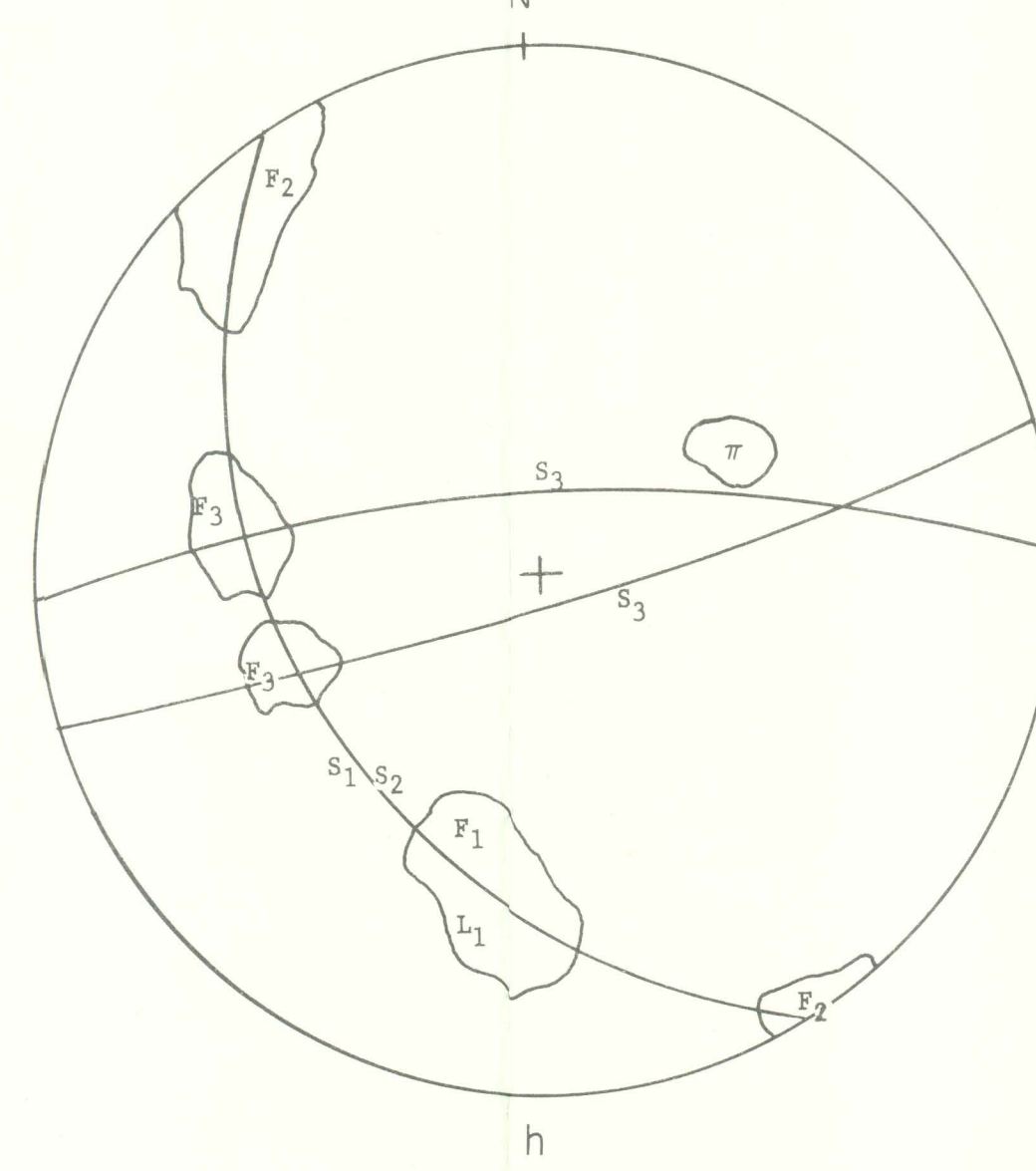
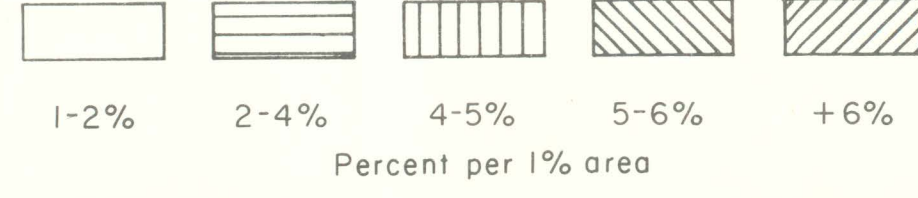
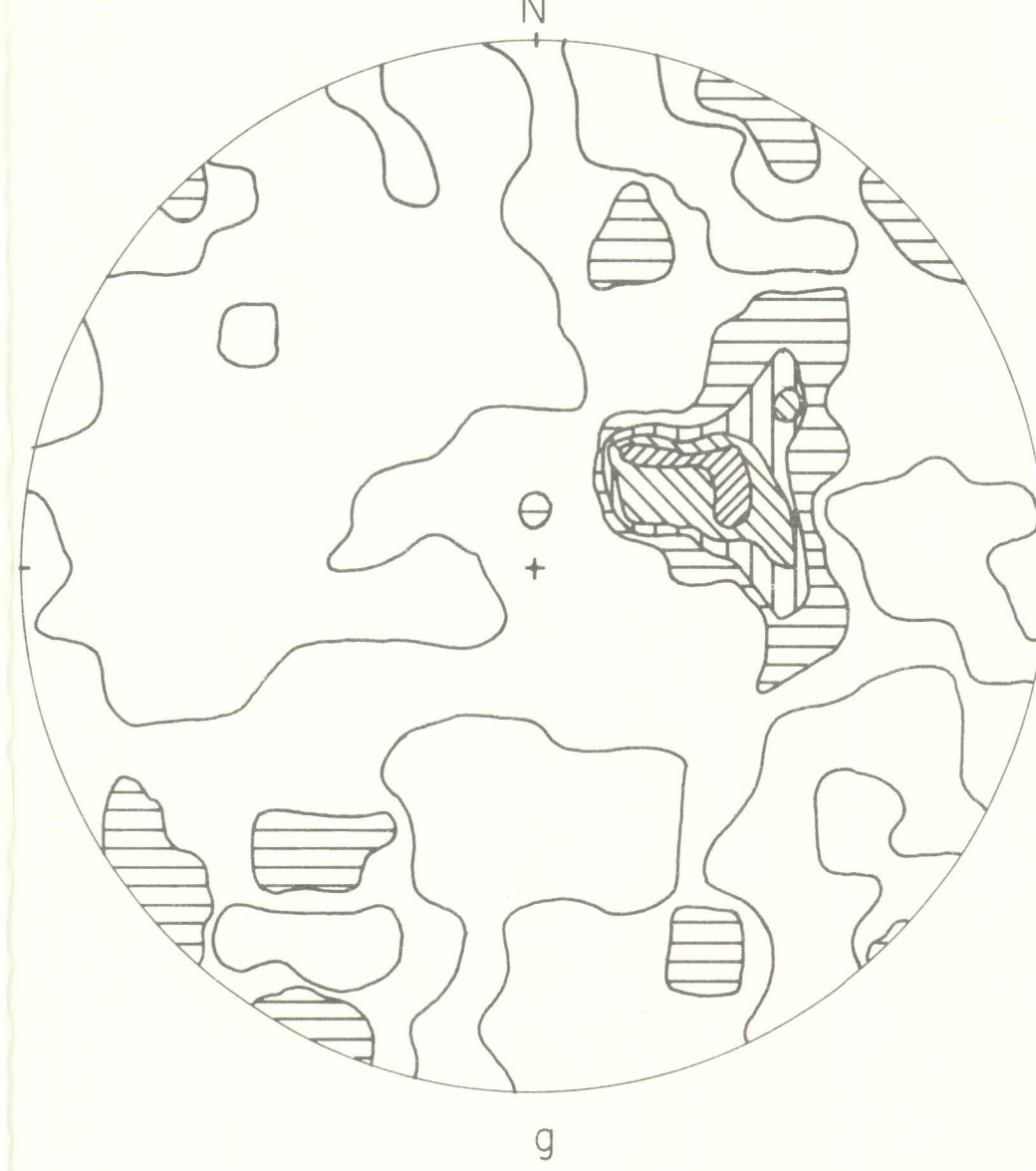
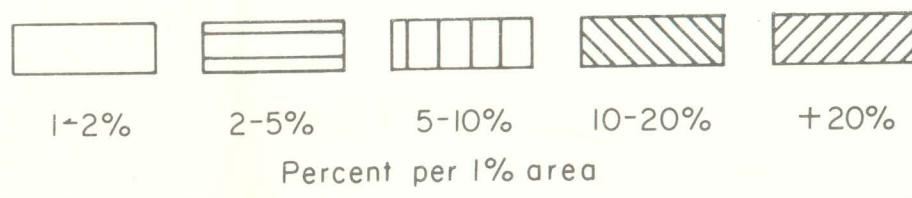
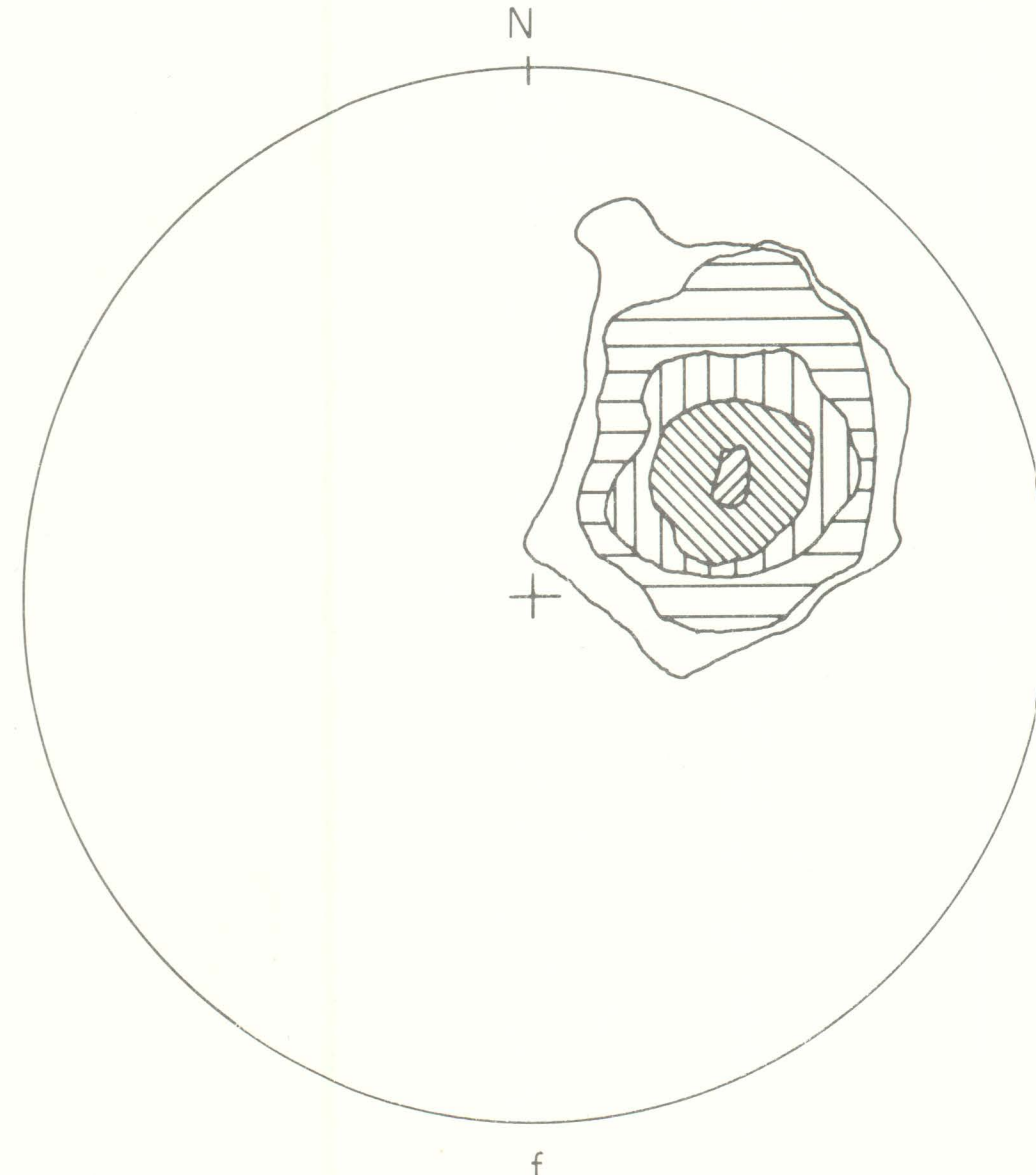
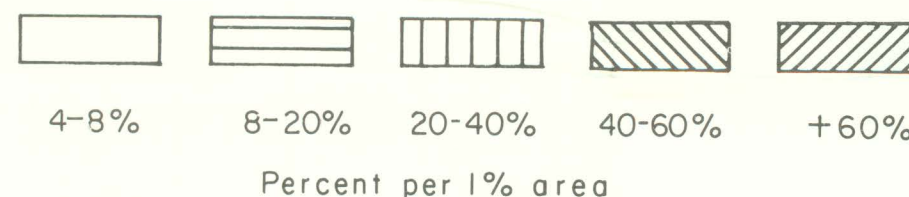
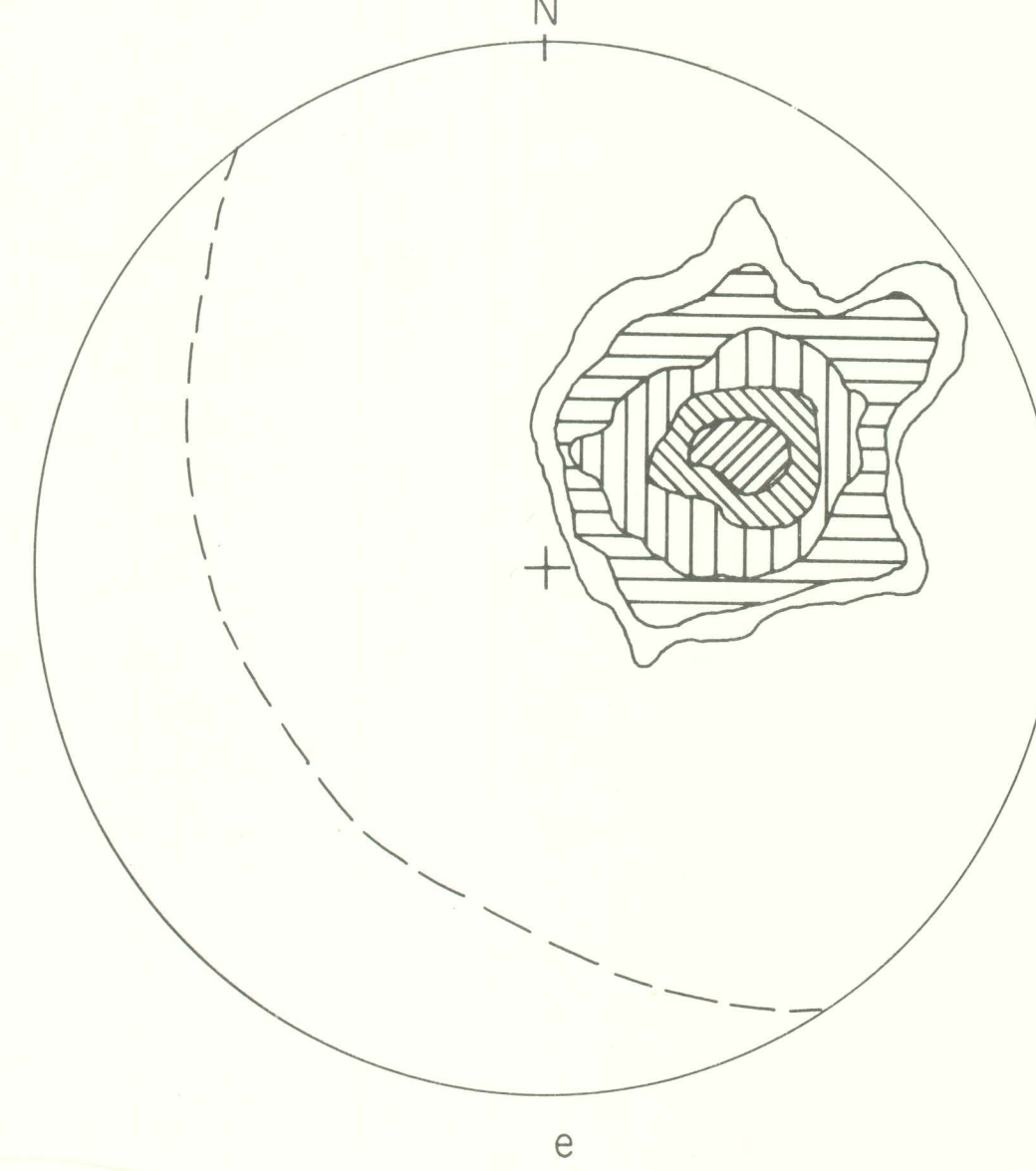
GEOLOGIC MAP LA MADERA SEVEN AND ONE HALF-MINUTE QUADRANGLE, NEW MEXICO

Base map from U.S. Geological Survey
La Madera Quadrangle 7 1/2 min. series.

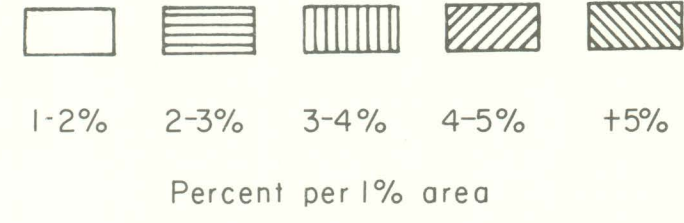
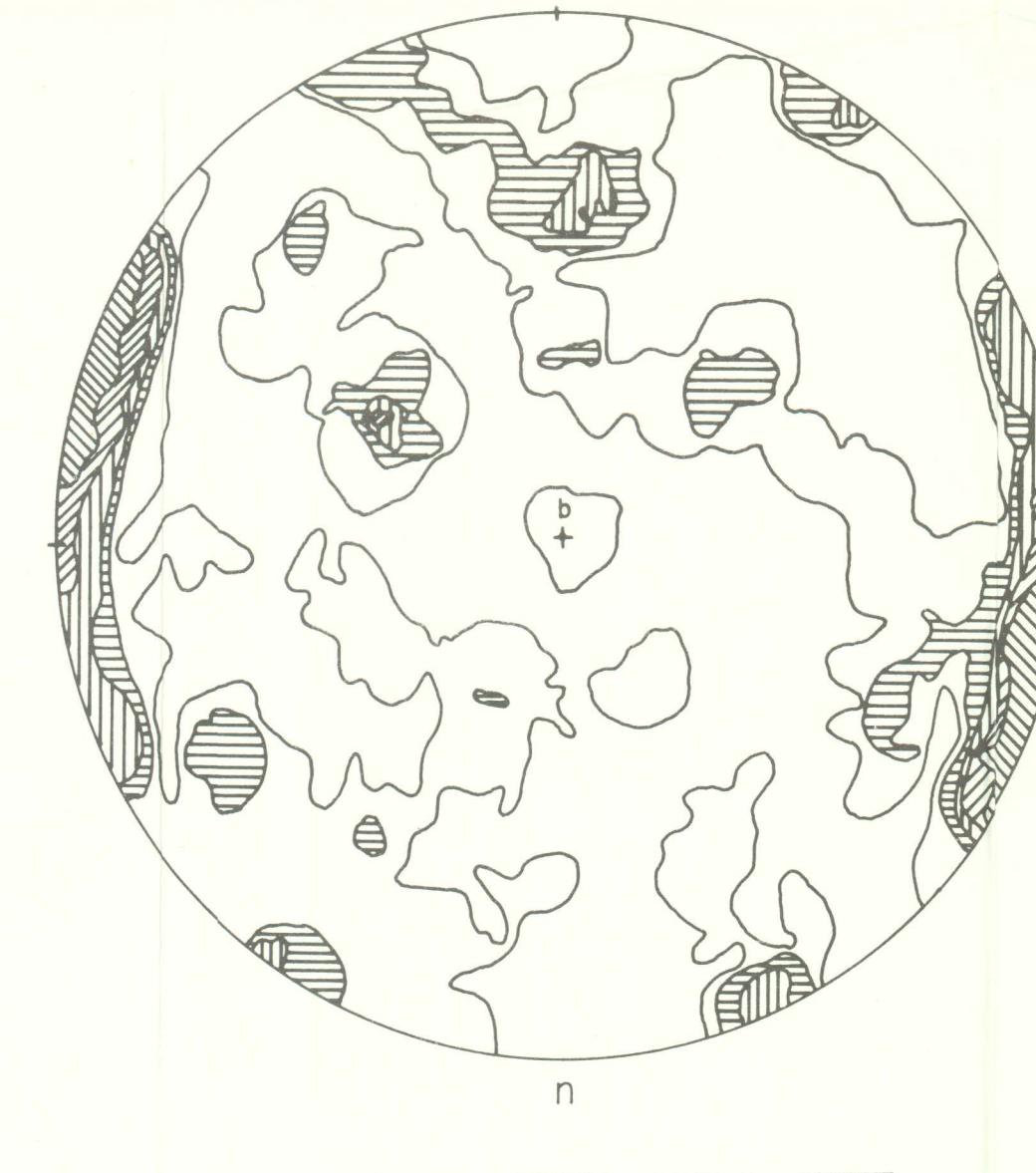
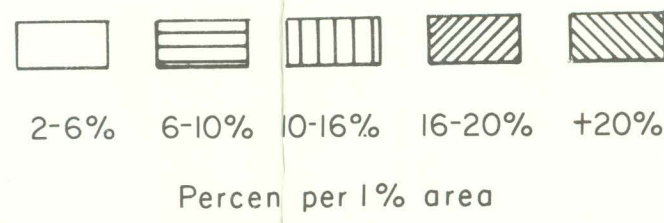
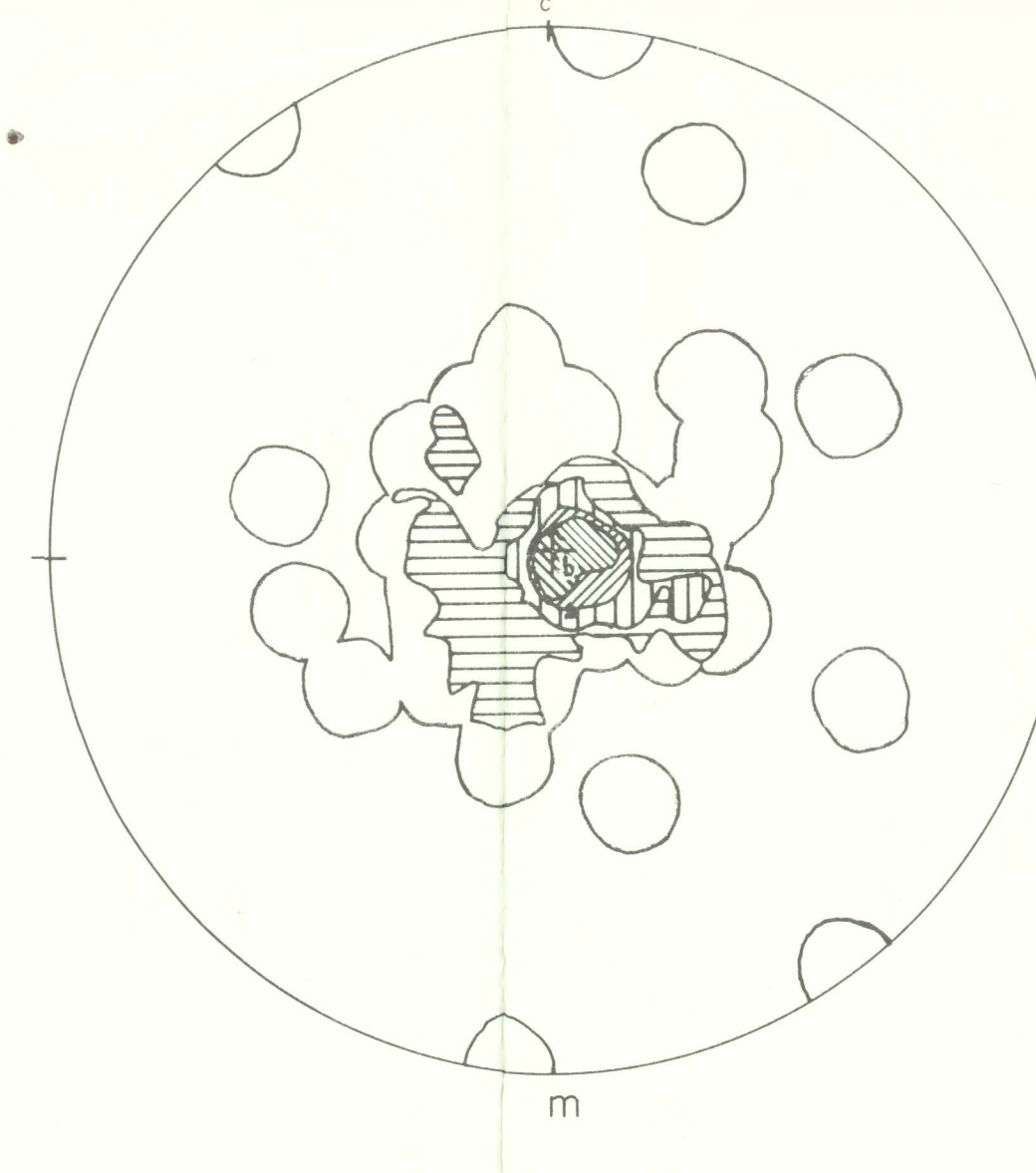
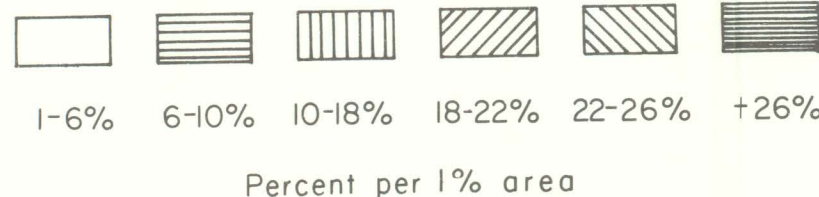
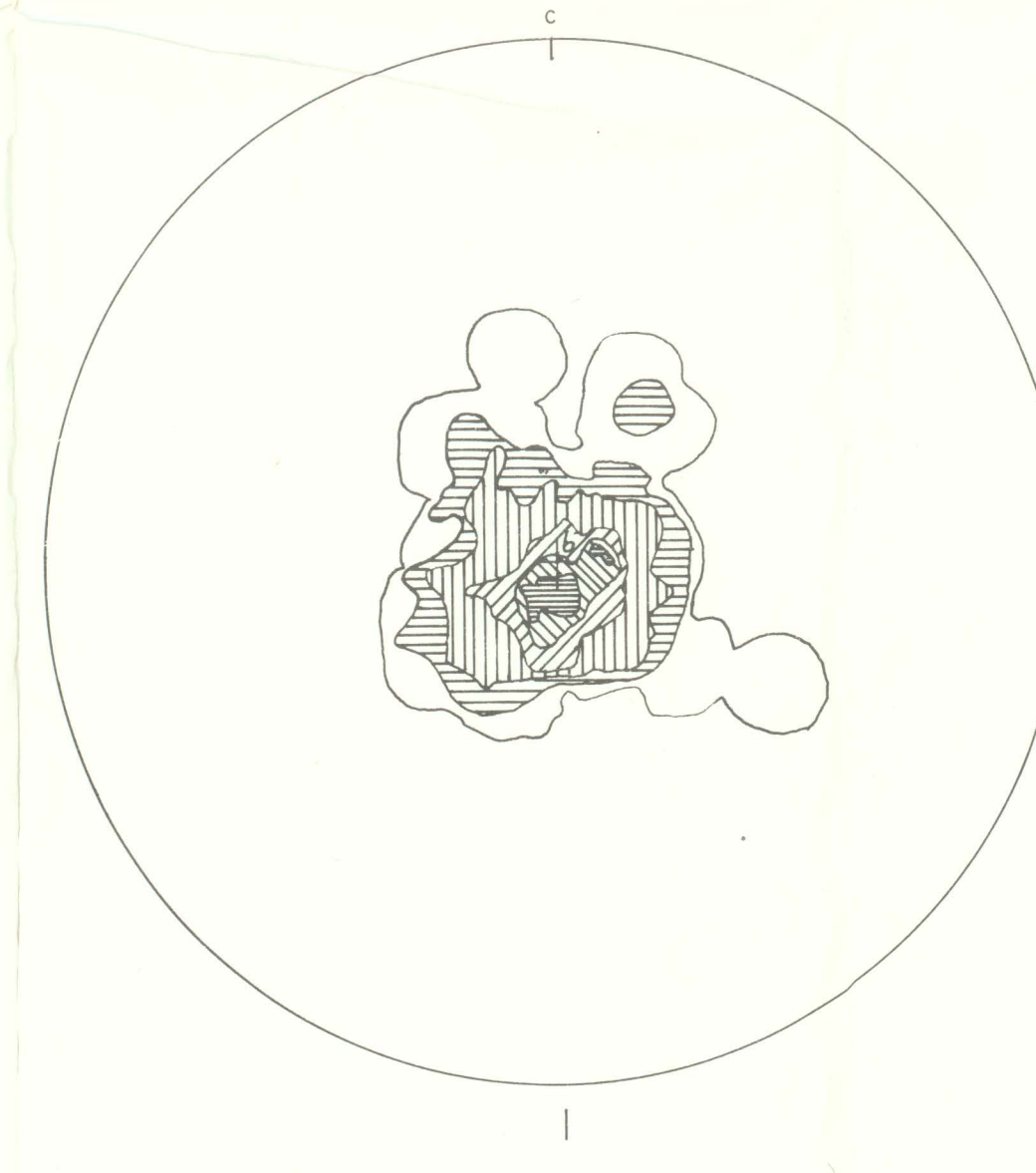
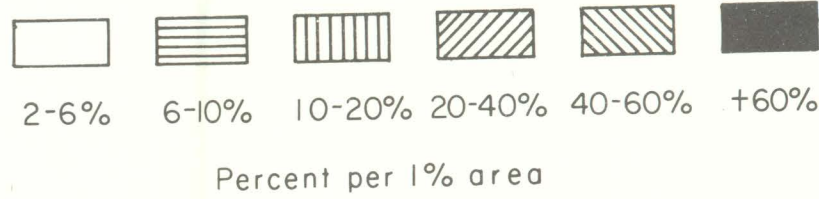
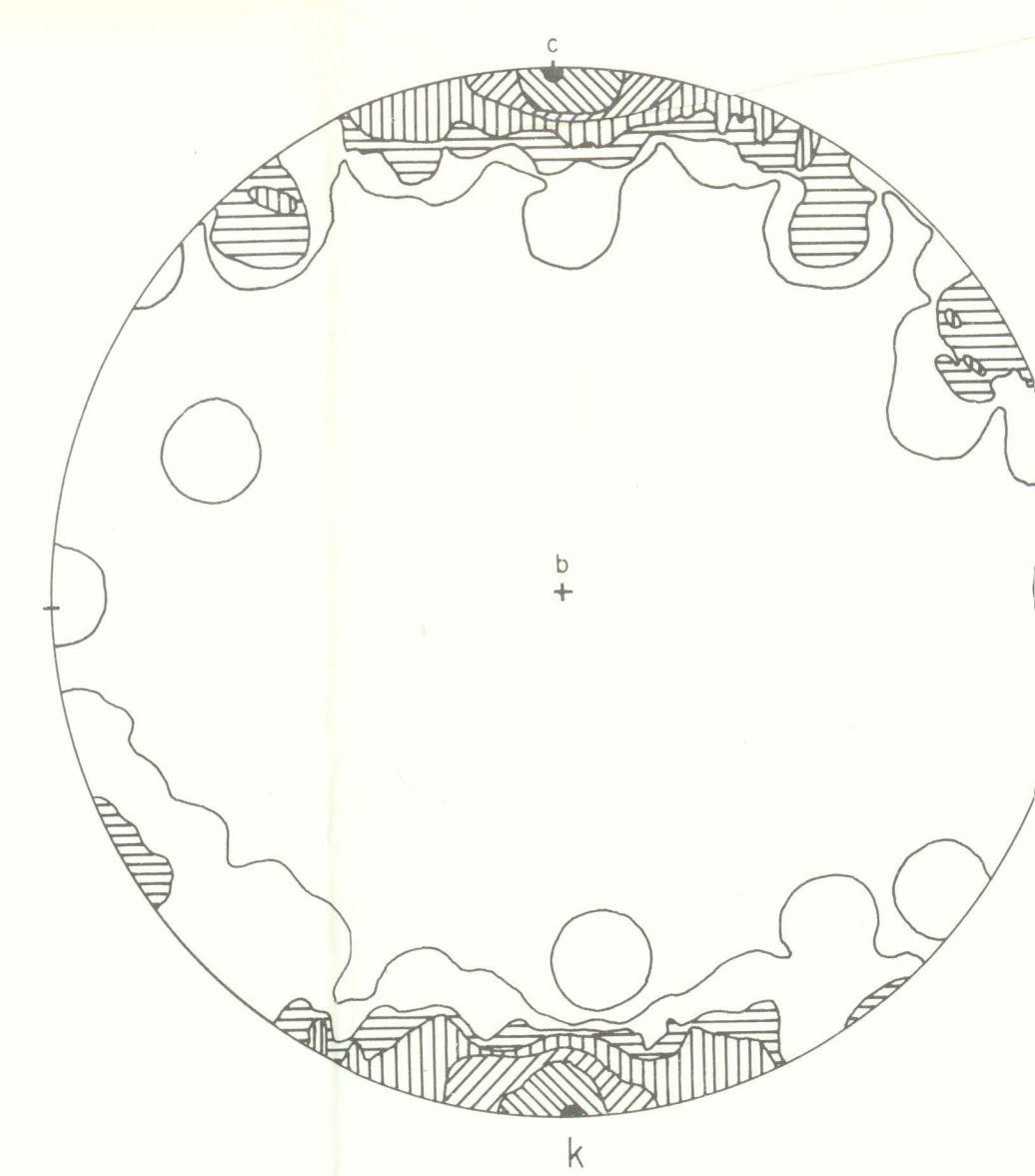
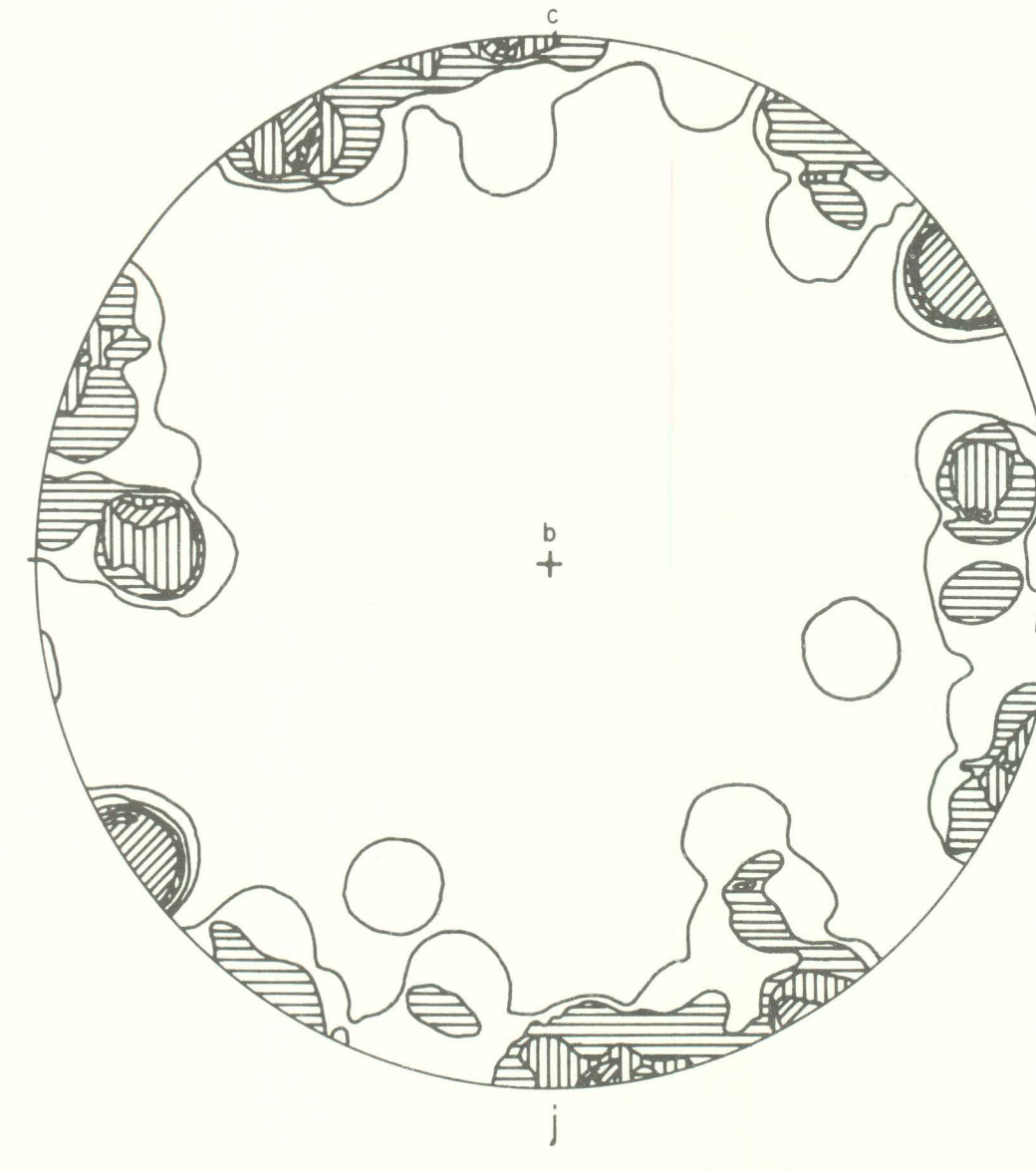
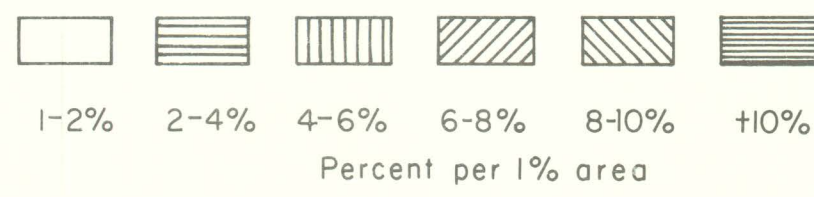
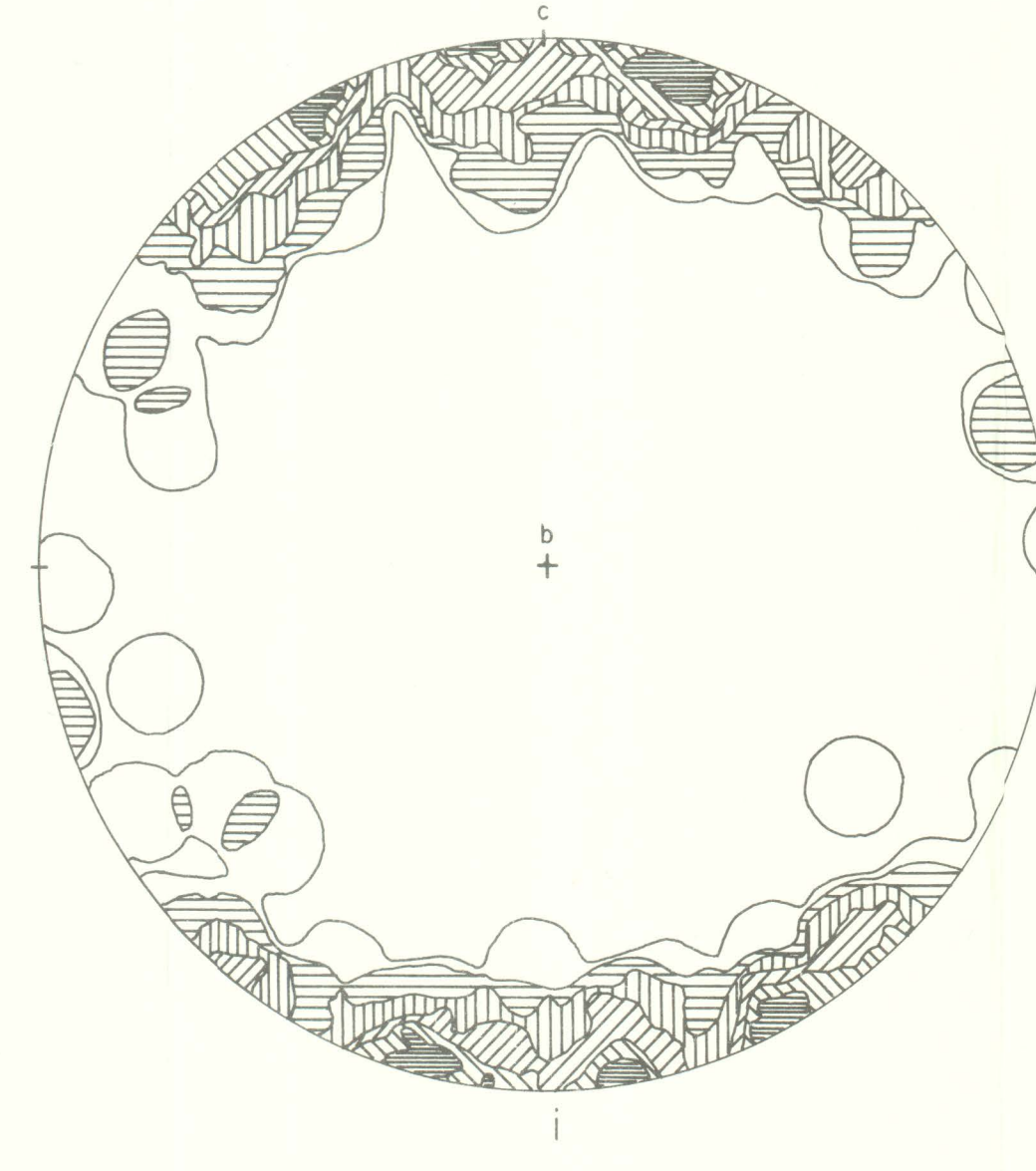
Geology by E. C. Binger, 1961-1963.
Geologic cartography by Bob Price.



d



h



EXPLANATION

- a. Mineralogic and textural lineation
- b. Lineation produced by intersecting planes
- c. Mesoscopic fold axes
- d. Domain (ruled area) in which third-deformation fold axes can occur as a function of known range in orientation of S_1 , S_2 and S_3
- e. Poles to flow cleavage
- f. Poles to relict fracture cleavage in quartzite
- g. Poles to fracture and slip cleavage
- h. Synoptic diagram of structural elements in Precambrian fold systems
- i. Poles to (001) of chlorite. Hornblende-chlorite schist. Section cut normal to schistosity and lineation
- j. Poles to (110) of hornblende. Hornblende-chlorite schist. Section cut normal to schistosity and lineation
- k. Poles to (001) of muscovite. Muscovitic quartzite. Section cut normal to schistosity and lineation
- l. b-axes of epidote. Hornblende-chlorite schist. Section cut normal to schistosity and lineation
- m. c-axes of hornblende. Hornblende-chlorite schist. Section cut normal to schistosity and lineation
- n. c-axes of quartz. Muscovitic quartzite. Section cut normal to schistosity and lineation

All diagrams are lower-hemisphere equal-area projections